


RESEARCH ARTICLE

Fast estimation of time-varying infectious disease transmission rates

Mikael Jagan^{1,2}[✉], Michelle S. deJonge¹[✉], Olga Krylova¹[✉], David J. D. Earn^{1,2*}

1 Department of Mathematics & Statistics, McMaster University, Hamilton, Ontario, Canada, **2** M.G. DeGroot Institute for Infectious Disease Research, McMaster University, Hamilton, Ontario, Canada

 These authors contributed equally to this work.

[✉] Current address: Applied Mathematics, University of Waterloo, Waterloo, Ontario, Canada

[✉] Current address: Integrated Decision Support, Hamilton Health Sciences, Hamilton, Ontario, Canada

[✉] Current address: Advanced Analytics, Canadian Institute for Health Information, Ottawa, Ontario, Canada

* earn@math.mcmaster.ca



Abstract

Compartmental epidemic models have been used extensively to study the historical spread of infectious diseases and to inform strategies for future control. A critical parameter of any such model is the transmission rate. Temporal variation in the transmission rate has a profound influence on disease spread. For this reason, estimation of time-varying transmission rates is an important step in identifying mechanisms that underlie patterns in observed disease incidence and mortality. Here, we present and test fast methods for reconstructing transmission rates from time series of reported incidence. Using simulated data, we quantify the sensitivity of these methods to parameters of the data-generating process and to misspecification of input parameters by the user. We show that sensitivity to the user's estimate of the initial number of susceptible individuals—considered to be a major limitation of similar methods—can be eliminated by an efficient, “peak-to-peak” iterative technique, which we propose. The method of transmission rate estimation that we advocate is extremely fast, for even the longest infectious disease time series that exist. It can be used independently or as a fast way to obtain better starting conditions for computationally expensive methods, such as iterated filtering and generalized profiling.

 OPEN ACCESS

Citation: Jagan M, deJonge MS, Krylova O, Earn DJD (2020) Fast estimation of time-varying infectious disease transmission rates. *PLoS Comput Biol* 16(9): e1008124. <https://doi.org/10.1371/journal.pcbi.1008124>

Editor: Jane M. Heffernan, York University, CANADA

Received: September 5, 2019

Accepted: July 6, 2020

Published: September 21, 2020

Copyright: © 2020 Jagan et al. This is an open access article distributed under the terms of the [Creative Commons Attribution License](https://creativecommons.org/licenses/by/4.0/), which permits unrestricted use, distribution, and reproduction in any medium, provided the original author and source are credited.

Data Availability Statement: All relevant data are found within the manuscript and Supporting Information files. Specifically, all of the data are simulated and can be generated reproducibly by running the R scripts contained in the Supporting Information files.

Funding: MJ was supported by an Undergraduate Student Research Award from the Natural Sciences and Engineering Research Council of Canada (NSERC) and a Student Fellowship from the M. G. DeGroot Institute for Infectious Disease Research. OK was supported by a Postgraduate Scholarship

Author summary

Many pathogens cause recurrent epidemics. Patterns of recurrence are strongly affected by seasonality of the transmission rate, which can arise from seasonal changes in weather and host population behaviour (*e.g.*, aggregation of children in schools). To understand and predict recurrent epidemic patterns, it is essential to reconstruct the time-varying transmission rate, which is never observed directly. Existing transmission rate estimation methods tend to fall into one of two categories: accurate but too slow to apply to long time series of reported incidence, or fast but inaccurate unless the number of individuals initially susceptible to infection is known precisely. Here, we introduce and compare fast methods inspired by the algorithm that Fine and Clarkson pioneered in the early 1980s.

from NSERC. DJDE was supported by a Discovery Grant from NSERC. The funders had no role in study design, data collection and analysis, decision to publish, or preparation of the manuscript.

Competing interests: The authors have declared that no competing interests exist.

The method that we suggest accurately reconstructs seasonally varying transmission rates, even with crude information about the initial size of the susceptible population.

1 Introduction

The transmission rate of an infectious disease is a salient quantity in the study of epidemics. Changes in the transmission rate over time greatly influence the spread of infection [1, 2]. Quantifying how it changes over time can elucidate factors governing disease spread (*e.g.*, weather [3], contact patterns [4]), inform epidemic forecasts, and suggest strategies for epidemic control [5].

In practice, we do not observe transmission directly. Instead, we observe the number of cases of infection (disease incidence) or number of deaths from infection (disease mortality) reported over time, and must reconstruct time-varying transmission rates from these data [6–13]. Utilizing historical mortality records, it is possible to identify patterns in transmission dating far back in time. Most notably, the London Bills of Mortality and the Registrar General’s Weekly Returns enable investigation of transmission patterns continuously from the mid-17th century to the present, for a number of infectious diseases including cholera [14] and smallpox [15].

A mechanistic understanding of long infectious disease time series—three centuries of weekly data in the case of smallpox [15]—requires methods of transmission rate estimation that are both accurate and fast, and therefore tractable for long time scales. Simulation-based methods of transmission rate estimation from reported incidence or mortality have been developed using the susceptible-infected-removed (SIR) model for infectious disease dynamics [16]. Markov chain Monte Carlo (MCMC [17, 18]) and sequential Monte Carlo (as in iterated filtering [8, 19, 20]) methods are statistically rigorous, but not tractable for long time scales owing to high computational cost. Generalized profiling [21, 22], which combines trajectory and gradient matching, is faster, but still too slow for convenient exploration of time series spanning hundreds of years. (Several CPU hours were required to apply generalized profiling to just 26 years of weekly data [22].)

In comparison, Finkenstädt and Grenfell’s popular “time series SIR” (tSIR) method [7, 23] is extremely fast, using a simple discretization of a continuous-time SIR model to reduce transmission rate estimation to a local regression problem. However, the tSIR method assumes that the duration of infection is equal to the time step, that natural death of susceptible individuals can be ignored, and that cumulative incidence approximates cumulative births. The latter two assumptions are reasonable for pre-vaccination measles, when most susceptible individuals were eventually infected [6]. However, in many contexts (*e.g.*, with pathogens less transmissible than measles), susceptible mortality over time scales of interest and the difference between incidence and births are non-negligible.

In their unpublished PhD and MSc theses, Krylova (Ch. 4 in [24]) and deJonge [25] separately modified a fast discretization method originally proposed by Fine and Clarkson [6]. Krylova’s approach has been employed to estimate the amplitude of seasonal variation in measles transmission in 20th century New York City [9]. Unlike the tSIR method and unlike Fine and Clarkson, Krylova’s and deJonge’s methods do not place constraints on the infectious period or ignore susceptible mortality.

Here, we present a new algorithm based on deJonge’s method and compare its performance to the methods of Fine and Clarkson and Krylova. Our main investigative approach is to apply

each method to simulated reported incidence data with known underlying transmission rate, so that error in transmission rate estimates can be quantified exactly.

Our analysis of the methods reveals a shared sensitivity to process and observation error. We mitigate this issue by introducing a smoothing step. The methods are additionally sensitive to error in the user's estimate of the initial number of susceptible individuals, which is rarely known with any precision. We propose a fast, iterative technique for estimating this parameter from time series of incidence, births, and natural mortality, eliminating a long-standing barrier to the use of fast methods of transmission rate reconstruction.

2 Methods

In §§2.1 and 2.2 below, we present three fast methods for estimating time-varying transmission rates, based on a mechanistic model of disease spread. In §§2.3–2.7, we outline our systematic analysis of the sensitivity of the methods to parameters of the data-generating process and to error in the user-specified values of input parameters. Finally, in §2.8, we introduce peak-to-peak iteration (PTPI), a technique for estimating the initial number of susceptible individuals. Essential notation is summarized in [Table 1](#).

2.1 Model of disease transmission

We assume that the principal mechanisms of disease spread in the focal population are captured by the SIR model [16], formulated with time-varying rates of birth, death, and transmission. Expressing the model as a system of ordinary differential equations, we write

$$\frac{dS}{dt} = v(t)\hat{N}_0 - \beta(t)SI - \mu(t)S, \quad (1a)$$

$$\frac{dI}{dt} = \beta(t)SI - \gamma I - \mu(t)I, \quad (1b)$$

$$\frac{dR}{dt} = \gamma I - \mu(t)R, \quad (1c)$$

where S , I , and R are the numbers of individuals who are susceptible, infected, and removed, respectively; $N = S + I + R$ is the population size; and $\hat{N}_0 = N(0)$ is the population size at an initial time, defined to be 0 years for simplicity. (We reserve the notation N_0 for $N(t_0)$, where $t_0 > 0$ years is the length of a transient; see [Table 1](#).)

The time-varying parameters are

$v(t)$ birth rate, the number of births per unit time relative to \hat{N}_0 ;

$\mu(t)$ natural mortality rate, the number of natural deaths per unit time *per capita* (i.e., relative to N); and

$\beta(t)$ transmission rate, the number of infections per unit time per susceptible per infected.

The constant parameter γ is the rate of removal from the infected compartment (due to recovery or death from disease) per infected individual.

In [Eq \(1a\)](#) and [Eq \(1b\)](#), we use mass action incidence $\beta(t)SI$ rather than standard incidence $\beta(t)SI/N$. Mass action incidence is essential for reproducing transitions in epidemic patterns resulting from changes in the birth rate [2, 28]. In [Eq \(1a\)](#), we write the net birth rate as $v(t)\hat{N}_0$ rather than $v(t)$. This formulation is for convenience: the factor of \hat{N}_0 does not affect dynamics, but ensures that $v(t)$ and $\mu(t)$ have the same scale.

Table 1. Notation. Unless otherwise stated, simulations of reported incidence time series use the reference values listed here. If a symbol is to be interpreted differently in relation to disease incidence and disease mortality data, then the correct definition is indicated by (I) and (M), respectively.

Symbol	Name	Definition	Ref. val.	Unit	Notes
t_k	k th observation time	Time of the k th observation in time series data, for $k = 0, \dots, n$.	$t_0 + k\Delta t$	years	
t_0	Transient period	Duration of the transient in system (1) that is ignored in simulations of reported incidence, before observations are recorded.	2000	years	System (1) is numerically integrated between $t = 0$ years and $t = t_0$, and observed starting at $t = t_0$. This is done so that simulations reflect dynamics near the attractor of system (1).
Δt	Observation interval	Time between successive observations in time series data.	1	weeks	Disease mortality is reported weekly in the London Bills of Mortality.
n	Time series length	Time between the initial and final observations in time series data, in units Δt , given by $(t_n - t_0)/\Delta t$.	1042	—	If $\Delta t = 1$ week, then $1042\Delta t = \lfloor 20 \times 365/7 \rfloor \Delta t \simeq 20$ years.
$[\cdot]_{\Delta t}$	Nearest $k\Delta t$ rounding	For time lengths t , $[t]_{\Delta t} = \lfloor \frac{t}{\Delta t} \rfloor \Delta t$, where $[\cdot]$ denotes nearest integer rounding.	—	—	
$\langle \cdot \rangle$	Long-term averaging	For functions $x(t)$, $\langle x \rangle = \lim_{T \rightarrow \infty} \frac{1}{T} \int_0^T x(s) ds$. For sequences x_k , $\langle x \rangle = \lim_{n \rightarrow \infty} \frac{1}{n} \sum_{k=0}^n x_k$.	—	—	
$(S(t), I(t), R(t))$	State	Number of (susceptible, infected, removed) individuals in the population at time t .	—	—	“Removed” individuals have either recovered from the disease and gained permanent immunity or died from the disease.
$N(t)$	Population size	$S(t) + I(t) + R(t)$.	—	—	
$B(t)$	Births	Number of births that occur during the time interval $[t - \Delta t, t)$.	—	—	
$Q(t)$	Cumulative incidence	Number of susceptibles who become infected during the time interval $[t_0, t)$.	—	—	
$Z(t)$	Incidence	Number of susceptibles who become infected during the time interval $[t - \Delta t, t)$.	$Q(t) - Q(t - \Delta t)$	—	
$C(t)$	Reported disease (I) incidence or (M) mortality	Number of (I) infections or (M) disease-induced deaths reported during the time interval $[t - \Delta t, t)$.	Eq (31)	—	C is an abbreviation of “cases”, which are reported as infections or as deaths.
(S_0, I_0, R_0)	Initial state ($t = t_0$)	$(S(t_0), I(t_0), R(t_0))$.	(S^*, I^*, R^*)	—	(S^*, I^*, R^*) denotes the state of system (1) after numerical integration between $t = 0$ years and $t = t_0$ with seasonally forced transmission rate $\beta(t)$ (Eq (27)), constant vital rates v_c and μ_c , and initial state ($t = 0$ years) $(\hat{S}, \hat{I}, \hat{R})$ (Eq (32); see below).
N_0	Initial population size ($t = t_0$)	$N(t_0)$.	$S^* + I^* + R^*$	—	
$(\hat{S}, \hat{I}, \hat{R})$	Endemic equilibrium	Endemic equilibrium of system (1) with constant transmission rate ($\beta \equiv \langle \beta \rangle$) and constant vital rates ($v \equiv \mu \equiv \mu_c$).	Eq (32)	—	
\hat{N}_0	Initial population size ($t = 0$ years)	$N(0)$.	10^6	—	
x_k	Estimation input/output	Within an estimation algorithm (Boxes 1–3), the supplied or estimated value of $x(t_k)$ ($x = C, B, \mu, Z, S, I, \beta$).	—	varies	
$v(t)$	Birth rate	Number of births per unit time relative to \hat{N}_0 , at time t .	v_c	year ⁻¹	In simulations of reported incidence, $v(t)$ is modeled as a constant v_c . In general, estimation of $\beta(t)$ from data does not require the underlying $v(t)$ to be constant.
v_c	Birth rate (constant)	See $v(t)$ above.	0.04	year ⁻¹	
$\mu(t)$	Natural mortality rate	Number of natural deaths per unit time <i>per capita</i> , at time t .	μ_c	year ⁻¹	In simulations of reported incidence, $\mu(t)$ is modeled as a constant μ_c . In general, estimation of $\beta(t)$ from data does not require the underlying $\mu(t)$ to be constant.
μ_c	Natural mortality rate (constant)	See $\mu(t)$ above.	0.04	year ⁻¹	

(Continued)

Table 1. (Continued)

Symbol	Name	Definition	Ref. val.	Unit	Notes
t_{gen}	Mean generation interval	Mean time between onset of infection (in infector) and subsequent transmission of infection (by infector) [26, 27].	13	days	The reference value is the sum of the observed mean latent and infectious periods, which for measles are 8 days and 5 days, respectively [16].
γ	Removal rate	Number of removals (recoveries or deaths from disease) per unit time per infected.	$1/t_{\text{gen}}$	day ⁻¹	
p_{rep}	Case reporting probability	(I) Probability that an infection is reported, or (M) the case fatality ratio times the probability that a death from disease is reported.	0.25 or 1	—	If we simulate data with under-reporting, then we use $p_{\text{rep}} = 0.25$ as a reference value. Otherwise, we set $p_{\text{rep}} = 1$.
t_{rep}	Mean case reporting delay	Mean time between infection and reporting of (I) infection or (M) disease-induced death.	2 or 0	weeks	If we simulate data with reporting delays, then we use $t_{\text{rep}} = 2$ weeks as a reference value. Otherwise, we set $t_{\text{rep}} = 0$ weeks.
$\beta(t)$	Transmission rate	Number of infections per unit time per susceptible per infected, at time t .	Eq (27)	year ⁻¹	In simulations of reported incidence, $\beta(t)$ is modeled by the seasonal forcing function defined in Eq (27). In general, estimation of $\beta(t)$ from data does not require it vary seasonally or even periodically.
$\langle\beta\rangle$	Mean transmission rate	Continuous-time average of the seasonally forced $\beta(t)$, equal to $\lim_{T \rightarrow \infty} \frac{1}{T} \int_0^T \beta(s) ds$.	β^*	year ⁻¹	$\beta^* \approx 5.6 \times 10^{-4} \text{year}^{-1}$ is the value of $\langle\beta\rangle$ that satisfies Eq (2) with $\mathcal{R}_0 = 20$, $\nu_c = \mu_c = 0.04 \text{year}^{-1}$, $t_{\text{gen}} = \gamma^{-1} = 13$ days, and $\hat{N}_0 = 10^6$.
\mathcal{R}_0	Basic reproduction number	Number of individuals that a typical infected person is expected to infect in an otherwise completely susceptible population.	Eq (2)	—	For measles in the 20th century, $\mathcal{R}_0 \approx 20$ [16].
α	Seasonal amplitude	Amplitude of the seasonally forced $\beta(t)$ relative to $\langle\beta\rangle$.	0.08	—	For measles, $\alpha \approx 0.08$ [2]. We require $\alpha \in [0, 1]$ to ensure that the seasonal forcing function defined in Eq (27) is non-negative.
$\phi(t; \epsilon)$	Environmental noise (realized)	Phase shift in the seasonally forced $\beta(t)$, at time t .	Normal(0, ϵ^2)	—	ϕ is a realization of a continuous-time stochastic process defined by a set $\{\Phi(t; \epsilon)\}$ of independent and Normal(0, ϵ^2)-distributed random variables.
ϵ	Standard deviation of environmental noise	See $\phi(t; \epsilon)$ above.	0.5	—	
q	Loess smoothing parameter	Rough number of nearest neighbours weighted in local regression (i.e., when fitting loess curves to time series), determining the degree of smoothing.	—	—	See §2.2.6 for an exact definition.

<https://doi.org/10.1371/journal.pcbi.1008124.t001>

The SIR model (1) assumes that the focal population is homogeneously mixed and subject to the mass action principle, which states that incidence is proportional to the product of the densities of susceptibles and infecteds [16]. The model further assumes that the latent period (time from infection to onset of infectiousness) can be ignored and that the infectious period (time from onset of infectiousness to recovery or death from disease) is exponentially distributed [29]. The distributions of the latent and infectious periods affect disease dynamics [28, 30, 31], but Krylova and Earn [28] showed that the effect on long-term dynamical structure is typically small when the mean generation interval is fixed (see Fig 11 in [28]). For this reason, we assign the mean generation interval implied by the SIR model (1) ($t_{\text{gen}} = \gamma^{-1}$) the value of the sum of the observed mean latent and infectious periods. This sum is the true mean generation interval if the latent and infectious periods are both exponentially distributed, and is a good estimate of the true mean generation interval more generally [28].

Transmissibility of infection is typically measured by the basic reproduction number \mathcal{R}_0 , defined as the number of individuals that a typical infected person is expected to infect in an otherwise completely susceptible population [16]. If the birth and death rates are constant ($\nu \equiv \nu_c$ and $\mu \equiv \mu_c$), and if the transmission rate has a well-defined average $\langle\beta\rangle$ [32], then the

basic reproduction number for the SIR model (1) can be written as [28]

$$\mathcal{R}_0 = \frac{v_c \hat{N}_0}{\mu_c} \cdot \frac{\langle \beta \rangle}{\gamma + \mu_c}. \quad (2)$$

2.2 Estimating $\beta(t)$ from time series data

Here, we examine three fast methods for estimating time-varying transmission rates $\beta(t)$. The methods take as input (i) time series of reported disease incidence or disease mortality, (ii) time series of births and natural mortality, and (iii) values for input parameters, such as the mean generation interval t_{gen} . By assumption, the time series data are available at discrete, equally spaced time points

$$t_k = t_0 + k\Delta t, \quad k = 0, \dots, n, \quad (3)$$

where Δt is the observation interval. The methods return as output a time series estimate of $\beta(t)$, denoted by $\{(t_k, \beta_k)\}_{k=0}^n$ or simply β_k , which can be averaged (§2.2.5) or smoothed (§2.2.6) to distill temporal patterns of interest.

Missing data must be imputed: the three methods are recursive, so they break down as soon as they encounter a missing value. Imputation can be accomplished most simply via linear interpolation between available data. More sophisticated techniques accounting for uncertainty in missing values are described in [33].

2.2.1 FC method. We review the method first described by Fine and Clarkson [6], referred to here as the “FC method”. Let $S(t)$ and $I(t)$ be the number of susceptibles and infecteds in the population at time t . S decreases when susceptibles become infected or die and increases when susceptibles are born. Let $Z(t)$ and $B(t)$ be the number of infections and births, respectively, that occur during the time interval $[t - \Delta t, t)$. Assuming that natural mortality was negligible, Fine and Clarkson reconstructed S from Z and B with the recursion

$$S(t + \Delta t) \approx S(t) + B(t + \Delta t) - Z(t + \Delta t). \quad (4)$$

Fine and Clarkson further assumed that the observation interval Δt was equal to the mean generation interval t_{gen} , so that prevalence could be approximated by incidence. That is,

$$I(t) \approx Z(t) \quad (5)$$

for all t . They derived an expression for $Z(t + \Delta t)$ via the mass action principle

$$Z(t + \Delta t) \approx \beta(t)S(t)I(t)\Delta t. \quad (6)$$

Rearranging Eq (6), they obtained an estimate of $\beta(t)$, given by

$$\beta(t) \approx \frac{Z(t + \Delta t)}{S(t)I(t)\Delta t}. \quad (7)$$

Fine and Clarkson applied Eqs (4), (5), and (7) to estimate $S(t_k)$, $I(t_k)$, and $\beta(t_k)$ (for $k = 0, \dots, n$), after specifying (i) the initial number of susceptibles $S_0 = S(t_0)$, and (ii) values of $Z(t_k)$ and $B(t_k)$ from incidence and birth data, respectively.

A limitation of the FC method is the constraint requiring $\Delta t = t_{\text{gen}}$. For some diseases, this is a minor issue, because incidence and birth data can be aggregated so that the time between successive aggregates is approximately equal to t_{gen} . For example, the mean generation interval of measles is approximately two weeks, so Fine and Clarkson [6] aggregated pairs of weekly

observations. A second, more serious limitation is the assumption, implicit in Eqs (4) and (5), that natural mortality is negligible. We discuss this issue in §3.1.

2.2.2 S method. Krylova (Ch. 4 in [24]) generalized the FC method in order to eliminate the constraint requiring $\Delta t = t_{\text{gen}}$ and account for natural mortality. Her approach is based on the SEIR model, which distinguishes “exposed” individuals in the latent stage of infection from infectious individuals. Here, we adapt Krylova’s approach to the SIR model (1) and refer to our approach as the “S method.”

We define S , I , Z , and B as in the FC method. Let $\mu(t)$ be the *per capita* natural mortality rate at time t , and let $Q(t)$ be the total number of infections occurring between the initial observation time t_0 and current time t (*i.e.*, cumulative incidence). The observation interval Δt is no longer constrained to be equal to the mean generation interval t_{gen} .

We reconstruct S recursively by discretizing Eq (1a):

$$S(t + \Delta t) \approx S(t) + B(t + \Delta t) - Z(t + \Delta t) - \mu(t)S(t)\Delta t. \tag{8}$$

Eq (8) is the result of applying the forward Euler method for numerical integration to Eq (1a), and replacing the incidence and birth terms with $Z(t + \Delta t)$ and $B(t + \Delta t)$, respectively. Eq (8) is identical to Eq (4) of the FC method, except that it includes a natural mortality term.

In order to estimate $\beta(t)$, we note that, by definition, dQ/dt is the rate at which individuals enter the infected compartment. From Eq (1b), this is

$$\frac{dQ}{dt} = \beta(t)S(t)I(t). \tag{9}$$

If the mean generation interval t_{gen} is short enough that I and μ are roughly constant between times t and $t + t_{\text{gen}}$, then $dI/dt \approx 0$ in that interval, and using Eq (1b) we can write

$$\beta(t)S(t)I(t) \approx (\gamma + \mu(t))I(t) \approx (\gamma + \mu(t + t_{\text{gen}}))I(t + t_{\text{gen}}). \tag{10}$$

In this case, dQ/dt is also (approximately) the rate at which individuals leave the infected compartment, t_{gen} time after infection:

$$\frac{dQ}{dt} \approx (\gamma + \mu(t + t_{\text{gen}}))I(t + t_{\text{gen}}). \tag{11}$$

Note that Eq (11) is also valid if the generation interval is narrowly distributed around its mean t_{gen} (even if t_{gen} is long).

Discretizing Eqs (9) and (11) using forward Euler, we obtain two approximations of $Z(t + \Delta t)$:

$$Z(t + \Delta t) = Q(t + \Delta t) - Q(t) \approx \begin{cases} \beta(t)S(t)I(t)\Delta t & \text{from Eq (9),} \\ (\gamma + \mu(t + t_{\text{gen}}))I(t + t_{\text{gen}})\Delta t & \text{from Eq (11).} \end{cases} \tag{12}$$

Rearranging Eq (12) yields an estimate of $\beta(t)$, given by

$$\beta(t) \approx \frac{Z(t + \Delta t)}{S(t)I(t)\Delta t}, \tag{13}$$

and an estimate of $I(t)$, given by

$$I(t) \approx \frac{Z(t + \Delta t - t_{\text{gen}})}{(\gamma + \mu(t))\Delta t}. \tag{14}$$

Since data are available only at the observation times t_k (Eq (3)), the value of $Z(t + \Delta t - t_{\text{gen}})$ in

Eq (14) will be observed only if t_{gen} is an integer multiple of Δt . In general, t_{gen} is not divisible by Δt . Therefore, in practice, we replace t_{gen} in $Z(t + \Delta t - t_{\text{gen}})$ with the nearest integer multiple of Δt , denoted here by $[t_{\text{gen}}]_{\Delta t}$:

$$I(t) \approx \frac{Z(t + \Delta t - t_{\text{gen}})}{(\gamma + \mu(t))\Delta t} \tag{15}$$

Thus, the S method is defined by Eq (13), coupled with Eqs (8) and (15) for the reconstruction of S and I . The S method requires users to specify (i) input parameters $S_0 = S(t_0)$ and $t_{\text{gen}} = \gamma^{-1}$, and (ii) values of $Z(t_k)$, $B(t_k)$, and $\mu(t_k)$ from incidence, birth, and natural mortality data, respectively.

The FC method is a special case of the S method, obtained by setting $\Delta t = t_{\text{gen}}$ and $\mu(t) \equiv 0$.

2.2.3 SI method. DeJonge [25] improved Krylova’s method (Ch. 4 in [24]) by reconstructing I directly from Eq (1b) instead of relying on the approximation in Eq (11). Here, we improve deJonge’s discretization, which employs the forward Euler method, by instead combining forward and backward Euler. One way to do this is to use the trapezoidal method: whereas forward and backward Euler take $f'(t)\Delta t$ and $f'(t + \Delta t)\Delta t$, respectively, to approximate integrals $\int_t^{t+\Delta t} f'(\tau) d\tau$, the trapezoidal method takes the average $\frac{1}{2}[f'(t) + f'(t + \Delta t)]\Delta t$, which is less prone to error. Our discretization, which we call the “SI method”, is consistently more accurate than deJonge’s and others (see §S9 of S1 Text for a comparison of nine possible algorithms). Numerically integrating Eq (1a) and Eq (1b) using the trapezoidal method, and replacing the incidence and birth terms with $Z(t + \Delta t)$ and $B(t + \Delta t)$, respectively, we obtain

$$S(t + \Delta t) \approx \frac{[1 - \frac{1}{2}\mu(t)\Delta t]S(t) + B(t + \Delta t) - Z(t + \Delta t)}{1 + \frac{1}{2}\mu(t + \Delta t)\Delta t} \tag{16}$$

and

$$I(t + \Delta t) \approx \frac{[1 - \frac{1}{2}(\gamma + \mu(t))\Delta t]I(t) + Z(t + \Delta t)}{1 + \frac{1}{2}(\gamma + \mu(t + \Delta t))\Delta t} \tag{17}$$

Eq (17) eliminates an important problem with Eq (15) of the S method, which estimates $I(t) \approx 0$ if $Z(t + \Delta t - [t_{\text{gen}}]_{\Delta t}) = 0$, leading to division by zero in Eq (13).

Discretizing Eq (9) using forward and backward Euler, we obtain two approximations of $Z(t + \Delta t)$:

$$Z(t + \Delta t) = Q(t + \Delta t) - Q(t) \approx \begin{cases} \beta(t)S(t)I(t)\Delta t & \text{from forward Euler,} \\ \beta(t + \Delta t)S(t + \Delta t)I(t + \Delta t)\Delta t & \text{from backward Euler.} \end{cases} \tag{18}$$

Rearranging Eq (18) yields two estimates of $\beta(t)$,

$$\beta(t) \approx \begin{cases} \frac{Z(t+\Delta t)}{S(t)I(t)\Delta t} & \text{from forward Euler,} \\ \frac{Z(t)}{S(t)I(t)\Delta t} & \text{from backward Euler,} \end{cases} \tag{19}$$

whose average supplies a more accurate estimate (see §S9 of S1 Text), given by

$$\beta(t) \approx \frac{Z(t) + Z(t + \Delta t)}{2S(t)I(t)\Delta t} \tag{20}$$

Thus, the SI method is defined by Eq (20), coupled with Eqs (16) and (17) for the reconstruction of S and I . Compared to the S method, the SI method, in principle, requires one

additional input parameter, namely the initial number of infecteds $I_0 = I(t_0)$. In §3.6, we show that, in practice, this additional information is not necessary.

2.2.4 Estimating true incidence from reported incidence. Let $C(t)$ be the number of infections reported during the time interval $[t - \Delta t, t)$. We estimate true incidence Z from reported incidence C via

$$Z(t) \approx \frac{1}{p_{\text{rep}}} C(t + [t_{\text{rep}}]_{\Delta t}), \quad (21)$$

where p_{rep} is the probability that an infection is reported and $[t_{\text{rep}}]_{\Delta t}$ is the mean time between infection and reporting, rounded to the nearest integer multiple of the observation interval Δt .

Eq (21) has the limitation that multiplying by p_{rep}^{-1} does not correct for under-reporting if, by chance, $C(t + [t_{\text{rep}}]_{\Delta t}) = 0$. In this situation, not only is the result $Z(t) \approx 0$ incorrect, but we divide by zero in the FC and S methods when we substitute Eqs (5) and (15) in Eqs (7) and (13), respectively. If $C(t + [t_{\text{rep}}]_{\Delta t}) = C(t + [t_{\text{rep}}]_{\Delta t} + \Delta t) = 0$, then the SI method also suffers: Eq (20) gives $\beta(t) \approx 0$. To circumvent these issues, we replace zeros in reported incidence time series by linearly interpolating between nonzero values prior to estimating true incidence using Eq (21). We do not replace leading and trailing zeros.

If what we observe is deaths from disease, rather than infections, then we have the complication that only a fraction of infections end in death. In this situation, we can still use Eq (21) to estimate Z , provided we interpret (i) C as reported disease mortality, (ii) p_{rep} as the case fatality ratio times the probability that a death from disease is reported, and (iii) t_{rep} as the mean time between infection and reporting of disease-induced death.

A more sophisticated method of inferring true incidence from reported data is described in [34].

2.2.5 Averaging raw estimates of $\beta(t)$. Given fixed time series data and input parameters, the FC, S, and SI methods return estimates of $\beta(t)$ that are entirely determined (not random). In the absence of additional data observed from the same population, it is difficult to assign confidence to the output.

However, if an estimate $\tilde{\beta}(t)$ is approximately periodic (with apparent period T) and contains m complete cycles, and if we assume $\beta(t)$ is truly periodic, then we can view $\tilde{\beta}(t)$ as containing a sample of m estimates of the true cycle, with some variance, and use its mean as an estimator instead of any one of the m cycles. For such an estimate $\tilde{\beta}(t)$ defined on the interval $[t_0, t_0 + mT)$, the mean and variance are given by

$$\bar{x}(t) = \frac{1}{m} \sum_{i=0}^{m-1} \tilde{\beta}(t + iT), \quad t \in [t_0, t_0 + T), \quad (22a)$$

$$s^2(t) = \frac{1}{m-1} \sum_{i=0}^{m-1} [\tilde{\beta}(t + iT) - \bar{x}(t)]^2, \quad t \in [t_0, t_0 + T). \quad (22b)$$

In §3.3, we apply the S and SI methods to simulated data to estimate an underlying, seasonally forced $\beta(t)$ (Eq (27)), which has a period of 1 year. We linearly interpolate the raw time series estimate β_k and compute the average 1-year cycle in the interpolant $\beta_{\text{int}}(t)$ using Eq (22a).

Comparing this average to the true 1-year cycle, we are able to assess bias in the two methods.

Note that $\bar{x}(t)$ and $s^2(t)$ can be used to obtain a formal, likelihood-based measure of confidence in estimates $\tilde{\beta}(t)$ (see §2.3.4 in [35]).

2.2.6 Smoothing raw estimates of $\beta(t)$. Process and observation error introduce random fluctuations in reported incidence on top of longer-term (e.g., seasonal) variation. In §3.2, we show that noise in reported incidence is spuriously amplified in β_k , the raw time series estimate of $\beta(t)$.

To distill temporal patterns of interest from the noise, we fit a smooth loess (short for local regression; see Ch. 8.1 in [36]) curve $\beta_{\text{loess}}(t; q)$ to the points $\{(t_k, \beta_k)\}_{k=0}^n$ and use $\beta_{\text{loess}}(t; q)$ as our final estimate of $\beta(t)$. Here, $q \in \{5, \dots, n + 1\}$ is an integer-valued parameter controlling the degree of smoothing. At times $t \in [t_0, t_n]$, the fitted value $\beta_{\text{loess}}(t; q)$ is obtained as follows:

1. Order the distances $d_k = |t_k - t|$ of the time points t_k (Eq (3)) from t , letting d_{k_i} denote the i th smallest distance (for $i = 1, \dots, n + 1$).
2. Fit a quadratic polynomial $p_2(t)$ to the points $\{(t_k, \beta_k)\}_{k=0}^n$. This is done by weighted least squares using tricube weights

$$w_k = \begin{cases} \left(1 - \left(\frac{d_k}{d_{k_q}}\right)^3\right)^3 & \text{if } 0 \leq d_k < d_{k_q}, \\ 0 & \text{if } d_k \geq d_{k_q}. \end{cases} \tag{23}$$

Hence only time points t_k nearer to t than the q th nearest time point are weighted in the fit.

3. Define $\beta_{\text{loess}}(t; q) = p_2(t)$.

Typically, smoother fits are obtained with greater q [36, 37].

The optimal value of q for a given time series β_k , denoted by q_{opt} , is that which minimizes error in $\beta_{\text{loess}}(t; q)$ relative to $\beta(t)$. In §3.4, we estimate $\beta(t)$ from simulated data, smooth β_k using each value of q on a grid, and use our knowledge of $\beta(t)$ to determine q_{opt} . We show that it is possible for smoothing to eliminate much of the error in β_k attributable to process and observation error. Thus, in §2.2.7, we explicitly define the FC, S, and SI methods with loess smoothing as a final step.

In practice, $\beta(t)$ is not known, so we cannot determine q_{opt} . In this case, q_{opt} can be estimated using statistical methods, such as time series cross-validation [38]. However, reasonable results can be obtained much more quickly by inspecting $\beta_{\text{loess}}(t; q)$ directly and increasing q from 4 until a desirable degree of smoothing is achieved (e.g., until noise on the time scale of weeks is visibly reduced, and patterns on the time scale of months are easier to discern).

2.2.7 Summary. In Boxes 1–3 below, we summarize the three methods derived in §§2.2.1–2.2.6 for estimating time-varying transmission rates $\beta(t)$ from time series data with observation times t_k (Eq (3)). We use the notation x_k to refer to the value supplied or computed for $x(t_k)$ within the estimation algorithms ($x = C, B, \mu, Z, S, I, \beta$).

In Box 4, we provide instructions for input specification based on our analysis of the methods.

Box 1. FC method (Fine & Clarkson 1982 [6])

$$Z_k \leftarrow \frac{1}{p_{\text{rep}}} C_{k+r}, \quad \text{where } r = \frac{\lceil t_{\text{rep}} \rceil \Delta t}{\Delta t}, \tag{24a}$$

$$S_k \leftarrow S_{k-1} + B_k - Z_k, \tag{24b}$$

$$I_k \leftarrow Z_k, \tag{24c}$$

$$\beta_k \leftarrow \frac{Z_{k+1}}{S_k I_k \Delta t}, \tag{24d}$$

where Δt is assumed to be roughly equal to t_{gen} , and natural mortality is assumed to be negligible. Users must specify:

- a time series $\{(t_k, C_k)\}_{k=0}^n$ of reported incidence or reported disease mortality, with zeros replaced via linear interpolation between nonzero values;
- a time series $\{(t_k, B_k)\}_{k=0}^n$ of births;
- input parameters $S_0, t_{\text{gen}}, p_{\text{rep}}$, and t_{rep} .

Box 2. S method (adapted from Krylova 2011 [24])

$$Z_k \leftarrow \frac{1}{p_{\text{rep}}} C_{k+r}, \quad \text{where } r = \frac{\lceil t_{\text{rep}} \rceil \Delta t}{\Delta t}, \tag{25a}$$

$$S_k \leftarrow S_{k-1} + B_k - Z_k - \mu_{k-1} S_{k-1} \Delta t, \tag{25b}$$

$$I_k \leftarrow \frac{Z_{k+1-g}}{(\gamma + \mu_k) \Delta t}, \quad \text{where } g = \frac{\lceil t_{\text{gen}} \rceil \Delta t}{\Delta t}, \tag{25c}$$

$$\beta_k \leftarrow \frac{Z_{k+1}}{S_k I_k \Delta t}, \tag{25d}$$

$$\beta_{\text{loess}}(t; q) \leftarrow \text{loess curve fit to time series } \{(t_k, \beta_k)\}_{k=0}^n. \tag{25e}$$

Users must specify:

- a time series $\{(t_k, C_k)\}_{k=0}^n$ of reported incidence or reported disease mortality, with zeros replaced via linear interpolation between nonzero values;
- a time series $\{(t_k, B_k)\}_{k=0}^n$ of births;
- a time series $\{(t_k, \mu_k)\}_{k=0}^n$ of the *per capita* natural mortality rate;
- input parameters $S_0, t_{\text{gen}} = \gamma^{-1}, p_{\text{rep}}$, and t_{rep} ;
- loess smoothing parameter q .

Box 3. SI method (adapted from deJonge 2014 [25])

$$Z_k \leftarrow \frac{1}{p_{\text{rep}}} C_{k+r}, \quad \text{where } r = \frac{\lceil t_{\text{rep}} \rceil \Delta t}{\Delta t}, \quad (26a)$$

$$S_k \leftarrow \frac{[1 - \frac{1}{2} \mu_{k-1} \Delta t] S_{k-1} + B_k - Z_k}{1 + \frac{1}{2} \mu_k \Delta t}, \quad (26b)$$

$$I_k \leftarrow \frac{[1 - \frac{1}{2} (\gamma + \mu_{k-1}) \Delta t] I_{k-1} + Z_k}{1 + \frac{1}{2} (\gamma + \mu_k) \Delta t}, \quad (26c)$$

$$\beta_k \leftarrow \frac{Z_k + Z_{k+1}}{2 S_k I_k \Delta t}, \quad (26d)$$

$$\beta_{\text{loess}}(t; q) \leftarrow \text{loess curve fit to time series } \{(t_k, \beta_k)\}_{k=0}^n. \quad (26e)$$

Users must specify:

- a time series $\{(t_k, C_k)\}_{k=0}^n$ of reported incidence or reported disease mortality, with zeros replaced via linear interpolation between nonzero values;
- a time series $\{(t_k, B_k)\}_{k=0}^n$ of births;
- a time series $\{(t_k, \mu_k)\}_{k=0}^n$ of the *per capita* natural mortality rate;
- input parameters $S_0, I_0, t_{\text{gen}} = \gamma^{-1}, p_{\text{rep}}$, and t_{rep} ;
- loess smoothing parameter q .

Box 4. Instructions for input specification

- β_k is sensitive to mis-specification of S_0 , but not I_0 (cf. §3.6.1). If the user's estimate of S_0 is uncertain, and if the incidence time series Z_k is roughly periodic, then a more accurate estimate of S_0 may be obtained via peak-to-peak iteration (PTPI; cf. §3.7).
- If S_k is negative for any k , then it is likely that the case reporting probability p_{rep} was underestimated or that births were systematically under-reported by B_k . This can be resolved by correcting the estimate of p_{rep} or correcting B_k , then restarting the algorithm. Users should apply close to the minimal correction necessary to prevent negative S_k .
- q must be tuned to the β_k time series. An estimate of q_{opt} can be obtained using statistical methods, such as time series cross-validation [38]. However, q can be tuned quickly through visual inspection of $\beta_{\text{loess}}(t; q)$: one can increase q from 5 until a desirable degree of smoothing is achieved (e.g., until noise on the time scale of weeks is visibly reduced, and patterns on the time scale of months are easier to discern).

2.3 Simulating reported incidence data

In order to compare the performance of the FC, S, and SI methods in estimating $\beta(t)$, we apply the methods to simulated reported incidence data with known underlying $\beta(t)$. Here, we outline our methods for simulating these data using the SIR model (1).

2.3.1 Seasonal forcing of $\beta(t)$ with environmental stochasticity. We reproduce seasonal fluctuation in the transmission rate by modeling $\beta(t)$ in Eq (1) as a sinusoidal forcing function with period equal to one year:

$$\beta(t) = \langle \beta \rangle \left(1 + \alpha \cos \left(\frac{2\pi t}{1 \text{ year}} \right) \right). \quad (27)$$

Here, $\alpha \in [0, 1]$ is the amplitude of seasonal forcing relative to the mean $\langle \beta \rangle$. We introduce stochastic fluctuation by adding a randomly generated phase shift:

$$\beta_\phi(t) = \langle \beta \rangle \left(1 + \alpha \cos \left(\frac{2\pi t}{1 \text{ year}} + \phi(t; \epsilon) \right) \right). \quad (28)$$

ϕ is a realization of a continuous-time stochastic process consisting of independent, Normal(0, ϵ^2)-distributed random variables. It models **environmental stochasticity** leading to random noise in the transmission rate. Modeling environmental stochasticity with a random phase shift rather than additive noise conveniently avoids negative $\beta_\phi(t)$: $\beta_\phi(t)$ oscillates between $\langle \beta \rangle(1 - \alpha)$ and $\langle \beta \rangle(1 + \alpha)$ regardless of the distribution of the noise. In practice, we take the values of ϕ at times t_k (Eq (3)) and linearly interpolate to obtain values in between. This helps to make simulations of Eqs (1) and (9) with adaptive time steps (cf. §2.3.2) reproducible.

2.3.2 Generating incidence time series with demographic stochasticity. We supplement Eq (1) with Eq (9), so that trajectories of the resulting system record changes in cumulative incidence Q . In this system, we employ the noisy transmission rate $\beta_\phi(t)$ (Eq (28)) and constant vital rates ν_c and μ_c . We then either (i) numerically integrate the differential equations to approximate their solution, or (ii) treat the system more realistically as an event-driven, continuous-time Markov process (with event rates specified by terms in the differential equations) and use the adaptive tau-leaping algorithm for stochastic simulation [39, 40]. The latter approach accounts for **demographic stochasticity** in disease dynamics. We prevent disease fadeout in simulations with demographic stochasticity by setting the rates of infected recovery and death to zero whenever $I = 1$.

In both methods of simulation, we record the state of the system at times t_k (Eq (3)), choosing initial state

$$\begin{pmatrix} S(t_0) \\ I(t_0) \\ R(t_0) \\ Q(t_0) \end{pmatrix} = \begin{pmatrix} S_0 \\ I_0 \\ R_0 \\ 0 \end{pmatrix}, \quad (29)$$

where $S_0 + I_0 + R_0 = N_0 = N(t_0)$. Finally, we derive incidence Z from Q via first differences:

$$Z(t) = Q(t) - Q(t - \Delta t). \quad (30)$$

2.3.3 Introducing observation error. Observation error due to under-reporting ($p_{\text{rep}} < 1$) and reporting delays ($t_{\text{rep}} > 0$ weeks) creates discrepancies between true incidence Z and reported incidence C . We introduce random observation error to simulated incidence time

series with delayed binomial sampling:

$$C(t + [t_{\text{rep}}]_{\Delta t}) \sim \text{Binomial}(Z(t), p_{\text{rep}}). \tag{31}$$

For simulations without observation error, we set $p_{\text{rep}} < 1$ and $t_{\text{rep}} > 0$ weeks.

2.3.4 Parametrization. The simulation method outlined in §§2.3.1–2.3.3 is parametrized by

disease parameters	$\langle \beta \rangle, \alpha, \epsilon, t_{\text{gen}};$
population parameters	$\hat{N}_0 = N(0), S_0 = S(t_0), I_0 = I(t_0), \nu_c, \mu_c;$ and
reporting parameters	$p_{\text{rep}}, t_{\text{rep}}, t_0, \Delta t, n.$

For most simulations, we assign parameters the reference values listed in Table 1. We consider different values when we investigate the sensitivity of $\beta(t)$ estimates to data-generating parameters (cf. §2.6.1).

We bypass transient dynamics by choosing $t_0 = 2000$ years and numerically integrating system (1) between 0 years and t_0 in order to obtain a point (S^*, I^*, R^*) very near the attractor. For this step, we exclude environmental noise, defining $\beta(t)$ as in Eq (27), and take the initial state to be the endemic equilibrium of the unforced system (system (1) with $\beta \equiv \langle \beta \rangle$ and $\nu \equiv \mu \equiv \mu_c$):

$$\begin{pmatrix} S(0) \\ I(0) \\ R(0) \end{pmatrix} = \begin{pmatrix} \hat{S} \\ \hat{I} \\ \hat{R} \end{pmatrix} = \begin{pmatrix} \frac{\hat{N}_0}{\mathcal{R}_0} \\ \hat{N}_0 \left(1 - \frac{1}{\mathcal{R}_0}\right) \left(\frac{\mu_c}{\gamma + \mu_c}\right) \\ \hat{N}_0 \left(1 - \frac{1}{\mathcal{R}_0}\right) \left(\frac{\gamma}{\gamma + \mu_c}\right) \end{pmatrix}. \tag{32}$$

2.4 Creating mock birth and natural mortality time series

In addition to reported incidence data, the FC, S, and SI methods require time series of births and the *per capita* natural mortality rate. For simplicity, we create mock time series by (i) choosing constant vital rates ν'_c and μ'_c , then (ii) setting $B_k = \nu'_c \hat{N}_0 \Delta t$ and $\mu_k = \mu'_c$ for all k . Note that $\nu'_c \hat{N}_0 \Delta t$ is the result of integrating the net birth rate in the SIR model (1), given by $\nu(t) \hat{N}_0$, between successive observation times using $\nu \equiv \nu'_c$.

We specify $\nu'_c = \nu_c$ and $\mu'_c = \mu_c$, where ν_c and μ_c are the data-generating vital rates (cf. §2.3.4), except when we investigate the sensitivity of $\beta(t)$ estimates to incorrect vital data (cf. §2.6.2). For example, to model under-reporting of births, we simply set $\nu'_c < \nu_c$.

2.5 Measuring $\beta(t)$ estimation error

When we simulate reported incidence data, the underlying transmission rate $\beta(t)$ is defined beforehand via Eq (27) and known for all t . We use this knowledge to quantify the error in estimates of $\beta(t)$ obtained from the data. Specifically, given an estimate $\tilde{\beta}(t)$ defined at time points t_k (Eq (3)), we compute the relative root mean square error (RRMSE), defined as

$$\text{RRMSE}(\beta, \tilde{\beta}) := \sqrt{\frac{1}{n+1} \sum_{k=0}^n \left(\frac{\beta(t_k) - \tilde{\beta}(t_k)}{\tilde{\beta}} \right)^2}, \tag{33}$$

where

$$\bar{\beta} := \frac{1}{n+1} \sum_{k=0}^n \beta(t_k). \quad (34)$$

Note that by “underlying transmission rate” we mean the transmission rate *excluding* environmental noise. Although we simulate data using the noisy $\beta_\phi(t)$, defined in Eq (28), our aim is to reconstruct the noiseless $\beta(t)$, defined in Eq (27).

2.6 Sensitivity analysis

Error in $\beta(t)$ estimation from reported incidence data depends on how the data were generated. The number of cases reported over time is influenced by features of the disease (e.g., the natural history of infection), population (e.g., contact patterns), and case reporting (e.g., the frequency and accuracy of reports). In our simulations of reported incidence, there are 14 **data-generating parameters** (cf. §2.3.4), whose values are summarized in the vector

$$\theta = (\langle \beta \rangle, \alpha, \epsilon, \hat{N}_0, S_0, I_0, v_c, \mu_c, t_{\text{gen}}, p_{\text{rep}}, t_{\text{rep}}, t_0, \Delta t, n). \quad (35)$$

Estimation error also depends on how accurately certain data-generating parameters are specified by users of the FC, S, and SI methods. The initial observation time t_0 , observation interval Δt , and time series length n are always known exactly. Other parameters ($\langle \beta \rangle, \alpha, \epsilon, \hat{N}_0, v_c$, and μ_c) influence our simulations of reported incidence, but in practice are not parameters of the FC, S, and SI methods. In practice, users are required to specify only $S_0, t_{\text{gen}}, p_{\text{rep}}, t_{\text{rep}}$, and (with the SI method) I_0 . However, when we test the methods here, we do specify vital rates v_c and μ_c in order to create mock (constant) birth and natural mortality time series (cf. §2.4). The specified values of these 7 **input parameters** are summarized in the vector

$$\theta' = (S'_0, I'_0, v'_c, \mu'_c, t'_{\text{gen}}, p'_{\text{rep}}, t'_{\text{rep}}). \quad (36)$$

First, we investigate the sensitivity of the methods to the data-generating parameter values θ . Then, we examine their sensitivity to error in the user’s specification θ' of the input parameters. Here, we describe our analysis using the notation $\tilde{\beta}(t; \theta, \theta')$ to refer to transmission rate estimates constructed with user input θ' , from data generated by parameter values θ .

2.6.1 Sensitivity to data-generating parameters. In §3.5, we consider the ideal situation in which the input θ' corresponds exactly to the data-generating θ . In this case, how sensitive is error in $\tilde{\beta}(t; \theta, \theta')$ to θ ? For example, is $\beta(t)$ estimated more accurately for diseases with longer mean generation interval t_{gen} , etc.? To answer these questions, we perform the following steps on a grid of data-generating parameter values θ :

1. Simulate 1000 reported incidence time series using θ .
2. Create corresponding mock (constant) birth and natural mortality time series (cf. §2.4), specifying $v'_c = v_c$ and $\mu'_c = \mu_c$ in the input θ' .
3. Estimate $\beta(t)$ from the simulated data, specifying $S'_0 = S_0, I'_0 = I_0, t'_{\text{gen}} = t_{\text{gen}}, p'_{\text{rep}} = p_{\text{rep}}$, and $t'_{\text{rep}} = t_{\text{rep}}$ in the input θ' .
4. Compute the median RRMSE in the estimates $\tilde{\beta}(t_k; \theta, \theta')$ (1000 estimates corresponding to 1000 simulations).

We repeat this analysis 6 times, corresponding to 2 methods of $\beta(t)$ estimation (S or SI) and 3 methods of data simulation:

- *without* demographic stochasticity and *without* observation error (fixing $p_{\text{rep}} = 1$, $t_{\text{rep}} = 0$ weeks),
- *with* demographic stochasticity but *without* observation error (fixing $p_{\text{rep}} = 1$, $t_{\text{rep}} = 0$ weeks), or
- *with* demographic stochasticity and *with* observation error (fixing $p_{\text{rep}} = 0.25$ unless sensitivity to p_{rep} is considered, $t_{\text{rep}} = 2$ weeks).

Environmental stochasticity ($\epsilon = 0.5$) is included in all simulations.

2.6.2 Sensitivity to mis-specification of input parameters. In §3.6, we fix the data-generating θ and consider the more realistic situation in which components of the input θ' differ from the corresponding components of θ by a potentially large factor. In this case, how sensitive is error in $\tilde{\beta}(t; \theta, \theta')$ to error in θ' ? For example, how important is having an accurate estimate of t_{gen} , *etc.*? To answer these questions, we perform the following steps:

1. Simulate 1000 reported incidence time series using fixed data-generating parameter values θ . (We assign the reference values listed in Table 1.)
2. For each point on a grid of input parameter values θ' :
 - a. Create mock (constant) birth and natural mortality time series, taking v'_c and μ'_c from the input θ' .
 - b. Estimate $\beta(t)$ from the simulated data, taking $S'_0, I'_0, t'_{\text{gen}}, p'_{\text{rep}}$, and t'_{rep} from the input θ' .
 - c. Compute the median RRMSE in the estimates $\tilde{\beta}(t_k; \theta, \theta')$ (1000 estimates corresponding to 1000 simulations).

We repeat this analysis 6 times, as outlined at the end of §2.6.1.

2.7 Asymptotic analysis

Here, we examine analytically the propagation of input error to the output of the SI method. (Similar expressions for propagated errors are obtained by analyzing the S method.) Our analysis here supports numerical results presented in §3.6 concerning the sensitivity of $\beta(t)$ estimation error to mis-specification of input parameters.

2.7.1 Explicit solutions of the (S_k, I_k) difference equations. The SI method uses Eq (26a) to Eq (26c) to recursively reconstruct $S(t)$ and $I(t)$ from time series of reported incidence, births, and natural mortality. After substitution of Eq (26a), Eq (26b) and Eq (26c) can be written as

$$S_{k+1} = \frac{1 - \frac{1}{2}\mu_k\Delta t}{1 + \frac{1}{2}\mu_{k+1}\Delta t} S_k + \frac{B_{k+1} - \frac{1}{p_{\text{rep}}}C_{k+1+r}}{1 + \frac{1}{2}\mu_{k+1}\Delta t}, \quad k = 0, 1, \dots, \tag{37a}$$

$$I_{k+1} = \frac{1 - \frac{1}{2}(\gamma + \mu_k)\Delta t}{1 + \frac{1}{2}(\gamma + \mu_{k+1})\Delta t} I_k + \frac{\frac{1}{p_{\text{rep}}}C_{k+1+r}}{1 + \frac{1}{2}(\gamma + \mu_{k+1})\Delta t}, \quad k = 0, 1, \dots, \tag{37b}$$

where $r = \lceil t_{\text{rep}} \rceil_{\Delta t} / \Delta t$ is the mean case reporting delay in units of the observation interval, rounded to the nearest integer. Eq (37) are linear, first order difference equations, whose explicit solutions are obtained using standard algebraic techniques (see Eq 1.2.4 in [41]) and

given by

$$S_k = S_0 \prod_{j=0}^{k-1} \frac{1 - \frac{1}{2} \mu_j \Delta t}{1 + \frac{1}{2} \mu_{j+1} \Delta t} + \sum_{i=0}^{k-1} (B_{i+1} - \frac{1}{p_{\text{rep}}} C_{i+1+r}) \prod_{j=i+1}^{k-1} \frac{1 - \frac{1}{2} \mu_j \Delta t}{1 + \frac{1}{2} \mu_{j+1} \Delta t}, \quad k = 0, 1, \dots, \quad (38a)$$

$$I_k = I_0 \prod_{j=0}^{k-1} \frac{1 - \frac{1}{2} (\gamma + \mu_j) \Delta t}{1 + \frac{1}{2} (\gamma + \mu_{j+1}) \Delta t} + \sum_{i=0}^{k-1} \frac{1}{p_{\text{rep}}} C_{i+1+r} \prod_{j=i+1}^{k-1} \frac{1 - \frac{1}{2} (\gamma + \mu_j) \Delta t}{1 + \frac{1}{2} (\gamma + \mu_{j+1}) \Delta t}, \quad k = 0, 1, \dots, \quad (38b)$$

with the conventions $\prod_{i=b}^a x_i = 0$ and $\prod_{i=b}^a x_i = 1$ if $a < b$. As we show in §2.7.2, explicit solutions of Eq (37) facilitate asymptotic analysis.

2.7.2 Propagation of input error to (S_k, I_k) . We consider the special case in which the vital rates are constant and set $B_k = v_c \hat{N}_0 \Delta t$ and $\mu_k = \mu_c$ for all k (cf. §2.4). Then Eq (38) simplify to

$$\begin{aligned} & S_k(S_0, v_c, \mu_c, p_{\text{rep}}) \\ &= S_0 \left(\frac{1 - \frac{1}{2} \mu_c \Delta t}{1 + \frac{1}{2} \mu_c \Delta t} \right)^k + \sum_{i=0}^{k-1} \frac{v_c \hat{N}_0 \Delta t - \frac{1}{p_{\text{rep}}} C_{i+1+r}}{1 + \frac{1}{2} \mu_c \Delta t} \left(\frac{1 - \frac{1}{2} \mu_c \Delta t}{1 + \frac{1}{2} \mu_c \Delta t} \right)^{k-1-i} \end{aligned} \quad (39a)$$

$$\begin{aligned} & I_k(I_0, \mu_c, t_{\text{gen}}, p_{\text{rep}}) \\ &= I_0 \left(\frac{1 - \frac{1}{2} (\gamma + \mu_c) \Delta t}{1 + \frac{1}{2} (\gamma + \mu_c) \Delta t} \right)^k + \sum_{i=0}^{k-1} \frac{\frac{1}{p_{\text{rep}}} C_{i+1+r}}{1 + \frac{1}{2} (\gamma + \mu_c) \Delta t} \left(\frac{1 - \frac{1}{2} (\gamma + \mu_c) \Delta t}{1 + \frac{1}{2} (\gamma + \mu_c) \Delta t} \right)^{k-1-i} \end{aligned} \quad (39b)$$

where we have made explicit the dependence of S_k and I_k on input parameters $S_0, I_0, v_c, \mu_c, t_{\text{gen}} = \gamma^{-1}$, and p_{rep} . Using Eq (39), we can derive exact expressions for the error propagated to S_k and I_k in the SI method as a result of assigning an incorrect value to an input parameter.

If the initial number of susceptibles is truly S_0 , but we specify $S'_0 = \omega S_0$, where $\omega > 0$, then the error propagated to S_k is

$$\begin{aligned} \text{Err}(S_k, S_0 \leftarrow \omega S_0) &= S_k(\omega S_0, v_c, \mu_c, p_{\text{rep}}) - S_k(S_0, v_c, \mu_c, p_{\text{rep}}) \\ &= (\omega - 1) S_0 \left(\frac{1 - \frac{1}{2} \mu_c \Delta t}{1 + \frac{1}{2} \mu_c \Delta t} \right)^k \\ &= (\omega - 1) S_0 \left(\frac{1 - \frac{\Delta t}{2 t_{\text{life}}}}{1 + \frac{\Delta t}{2 t_{\text{life}}}} \right)^k \xrightarrow{k \rightarrow \infty} 0, \end{aligned} \quad (40)$$

where $t_{\text{life}} = \mu_c^{-1}$ is the life expectancy in the population. Similarly, specifying $I'_0 = \omega I_0$ for I_0 yields an error

$$\begin{aligned}
 \text{Err}(I_k, I_0 \leftarrow \omega I_0) &= I_k(\omega I_0, \mu_c, t_{\text{gen}}, p_{\text{rep}}) - I_k(I_0, \mu_c, t_{\text{gen}}, p_{\text{rep}}) \\
 &= (\omega - 1)I_0 \left(\frac{1 - \frac{1}{2}(\gamma + \mu_c)\Delta t}{1 + \frac{1}{2}(\gamma + \mu_c)\Delta t} \right)^k \\
 &= (\omega - 1)I_0 \left(\frac{1 - \frac{\Delta t}{2t_{\text{inf}}}}{1 + \frac{\Delta t}{2t_{\text{inf}}}} \right)^k \xrightarrow{k \rightarrow \infty} 0
 \end{aligned}
 \tag{41}$$

in I_k , where $t_{\text{inf}} = (\gamma + \mu_c)^{-1}$ is the mean time between infection and removal from the infected compartment, accounting for the possibility of natural death during infection. Eqs (40) and (41) show that the errors propagated to S_k and I_k vanish as $k \rightarrow \infty$; we exploit this fact to improve susceptible reconstruction (cf. §2.8).

Mis-specifying v_c by assigning a value $v'_c = \omega v_c$ creates an error in S_k that increases in magnitude over time and converges to a limit:

$$\begin{aligned}
 \text{Err}(S_k, v_c \leftarrow \omega v_c) &= S_k(S_0, \omega v_c, \mu_c, p_{\text{rep}}) - S_k(S_0, v_c, \mu_c, p_{\text{rep}}) \\
 &= \sum_{i=0}^{k-1} \frac{(\omega - 1)v_c \hat{N}_0 \Delta t}{1 + \frac{1}{2}\mu_c \Delta t} \left(\frac{1 - \frac{1}{2}\mu_c \Delta t}{1 + \frac{1}{2}\mu_c \Delta t} \right)^{k-1-i} \\
 &= \frac{(\omega - 1)v_c \hat{N}_0 \Delta t}{1 + \frac{1}{2}\mu_c \Delta t} \sum_{i=0}^{k-1} \left(\frac{1 - \frac{1}{2}\mu_c \Delta t}{1 + \frac{1}{2}\mu_c \Delta t} \right)^i \\
 &= \frac{(\omega - 1)v_c \hat{N}_0}{\mu_c} \left[1 - \left(\frac{1 - \frac{1}{2}\mu_c \Delta t}{1 + \frac{1}{2}\mu_c \Delta t} \right)^k \right] \xrightarrow{k \rightarrow \infty} (\omega - 1)v_c \hat{N}_0 t_{\text{life}}.
 \end{aligned}
 \tag{42}$$

Unlike Eq (42), the exact expression for $\text{Err}(S_k, \mu_c \leftarrow \omega \mu_c)$ is not readily simplified and is difficult to interpret:

$$\begin{aligned}
 \text{Err}(S_k, \mu_c \leftarrow \omega \mu_c) &= S_k(S_0, v_c, \omega \mu_c, p_{\text{rep}}) - S_k(S_0, v_c, \mu_c, p_{\text{rep}}) \\
 &= S_0 \left(\frac{1 - \frac{1}{2}\omega \mu_c \Delta t}{1 + \frac{1}{2}\omega \mu_c \Delta t} \right)^k + \sum_{i=0}^{k-1} \frac{v_c \hat{N}_0 \Delta t - \frac{1}{p_{\text{rep}}} C_{i+1+r}}{1 + \frac{1}{2}\omega \mu_c \Delta t} \left(\frac{1 - \frac{1}{2}\omega \mu_c \Delta t}{1 + \frac{1}{2}\omega \mu_c \Delta t} \right)^{k-1-i} \\
 &\quad - S_0 \left(\frac{1 - \frac{1}{2}\mu_c \Delta t}{1 + \frac{1}{2}\mu_c \Delta t} \right)^k - \sum_{i=0}^{k-1} \frac{v_c \hat{N}_0 \Delta t - \frac{1}{p_{\text{rep}}} C_{i+1+r}}{1 + \frac{1}{2}\mu_c \Delta t} \left(\frac{1 - \frac{1}{2}\mu_c \Delta t}{1 + \frac{1}{2}\mu_c \Delta t} \right)^{k-1-i}.
 \end{aligned}
 \tag{43}$$

However, if C_k has a well-defined long-term average $\langle C \rangle$ (this will be true if, for instance, C_k is periodic), then $\text{Err}(S_k, \mu_c \leftarrow \omega \mu_c)$ has a well-defined long-term average $\langle \text{Err}(S_k, \mu_c \leftarrow \omega \mu_c) \rangle$ with a simple form. Replacing C_{i+1+r} in Eq (43) with $\langle C \rangle$, simplifying the resulting expression,

then taking the limit as $k \rightarrow \infty$, we obtain

$$\begin{aligned} & \langle \text{Err}(S_k, \mu_c \leftarrow \omega \mu_c) \rangle \\ &= \lim_{k \rightarrow \infty} \left\{ S_0 \left(\frac{1 - \frac{1}{2} \omega \mu_c \Delta t}{1 + \frac{1}{2} \omega \mu_c \Delta t} \right)^k + \frac{v_c \hat{N}_0 \Delta t - \frac{1}{p_{\text{rep}}} \langle C \rangle}{\omega \mu_c \Delta t} \left[1 - \left(\frac{1 - \frac{1}{2} \omega \mu_c \Delta t}{1 + \frac{1}{2} \omega \mu_c \Delta t} \right)^k \right] \right. \\ & \quad \left. - S_0 \left(\frac{1 - \frac{1}{2} \mu_c \Delta t}{1 + \frac{1}{2} \mu_c \Delta t} \right)^k - \frac{v_c \hat{N}_0 \Delta t - \frac{1}{p_{\text{rep}}} \langle C \rangle}{\mu_c \Delta t} \left[1 - \left(\frac{1 - \frac{1}{2} \mu_c \Delta t}{1 + \frac{1}{2} \mu_c \Delta t} \right)^k \right] \right\} \\ &= \left(\frac{1}{\omega} - 1 \right) \left(v_c \hat{N}_0 \Delta t - \frac{1}{p_{\text{rep}}} \langle C \rangle \right) \frac{t_{\text{lifc}}}{\Delta t}, \end{aligned} \tag{44}$$

We can similarly show the following, still assuming that $\langle C \rangle$ is well-defined:

$$\langle \text{Err}(I_k, \mu_c \leftarrow \omega \mu_c) \rangle = \frac{\langle C \rangle (t'_{\text{inf}} - t_{\text{inf}})}{p_{\text{rep}} \Delta t}, \quad t'_{\text{inf}} = (\gamma + \omega \mu_c)^{-1}, \tag{45}$$

$$\langle \text{Err}(I_k, t_{\text{gen}} \leftarrow \omega t_{\text{gen}}) \rangle = \frac{\langle C \rangle (t'_{\text{inf}} - t_{\text{inf}})}{p_{\text{rep}} \Delta t}, \quad t'_{\text{inf}} = \left(\frac{1}{\omega} \gamma + \mu_c \right)^{-1}, \tag{46}$$

$$\langle \text{Err}(S_k, p_{\text{rep}} \leftarrow \omega p_{\text{rep}}) \rangle = \left(1 - \frac{1}{\omega} \right) \frac{\langle C \rangle t_{\text{lifc}}}{p_{\text{rep}} \Delta t}, \tag{47}$$

$$\langle \text{Err}(I_k, p_{\text{rep}} \leftarrow \omega p_{\text{rep}}) \rangle = \left(\frac{1}{\omega} - 1 \right) \frac{\langle C \rangle t_{\text{inf}}}{p_{\text{rep}} \Delta t}. \tag{48}$$

Here, t'_{inf} is the (incorrect) mean time spent infected that results when $\omega \mu_c$ is incorrectly specified for μ_c (Eq 45) or ωt_{gen} is incorrectly specified for t_{gen} (Eq 46).

2.7.3 Propagation of error in (S_k, I_k) to β_k . Let $\beta_k(Z_k, Z_{k+1}, S_k, I_k)$ be the raw SI method estimate of $\beta(t_k)$, given by the right hand side of Eq (26d). Suppose that, due to propagated error (cf. §2.7.2), the arguments are incorrect by a factor, so that

$$Z_k = \omega_Z Z(t_k), \quad Z_{k+1} = \omega_Z Z(t_{k+1}), \quad S_k = \omega_S S(t_k), \quad I_k = \omega_I I(t_k), \tag{49}$$

where $\omega_Z, \omega_S, \omega_I > 0$. Then the computed β_k will have relative error

$$\frac{\beta_k(Z_k, Z_{k+1}, S_k, I_k) - \beta_k(Z(t_k), Z(t_{k+1}), S(t_k), I(t_k))}{\beta_k(Z(t_k), Z(t_{k+1}), S(t_k), I(t_k))} = \frac{\omega_Z}{\omega_S \omega_I} - 1. \tag{50}$$

Hence severe underestimation of S_k or I_k ($\omega_S \ll 1$ or $\omega_I \ll 1$) causes the relative error in β_k to blow up.

2.8 Estimating S_0 via peak-to-peak iteration

Reconstruction of susceptibles $S(t)$ is a necessary step in the reconstruction of $\beta(t)$ using the FC, S, and SI methods. In §3.6, we show that susceptible reconstruction requires accurate specification of the initial number of susceptibles $S_0 = S(t_0)$. However, reliable estimates of S_0 have, to this point, been difficult to obtain in practice.

We propose a technique for iteratively improving estimates of S_0 , requiring only incidence, birth, and natural mortality data at times t_k (Eq (3)). Crucially, our technique, which we call

“peak-to-peak iteration” (PTPI), enables accurate susceptible reconstruction without direct observation of the susceptible population size at the initial time.

Our approach is motivated by application of the SI method to simulated data. When we incorrectly guessed the value of S_0 and attempted to reconstruct $S(t)$ via Eq (26b), the absolute error in the reconstruction $\{(t_k, S_k)\}_{k=0}^n$ decreased monotonically over time (k). (Eq (40) shows that the error propagated from S_0 to S_k vanishes as $k \rightarrow \infty$.) Consequently, if the underlying dynamics are at least approximately periodic, and if t_0 and t_n occur at the same phase of the cycle, then S_n is actually a better estimate of S_0 than our initial guess. In this situation, instead of reconstructing $\beta(t)$ directly, we can use S_n as an updated estimate of S_0 , and reconstruct $S(t)$ more accurately. This procedure can be repeated any number of times, and, with simulated data, we observe rapid convergence to an accurate estimate of S_0 (cf. §3.7).

The key point is that the reconstructed final state can be used as an improved estimate of the initial state only if the initial and final states occur at the same phase of the cycle. This will not be true unless the observation period (the time between the first and last observations in time series data) is an integer multiple of the period of the underlying dynamics. We can ensure this by choosing appropriate times at which to start and stop $S(t)$ reconstruction. In noisy periodic data, the points in a cycle that are easiest to identify robustly are the peaks. Consequently, we ignore observations (i) prior to the time t_a of the first peak in the incidence time series and (ii) after the time t_b of the last peak that occurs near an integer multiple of the apparent period after the first peak. For the truncated time series, the iterations converge to an accurate estimate of $S(t_a)$ starting from an initial guess, and we recover the corresponding accurate estimate of S_0 by solving Eq (26b) backwards in time, from t_a to t_0 :

$$S_{k-1} \approx \frac{[1 + \frac{1}{2}\mu_k\Delta t]S_k - B_k + Z_k}{1 - \frac{1}{2}\mu_{k-1}\Delta t}. \tag{51}$$

The complete PTPI algorithm, which consists of finding t_a and t_b (truncation step) and estimating S_0 (iteration step), is outlined in Boxes 5 and 6 below. In §3.7, we assess the performance of PTPI by applying the technique to simulated data with known underlying S_0 , starting from an incorrect initial estimate of S_0 .

Box 5. Peak-to-peak iteration: Truncation step

Goal: Given a roughly periodic time series $\{(t_k, Z_k)\}_{k=0}^n$ of incidence, we want to find the time t_a of the first peak and the time t_b of the last peak occurring at the same phase of the cycle. These times are necessary for the iteration step (Box 6).

Algorithm:

- i. Smooth the raw incidence time series Z_k by applying a $(2\ell_1 + 1)$ -point central moving average, computed via

$$\bar{Z}_k = \frac{1}{2\ell_1 + 1} \sum_{i=-\ell_1}^{\ell_1} Z_{k+i}, \quad k = \ell_1, \dots, n - \ell_1. \tag{52}$$

Choose minimal ℓ_1 large enough to remove spurious peaks in Z_k caused by noise, while retaining true peaks.

- ii. Identify the period T of the smoothed incidence time series $\{(t_k, \bar{Z}_k)\}_{k=\ell_1}^{n-\ell_1}$ from its power spectrum, and calculate the number of embedded cycles, given by $m = \lfloor \frac{t_{n-\ell_1} - t_{\ell_1}}{T} \rfloor$.

iii. Construct the set \mathcal{I} indexing peaks in $\{(t_k, \bar{Z}_k)\}_{k=\ell_1}^{n-\ell_2}$:

$$\mathcal{I} = \{k \in \{\ell_1 + \ell_2, \dots, n - \ell_1 - \ell_2\} : \bar{Z}_k > \bar{Z}_{k \pm i} \text{ for all } i = 1, \dots, \ell_2\}. \quad (53)$$

Choose minimal ℓ_2 large enough to ensure that \mathcal{I} indexes true peaks in \bar{Z}_k , but not spurious peaks caused by noise (any that remain after smoothing).

iv. Define $\mathcal{T} = \{t_k : k \in \mathcal{I}\}$, the set of times of peaks in \bar{Z}_k , and record the time of the first peak, given by $t_a = \min(\mathcal{T})$.

v. For $i = 0, \dots, m$, define $\tau_i = t_a + iT$ and find the element of \mathcal{T} nearest τ_i , namely $\arg \min_{\tau \in \mathcal{T}} |\tau_i - \tau|$. The resulting subset $\mathcal{T}_{\text{phase}}$ should contain successive time points that are roughly one period apart, *i.e.*, the corresponding peaks in \bar{Z}_k should occur at the same phase of the cycle.

vi. Record the time of the last such peak, given by $t_b = \max(\mathcal{T}_{\text{phase}})$.

Box 6. Peak-to-peak iteration: Iteration step

Goal: We want to produce an accurate estimate of the initial number of susceptibles $S_0 = S(t_0)$, given

- a roughly periodic time series $\{(t_k, Z_k)\}_{k=0}^n$ of incidence,
- a time series $\{(t_k, B_k)\}_{k=0}^n$ of births,
- a time series $\{(t_k, \mu_k)\}_{k=0}^n$ of the *per capita* natural mortality rate,
- times t_a and t_b as defined in the truncation step (Box 5), and
- an initial estimate of S_0 .

Algorithm:

- i. Define an initial estimate of $S(t_a)$. (We use the initial estimate of S_0 .)
- ii. Reconstruct $S(t)$ between times t_a and t_b using Eq (26b), starting with the current estimate of $S(t_a)$.
- iii. Update the estimate of $S(t_a)$ with the estimate of $S(t_b)$ obtained in (ii).
- iv. Repeat (ii) and (iii) until the sequence of estimates of $S(t_a)$ converges (to within a desirable tolerance).
- v. Reconstruct $S(t)$ between times t_0 and t_a using Eq (51), starting with the final estimate of $S(t_a)$ obtained in (iv). The reconstruction is performed backwards in time, from t_a to t_0 .
- vi. Record the estimate of $S_0 = S(t_0)$ computed in (v). This value can be passed back to Eq (26b), allowing for reconstruction of $S(t)$ between times t_0 and t_m as usual.

3 Results

In §3.1, we compare the performance of the FC, S, and SI methods in estimating $\beta(t)$ from an idealized reported incidence time series. In §3.2, we show how process and observation error create spurious noise in estimates of $\beta(t)$. In §§3.3 and 3.4, we examine averaging and smoothing as ways to distill temporal patterns of interest from noisy estimates of $\beta(t)$. In §§3.5 and 3.6, we summarize our systematic analysis of the sensitivity of $\beta(t)$ estimation error to data-generating parameters and to mis-specification of input parameters by the user. In §3.7, addressing apparent sensitivity to mis-specification of the initial number of susceptibles S_0 , we assess the performance of PTPI as a method of estimating S_0 . Finally, in §3.8, we report the run times of the S and SI methods and PTPI.

The results reported here are entirely reproducible using the annotated R code available in [S1 File](#).

3.1 Example of $\beta(t)$ estimation using the FC, S, and SI methods

We applied the FC, S, and SI methods without input error to estimate $S(t)$ and $\beta(t)$ from an idealized reported incidence time series, simulated without process or observation error. The time series estimates S_k and β_k are shown in [Fig 1](#). The S and SI methods estimated $S(t)$ and $\beta(t)$ accurately at every time point, whereas the FC method captured seasonality but failed otherwise. In the FC method, S_k neglects natural mortality ([Eq \(24b\)](#)), so it increases without bound while β_k decays to zero due to division by S_k ([Eq \(24d\)](#)).

[Fig 1A](#) confirms that the absolute error in the FC method estimate of $S(t)$ increases linearly as $\mu_c \langle S \rangle t$, where μ_c is the constant *per capita* natural mortality rate and $\langle S \rangle$ is the continuous-time average of $S(t)$. In practice, the FC method fails whenever natural mortality in the underlying population is non-negligible. Since the S and SI methods address this limitation at effectively no computational cost, we do not present further analysis of the FC method.

In [Fig 1B](#), the SI method estimate of $\beta(t)$ was very accurate (RRMSE $\approx 0.2\%$), whereas the S method estimate peaked too early and too high (RRMSE $\approx 2.4\%$).

3.2 Effects of process and observation error

We applied the S and SI methods without input error to four reported incidence time series C_k , simulated using the same parameter values but with different levels of process and observation noise. The first simulation was purely deterministic, while the remaining three included (i) environmental stochasticity [ES], (ii) ES and demographic stochasticity [ES+DS], or (iii) ES, DS, and observation error [ES+DS+OE]. [Fig 2](#) shows the resulting estimates Z_k , I_k , and β_k of true incidence $Z(t)$, prevalence $I(t)$, and the seasonally forced transmission rate $\beta(t)$.

Noise of any type introduces random fluctuations in C_k on top of longer-term (e.g., seasonal) variation. Noise in C_k is propagated to Z_k ([Fig 2A](#)) and I_k ([Fig 2B](#)), because (i) in both the S and SI methods, we scale C_{k+r} by a constant factor of $p_{\text{rep}}^{-1} \geq 1$ to compute Z_k (Eqs (25a) and (26a)); (ii) in the S method, we scale $C_{k+1-g+r}$ by a constant factor of $[p_{\text{rep}}(\gamma + \mu_k)\Delta t]^{-1}$ to compute I_k ([Eq \(25c\)](#) after substitution of [Eq \(25a\)](#)); and (iii) in the SI method, I_k contains a weighted sum of C_i terms ([Eq \(38b\)](#)).

Noise in Z_k and I_k is amplified in β_k ([Fig 2C](#)), distorting the correct temporal pattern, for the following reason. When Z and I are close to zero, small absolute changes in either yield large relative changes in the ratio Z/I and in turn β_k , which contains a factor of Z_{k+1}/I_k in the S method ([Eq \(25d\)](#)) and $(Z_k + Z_{k+1})/(2I_k)$ in the SI method ([Eq \(26d\)](#)). Hence low amplitude

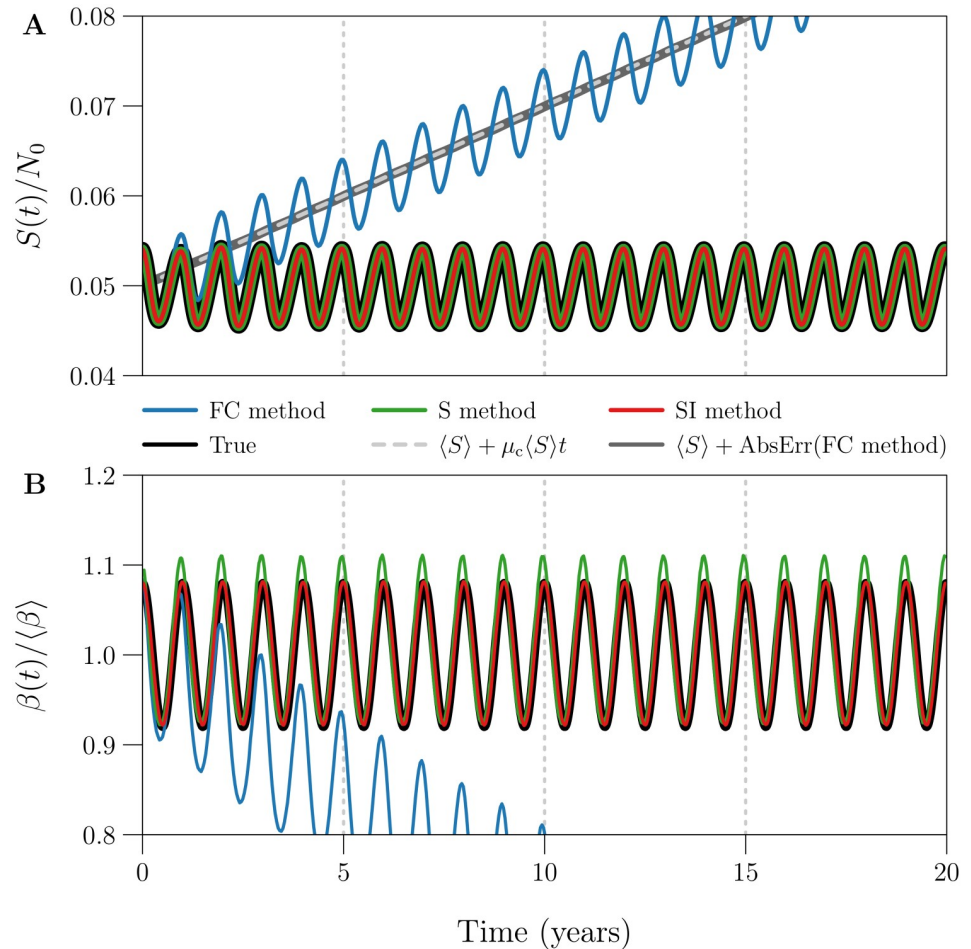


Fig 1. Example of $S(t)$ and $\beta(t)$ estimation using the FC, S, and SI methods. Plotted are the susceptible population size $S(t)$ and seasonally forced transmission rate $\beta(t)$ (Eq (27)) underlying 20 years of weekly reported incidence, together with time series estimates S_k and β_k obtained from the data by the FC [blue], S [green], and SI [red] methods. The reported incidence time series ($\Delta t = 1$ week, $n = \lfloor 20 \times 365/7 \rfloor = 1042$) was simulated without process or observation error ($\epsilon = 0, p_{rep} = 1$), using reference values (Table 1) for all other data-generating parameters. The three estimation methods were applied without input error, *i.e.*, all input parameters were assigned their true (data-generating) values. **[Panel A]** $S(t)$ scaled by $1/N_0$, describing the number of susceptibles as a proportion of the initial population size. Grey lines show that the absolute error in the FC method estimate of $S(t)$ increases linearly as $\mu_c \langle S \rangle t$, where μ_c is the constant *per capita* natural mortality rate and $\langle S \rangle$ is the continuous-time average of $S(t)$. **[Panel B]** $\beta(t)$ scaled by $1/\langle \beta \rangle$, describing the transmission rate relative to its mean. RRMSE (Eq (33)) in the β_k time series generated by the (FC, S, SI) method is roughly (0.3355, 0.0240, 0.0021).

<https://doi.org/10.1371/journal.pcbi.1008124.g001>

noise in Z_k and I_k appears as spurious, higher amplitude noise in β_k . This is an important issue in practice, because the incidence of endemic diseases is typically very small relative to the population size, and periodic fluctuations bringing incidence even closer to zero are common for many diseases [4, 14, 42].

Fig 2 shows that the SI method is much better than the S method at resisting noise propagation. One reason is the effective smoothing of incidence in the SI method, which replaces Z_{k+1} with $(Z_k + Z_{k+1})/2$ in the computation of β_k (compare Eqs (25d) and (26d)). We expose a second reason in §3.2.1 below by comparing the variance in I_k induced by observation error, between the two methods. (We expect similar results for process error.)

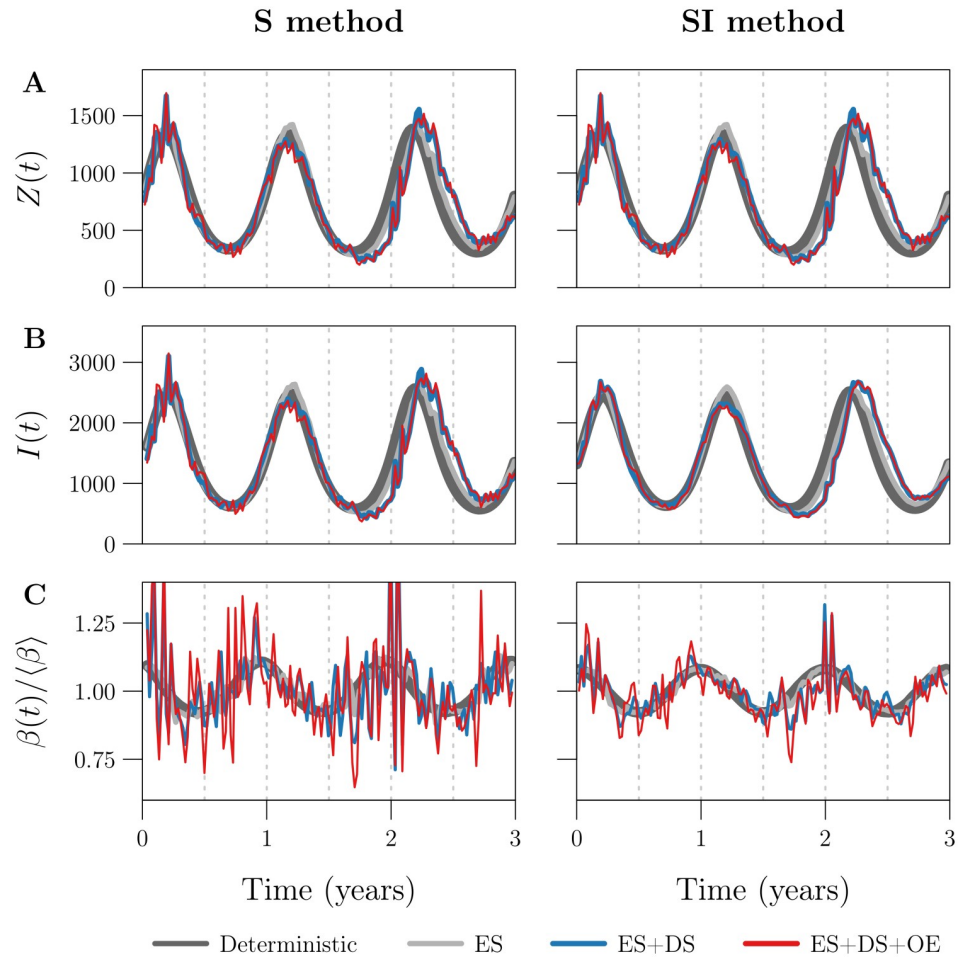


Fig 2. Effects of process and observation error on the S and SI methods. Plotted are the estimates [Row A] Z_k , [Row B] I_k , and [Row C] β_k of true incidence $Z(t)$, prevalence $I(t)$, and the seasonally forced transmission rate $\beta(t)$ (Eq (27)) obtained by applying the [Left] S and [Right] SI methods without input error to each of four simulated reported incidence time series (indicated by the legend; $\Delta t = 1$ week, $n = \lfloor 3 \times 365/7 \rfloor = 156$). The first simulation was purely deterministic [dark grey] ($\epsilon = 0, p_{\text{rep}} = 1$), while the remaining three accounted for (i) environmental stochasticity [ES, light grey] ($\epsilon = 0.5, p_{\text{rep}} = 1$), (ii) ES and demographic stochasticity [ES+DS, blue] ($\epsilon = 0.5, p_{\text{rep}} = 1$), or (iii) ES, DS, and observation error [ES+DS+OE, red] ($\epsilon = 0.5, p_{\text{rep}} = 0.25$). Reference values (Table 1) were assigned to all other data-generating parameters, in all four simulations. The left and right panels in Row A are identical, because the S and SI methods compute Z_k identically (compare Eqs (25a) and (26a)). RRMSE in the β_k time series is (0.0239, 0.0375, 0.1126, 0.1432) with the S method and (0.0021, 0.0153, 0.0494, 0.0591) with the SI method (order follows the legend). Note that the underlying $\beta(t)$ was the same in all simulations; it is not plotted in Row C, but is close to perfectly represented by the dark grey curve in the right panel (RRMSE $\approx 0.2\%$). Due to process error, the underlying $Z(t)$ and $I(t)$ (also not shown) varied between the deterministic, ES, and ES+DS simulations.

<https://doi.org/10.1371/journal.pcbi.1008124.g002>

3.2.1 Propagation of noise from C_k to I_k . Consider the S and SI method estimates of prevalence $I(t_k)$,

$$I_k^{[S]} = \frac{C_{k+1-g+r}}{p_{\text{rep}}(\gamma + \mu_c)\Delta t}, \tag{54a}$$

$$I_k^{[SI]} = I_0 \left(\frac{1 - \frac{1}{2}(\gamma + \mu_c)\Delta t}{1 + \frac{1}{2}(\gamma + \mu_c)\Delta t} \right)^k + \sum_{i=0}^{k-1} \frac{C_{i+1+r}}{p_{\text{rep}}[1 + \frac{1}{2}(\gamma + \mu_c)\Delta t]} \left(\frac{1 - \frac{1}{2}(\gamma + \mu_c)\Delta t}{1 + \frac{1}{2}(\gamma + \mu_c)\Delta t} \right)^{k-1-i}. \tag{54b}$$

Here, $g = \lceil t_{\text{gen}} \rceil \Delta t / \Delta t$ and $r = \lceil t_{\text{rep}} \rceil \Delta t / \Delta t$ are the mean generation interval and case reporting delay in units of the observation interval, rounded to the nearest integer. These estimates are obtained from Eq (25c) (after substitution of Eqs (25a) and (38b) when we assume a constant natural mortality rate μ_c). Following §2.3.3, suppose reported incidence is generated from true incidence $Z(t_k)$ via $C_{k+r} \stackrel{\text{ind.}}{\sim} \text{Binomial}(Z(t_k), p_{\text{rep}})$. Then the variance of C_{k+r} is

$$\text{Var}(C_{k+r}) = Z(t_k)p_{\text{rep}}(1 - p_{\text{rep}}). \tag{55}$$

It follows from Eqs (54) and (55) and the identity $\text{Var}(aX) = a^2 \text{Var}(X)$ that

$$\text{Var}(I_k^{[S]}) = \frac{(1 - p_{\text{rep}})Z(t_{k+1-g})}{p_{\text{rep}}[(\gamma + \mu_c)\Delta t]^2}, \tag{56a}$$

$$\text{Var}(I_k^{[SI]}) = \sum_{i=0}^{k-1} \frac{(1 - p_{\text{rep}})Z(t_{i+1})}{p_{\text{rep}}[1 + \frac{1}{2}(\gamma + \mu_c)\Delta t]^2} \left(\frac{1 - \frac{1}{2}(\gamma + \mu_c)\Delta t}{1 + \frac{1}{2}(\gamma + \mu_c)\Delta t} \right)^{2(k-1-i)}. \tag{56b}$$

If $Z(t)$ has a well-defined average $\langle Z \rangle$, then replacing instances of Z in Eq (56) with $\langle Z \rangle$ and taking the limit as $k \rightarrow \infty$, we obtain the average variances

$$\langle \text{Var}(I_k^{[S]}) \rangle = \frac{(1 - p_{\text{rep}})\langle Z \rangle}{p_{\text{rep}}[(\gamma + \mu_c)\Delta t]^2}, \tag{57a}$$

$$\begin{aligned} \langle \text{Var}(I_k^{[SI]}) \rangle &= \lim_{k \rightarrow \infty} \left\{ \frac{(1 - p_{\text{rep}})\langle Z \rangle}{p_{\text{rep}}[1 + \frac{1}{2}(\gamma + \mu_c)\Delta t]^2} \sum_{i=0}^{k-1} \left(\frac{1 - \frac{1}{2}(\gamma + \mu_c)\Delta t}{1 + \frac{1}{2}(\gamma + \mu_c)\Delta t} \right)^{2i} \right\} \\ &= \lim_{k \rightarrow \infty} \left\{ \frac{(1 - p_{\text{rep}})\langle Z \rangle}{2p_{\text{rep}}(\gamma + \mu_c)\Delta t} \left[1 - \left(\frac{1 - \frac{1}{2}(\gamma + \mu_c)\Delta t}{1 + \frac{1}{2}(\gamma + \mu_c)\Delta t} \right)^{2k} \right] \right\} \\ &= \frac{(1 - p_{\text{rep}})\langle Z \rangle}{2p_{\text{rep}}(\gamma + \mu_c)\Delta t}. \end{aligned} \tag{57b}$$

Comparing these with $\langle \text{Var}(C_k) \rangle = \langle Z \rangle p_{\text{rep}}(1 - p_{\text{rep}})$ using reference parameter values $t_{\text{gen}} = \gamma^{-1} = 13$ days, $\mu_c = 0.04 \text{ year}^{-1}$, and $\Delta t = 1$ week, we obtain

$$\frac{\langle \text{Var}(I_k^{[S]}) \rangle}{\langle \text{Var}(C_k) \rangle} = \frac{1}{p_{\text{rep}}^2[(\gamma + \mu_c)\Delta t]^2} = \frac{1}{p_{\text{rep}}^2} \left(\frac{t_{\text{inf}}}{\Delta t} \right)^2 \approx \frac{3.44}{p_{\text{rep}}^2}, \tag{58a}$$

$$\frac{\langle \text{Var}(I_k^{[SI]}) \rangle}{\langle \text{Var}(C_k) \rangle} = \frac{1}{2p_{\text{rep}}^2[(\gamma + \mu_c)\Delta t]^2} = \frac{1}{2p_{\text{rep}}^2} \left(\frac{t_{\text{inf}}}{\Delta t} \right)^2 \approx \frac{0.93}{p_{\text{rep}}^2}, \tag{58b}$$

where $t_{\text{inf}} = (\gamma + \mu_c)^{-1}$ is the mean time spent infected. Hence, while both the S and SI methods suffer from propagation of noise from reported incidence C_k to estimated prevalence I_k , particularly for $p_{\text{rep}} \ll 1$, the S method tends to be much worse (by a factor of $3.44/0.93 \approx 3.7$ in this example). Comparative resistance to noise propagation is a distinct advantage of the SI method over the S method.

3.3 Averaging the raw estimate of $\beta(t)$

Fig 3A displays two raw estimates β_k (S and SI methods, applied without input error) of a seasonally forced $\beta(t)$, each spanning 1000 years (only the first 10 years are shown). The estimates

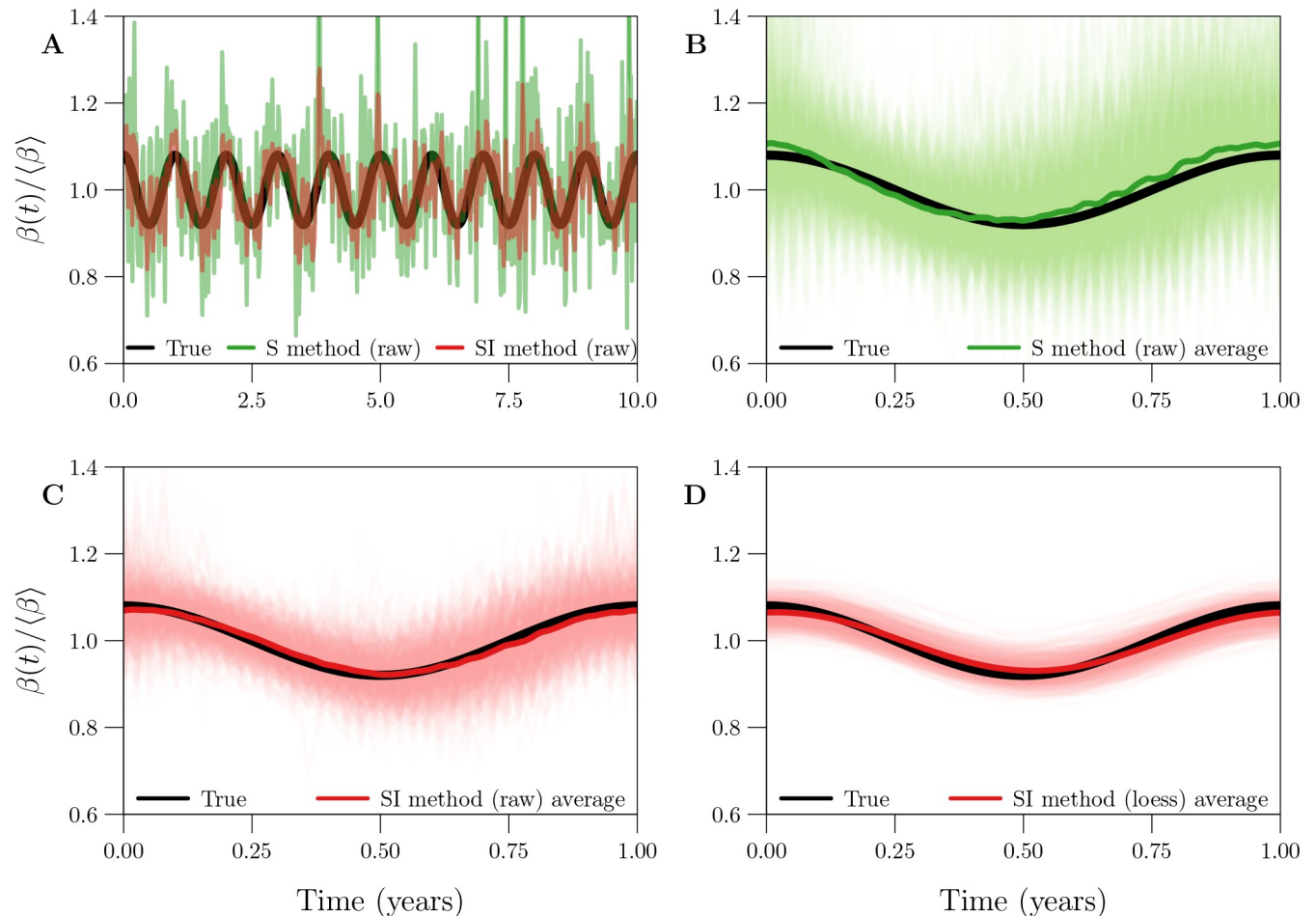


Fig 3. Bias and variance in 1-year cycles embedded in three estimates of a seasonally forced $\beta(t)$. [Panel A] In black, the seasonally forced $\beta(t)$ (Eq (27)) underlying 1000 years of simulated reported incidence data. In (transparent) colour, raw estimates β_k obtained from the data by the S [green] and SI [red] methods, both applied without input error. Only the first 10 of 1000 years are shown. [Panels B and C] In black, the true 1-year cycle in the seasonally forced $\beta(t)$. In light (transparent) colour, the 1000 1-year cycles embedded in the linear interpolant $\beta_{\text{int}}(t)$ of β_k . In dark colour, the average 1-year cycle (Eq (22a)) in $\beta_{\text{int}}(t)$. Results are shown for both the S [Panel B, green] and SI [Panel C, red] methods. [Panel D] Like Panel C, except for a smooth loess curve $\beta_{\text{loess}}(t; q)$ ($q = 53$) fit to β_k , instead of the interpolant $\beta_{\text{int}}(t)$. [Details] A reported incidence time series with 1000 years of weekly observations ($\Delta t = 1$ week, $n = 52153$) was simulated with environmental noise in transmission ($\epsilon = 0.5$), demographic stochasticity, and random under-reporting of cases ($p_{\text{rep}} = 0.25$), using reference values (Table 1) for the remaining parameters.

<https://doi.org/10.1371/journal.pcbi.1008124.g003>

embed 1000 1-year cycles, which are displayed in Fig 3B and 3C together with their 1-year average (cf. §2.2.5).

Both estimates suffered from spurious noise distorting the correct seasonal pattern, caused by process and observation error in the data-generating process (cf. §3.2). As in Fig 2C, the variance was markedly smaller with the SI method. Averaging the embedded 1-year cycles recovered the true 1-year cycle from the noise. In the absence of input error, the S method appears to carry a slight bias (peaking early and too high, as in Fig 1), whereas the SI method is nearly unbiased.

While some existing infectious disease time series span several centuries [15], in practice, averaging as in Fig 3B and 3C is sensible only over time intervals during which the underlying seasonal pattern in transmission is roughly stationary.

3.4 Smoothing the raw estimate of $\beta(t)$

Regardless of whether averaging is employed, comparison of Fig 3C and 3D shows that it is helpful to smooth the β_k time series by fitting a loess curve $\beta_{\text{loess}}(t; q)$ (cf. §2.2.6). An appropriate degree of smoothing (*i.e.*, choice of loess smoothing parameter q) eliminated spurious noise without significantly increasing bias.

Fig 4A quantifies the effect of smoothing β_k using the optimal value q_{opt} for parameter q (cf. §2.2.6). It plots RRMSE before and after smoothing as a function of the amount of noise in the simulated reported incidence data, which was modulated by varying the case reporting probability p_{rep} between 0.01 and 1 (more noise for smaller p_{rep} ; see Eq (31)).

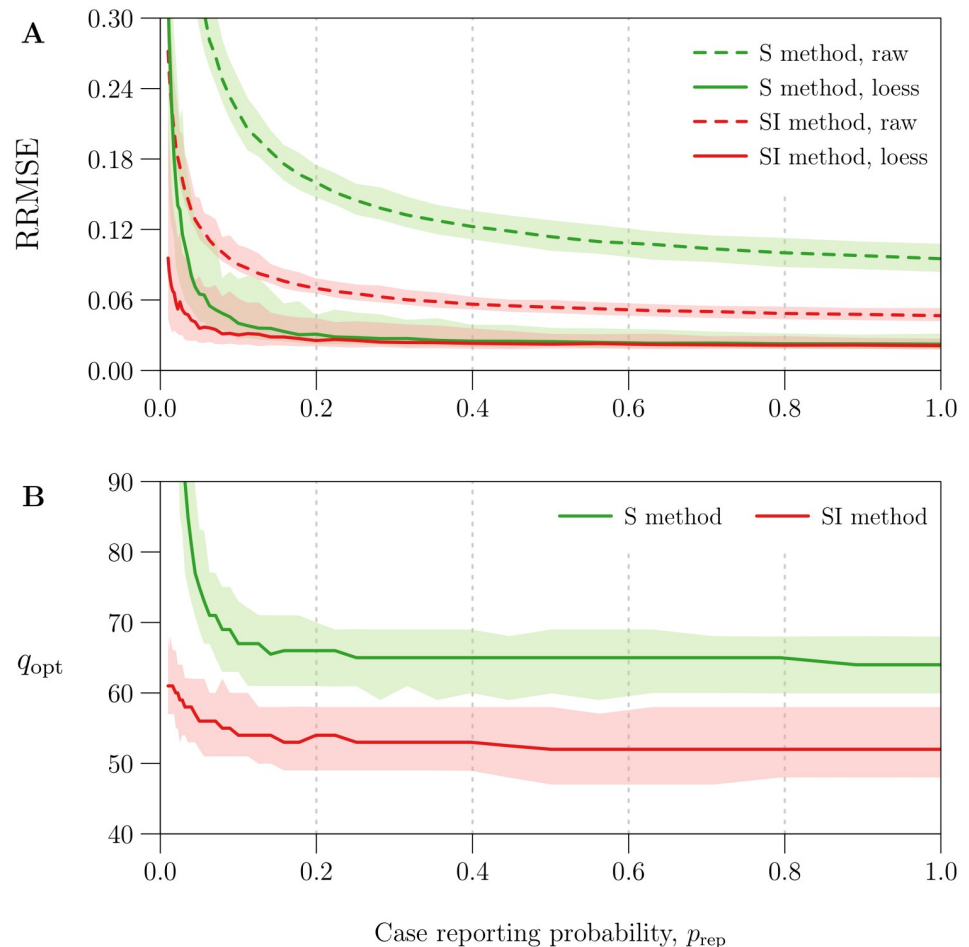


Fig 4. Reduction in $\beta(t)$ estimation error with optimal loess smoothing. The horizontal axis measures the case reporting probability p_{rep} , for which 41 values equally spaced on a logarithmic scale between 0.01 and 1 were considered. Using each value of p_{rep} and reference values (Table 1) for all other parameters, 100 reported incidence time series ($\Delta t = 1$ week, $n = 1042$) were simulated accounting for environmental noise in transmission ($\epsilon = 0.5$), demographic stochasticity, and random under-reporting of cases (measured by p_{rep}). The underlying seasonally forced $\beta(t)$ (Eq (27)) was estimated from reported incidence using the S and SI methods, both applied without input error, yielding two raw estimates β_k per simulation. Smooth loess curves $\beta_{\text{loess}}(t; q)$ ($q = 10, \dots, 110$; cf. §2.2.6) were fit to each β_k time series. The optimal q for a given time series, denoted by q_{opt} , was defined as the value that minimized RRMSE (Eq (33)) in $\beta_{\text{loess}}(t_k; q)$. Overall, for each value of p_{rep} and each $\beta(t)$ estimation method (S and SI), 100 values of q_{opt} were obtained corresponding to 100 β_k time series. Plotted on the vertical axis as functions of p_{rep} are the median and 5th and 95th percentiles of [Panel A] RRMSE in the raw estimates β_k [dashed lines] and optimal loess estimates $\beta_{\text{loess}}(t_k; q_{\text{opt}})$ [solid lines] and [Panel B] q_{opt} . Lines and bands indicate the median and 5th–95th percentile range, respectively. Results for the S and SI methods are shown in green and red, respectively.

<https://doi.org/10.1371/journal.pcbi.1008124.g004>

Using the optimal loess estimate $\beta_{\text{loess}}(t_k; q_{\text{opt}})$ instead of the raw estimate β_k significantly reduced RRMSE—by at least 46% for the S method and 17% for the SI method across all simulations. Although raw estimates generated by the SI method were consistently more accurate (expected in light of Fig 3B and 3C), optimal loess estimates were comparable between the S and SI methods for $p_{\text{rep}} > 0.2$ (RRMSE \approx 3%). For $p_{\text{rep}} < 0.2$ (severe under-reporting of cases), optimal smoothing failed to an increasing extent to recover the underlying $\beta(t)$ from noise in β_k . In this setting, the S method was greatly outperformed by the SI method, which is more resilient to noise in reported incidence (cf. §3.2).

Fig 4B shows that median q_{opt} was roughly constant for $p_{\text{rep}} > 0.1$, with

$$\text{median } q_{\text{opt}} \approx \begin{cases} 65 & \text{for the S method,} \\ 53 & \text{for the SI method.} \end{cases} \quad (59)$$

More smoothing (greater q) was required to minimize RRMSE for $p_{\text{rep}} > 0.1$. More generally, Fig 4 indicates that the S and SI methods should always include a smoothing step. Hence, in the remaining analysis, we always smooth β_k .

3.5 Sensitivity to data-generating parameters

Here, we characterize the sensitivity of $\beta(t)$ estimation error to parameters of the data-generating process. As in §§3.1–3.4, we consider the ideal case in which the user-specified values of all input parameters are equal to the true (data-generating) values. The details of our analysis are outlined in §2.6.1.

Fig 5 plots the median RRMSE in estimates of a seasonally forced $\beta(t)$ (Eq (27)) from 1000 realizations of a reported incidence time series, as a bivariate function of the mean $\langle\beta\rangle$ and amplitude α of seasonal forcing. To aid interpretation, the $\langle\beta\rangle$ axis was scaled to measure the basic reproduction number \mathcal{R}_0 (Eq (2)).

Fig 6 plots median RRMSE as a univariate function of each of 6 additional parameters—the initial states S_0 and I_0 , vital rates ν_c and μ_c , mean generation interval t_{gen} , and case reporting probability p_{rep} —with the focal parameter assigned values between $\frac{1}{4}$ and 4 times its reference value (Table 1). The horizontal axis measures the ratio of the focal parameter's data-generating value to its reference value, so that commensurate deviations from the reference case can be compared across the 6 parameters.

In order to produce Figs 5 and 6, we assigned reference values (Table 1) to all but the focal data-generating parameter(s) (e.g., all except $\langle\beta\rangle$ and α in Fig 5). We fit loess curves $\beta_{\text{loess}}(t; q)$ to all raw estimates β_k of $\beta(t)$, and recorded the RRMSE in $\beta_{\text{loess}}(t_k; q)$. Motivated by Fig 4B and Eq (59), we fixed $q = q^*$, taking $q^* = 65$ with the S method and $q^* = 53$ with the SI method.

A pattern in our interpretation of Figs 5 and 6 below is that error in $\beta(t)$ estimation is sensitive to a parameter if changes in that parameter (i) cause incidence $Z(t)$ or prevalence $I(t)$ to approach zero more frequently or more closely, or (ii) increase noise in estimated incidence Z_k or estimated prevalence I_k . Both outcomes incorrectly increase noise in β_k (cf. §3.2).

When the noise in β_k is extreme, setting $q = q^*$ can undersmooth the time series ($q^* < q_{\text{opt}}$). In this case, smaller RRMSE is attainable by determining q_{opt} and setting $q = q_{\text{opt}}$. Nevertheless, we did not find q_{opt} for each of the 5×10^6 time series considered by Figs 5 and 6, which would have increased the total computation time by a factor of 100. Consequently, Figs 5 and 6 may overestimate the sensitivity of $\beta(t)$ estimation error to data-generating parameters. (In §S5.3 of S1 Text, we show that the quantitative effect of choosing q^* over q_{opt} is likely to be small.)

3.5.1 Sensitivity to the basic reproduction number \mathcal{R}_0 and seasonal amplitude α (Fig 5). For fixed α , median RRMSE was a non-monotonic function of \mathcal{R}_0 . The reason is that

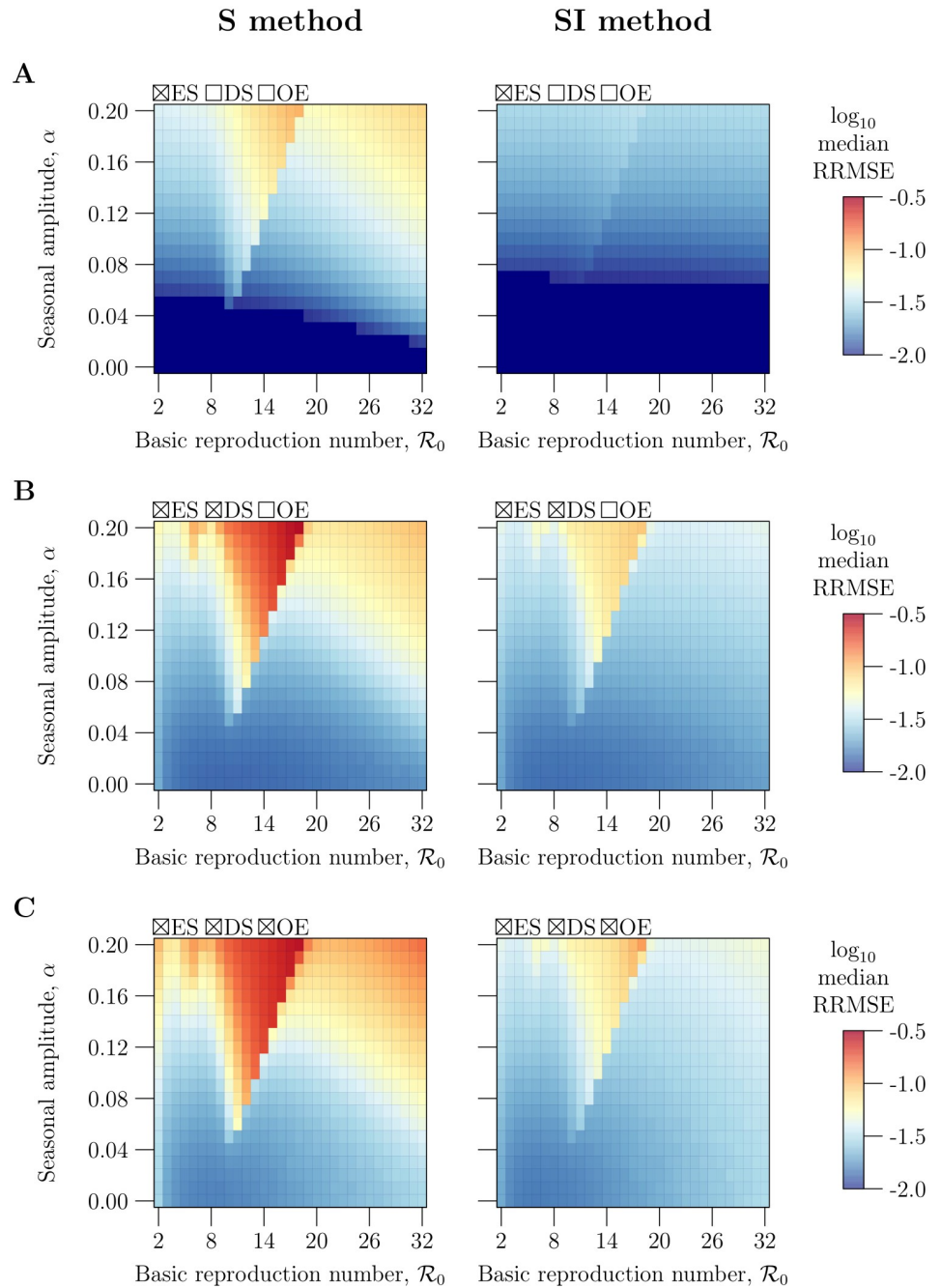


Fig 5. Sensitivity of $\beta(t)$ estimation error to the mean $\langle\beta\rangle$ and amplitude α of seasonal forcing. Contained in each panel are heatmaps of median RRMSE (Eq (33)) in estimates of a seasonally forced $\beta(t)$ (Eq (27)) from simulated reported incidence time series, as a bivariate function of the mean $\langle\beta\rangle$ and amplitude α of seasonal forcing. The $\langle\beta\rangle$ axis has been scaled to measure the basic reproduction number \mathcal{R}_0 (Eq (2)). When simulating reported incidence, reference values (Table 1) were assigned to all data-generating parameters except $\langle\beta\rangle$ and α . A grid of (\mathcal{R}_0, α) pairs with levels $\mathcal{R}_0 = 2, 3, \dots, 32$ and $\alpha = 0, 0.01, \dots, 0.2$ was considered, with $\langle\beta\rangle$ defined for each value of \mathcal{R}_0 via Eq (2). For each parametrization, 1000 simulations were performed with environmental stochasticity [ES] ($\epsilon = 0.5$) and with or without demographic stochasticity [DS] and observation error [OE], as indicated by row: [Row A] without DS or OE ($p_{\text{rep}} = 1, t_{\text{rep}} = 0$ weeks), [Row B] with DS but without OE ($p_{\text{rep}} = 1, t_{\text{rep}} = 0$ weeks), [Row C] with DS and OE ($p_{\text{rep}} = 0.25, t_{\text{rep}} = 2$ weeks). Corresponding mock birth and natural mortality time series were created, then $\beta(t)$ was estimated from the data using [Left] the S method and [Right] the SI method, all without input error. For each set of estimates of $\beta(t)$ (1000 estimates per parametrization, per simulation method, per estimation method), the median RRMSE was calculated (after smoothing with fixed q ; see Eq (59)) and displayed as one point in the appropriate heatmap, coloured according to the logarithmic scale on the right. The darkest blue indicates median RRMSE less than 0.01.

<https://doi.org/10.1371/journal.pcbi.1008124.g005>

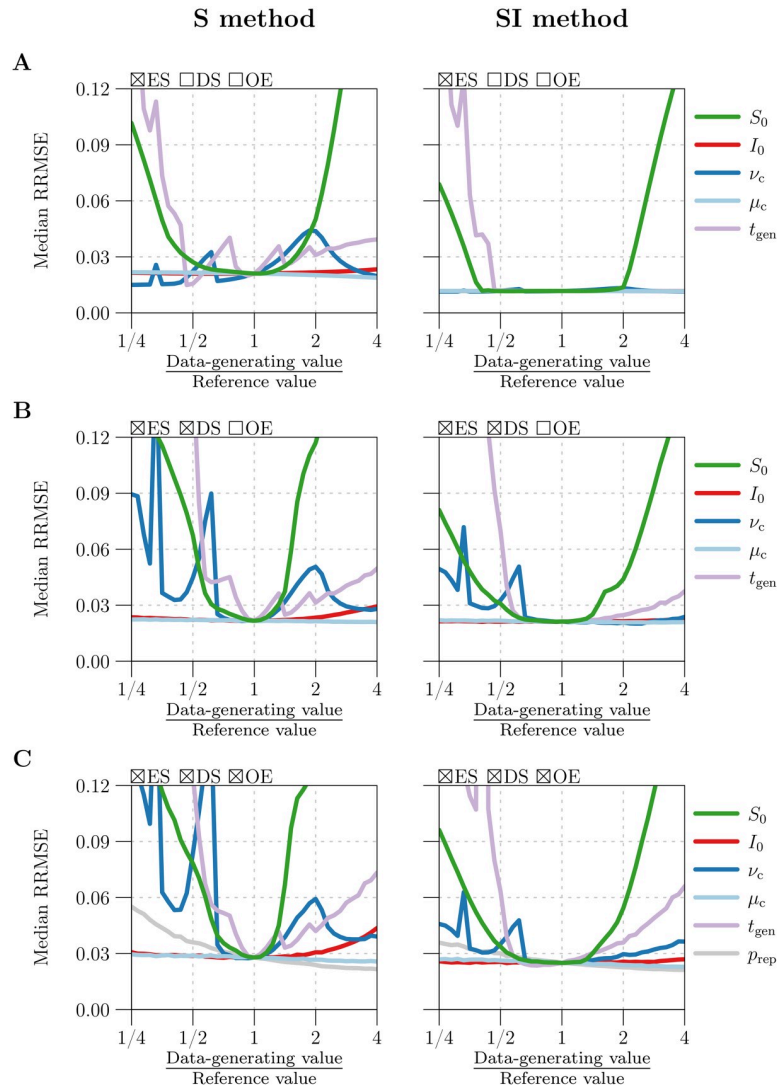


Fig 6. Sensitivity of $\beta(t)$ estimation error to data-generating parameters other than β and α . Plotted in each panel is the median RRMSE (Eq (33)) in estimates of a seasonally forced $\beta(t)$ (Eq (27)) from simulated reported incidence time series ($\Delta t = 1$ week, $n = 1042$), as a univariate function of each of 5 or 6 data-generating parameters (indicated by the legend). When simulating reported incidence, reference values (Table 1) were assigned to all but the focal parameter, which was assigned 41 values logarithmically spaced between $\frac{1}{4}$ and 4 times its reference value. The horizontal axis (logarithmic scale) measures the ratio of the focal parameter's true value to its reference value, so that commensurate deviations from the reference case can be compared across parameters. For each parametrization, 1000 simulations were performed with environmental stochasticity [ES] ($\epsilon = 0.5$) and with or without demographic stochasticity [DS] and observation error [OE], as indicated by row: **[Row A]** without DS or OE ($p_{\text{rep}} = 1$, $t_{\text{rep}} = 0$ weeks), **[Row B]** with DS but without OE ($p_{\text{rep}} = 1$, $t_{\text{rep}} = 0$ weeks), or **[Row C]** with DS and OE ($p_{\text{rep}} = 0.25$ except when p_{rep} is the focal parameter, $t_{\text{rep}} = 2$ weeks). Corresponding mock birth and natural mortality time series were created, then $\beta(t)$ was estimated from the data using **[Left]** the S method and **[Right]** the SI method, all without input error. For each set of estimates of $\beta(t)$ (1000 estimates per parametrization, per simulation method, per estimation method), the median RRMSE was calculated (after smoothing with fixed q ; see Eq (59)) and displayed as one point in the appropriate panel and graph.

changes in (effective) \mathcal{R}_0 are responsible for dynamical transitions that alter the structure of solutions of the SIR model (1) [28, 42, 43]. Specifically, as \mathcal{R}_0 is increased from 2 to 32, minimum incidence Z_{min} and minimum prevalence I_{min} on the attractor varies non-monotonically (see Fig 2 in [28]). Smaller Z_{min} and I_{min} yield more noise in β_k and correspondingly greater

RRMSE. For fixed \mathcal{R}_0 , I_{\min} decreases monotonically as α is increased from 0 to 1 (see Fig 11 in [43]), so we expect median RRMSE to increase monotonically with α , as observed in Fig 5.

3.5.2 Sensitivity to the initial state (S_0, I_0) (Fig 6). RRMSE is sensitive to the data-generating S_0 , but not I_0 . The reference values of S_0 and I_0 are taken from a point (S^*, I^*, R^*) on the attractor of the SIR model (1) with seasonally forced $\beta(t)$ and constant vital rates ν_c and μ_c (cf. §2.3.4). When S_0 is far from S^* , the solution of system (1) undergoes extreme fluctuation before relaxing to the attractor, and both Z and I approach zero during the transient, generating spurious noise at the start of the β_k time series.

Note that I_0 differing from I^* has a much smaller effect on dynamics than S_0 differing from S^* by the same factor. Since $I^* \ll S^*$, the perturbation of (S_0, I_0, R_0) from the attractor is much smaller.

3.5.3 Sensitivity to vital rates ν_c and μ_c (Fig 6). Median RRMSE was a non-monotonic function of the data-generating birth rate ν_c . This behaviour arises because scaling ν_c is dynamically equivalent to scaling \mathcal{R}_0 by the same factor [2, 28], and median RRMSE is a non-monotonic function of \mathcal{R}_0 (cf. §3.5.1 above).

Changing the data-generating natural mortality rate μ_c had a negligible effect on RRMSE. This is unsurprising, because natural death is dominated by recovery and disease-induced death in governing the rate of infected decrease. That is, $\gamma \gg \mu(t)$ in Eq (1b), so changes in μ_c by up to a factor of 4 have little effect on dynamics.

3.5.4 Sensitivity to the mean generation interval t_{gen} (Fig 6). Median RRMSE increased rapidly as the data-generating t_{gen} was made smaller than $2^{-4/5}$ (roughly 0.57) times its reference value of 13 days. A period-doubling bifurcation occurs near this value of t_{gen} , and the attractor of the SIR model (1) acquires a 2-year cycle with much smaller Z_{\min} and I_{\min} (see §5.3.1 of S1 Text). Propagation of noise to β_k intensifies, resulting in greater RRMSE.

The performance of the S method fluctuates more as a function of t_{gen} than that of the SI method. This occurs because the S method rounds t_{gen} in the numerator of Eq (25c) to the nearest integer multiple of Δt , and the rounding error oscillates as a function of t_{gen} . The SI method does not require rounding, so these fluctuations are not observed.

3.5.5 Sensitivity to the case reporting probability p_{rep} (Fig 6). When the reported incidence data contain observation error (Fig 6C), RRMSE is additionally sensitive to the case reporting probability p_{rep} . Decreasing p_{rep} increases noise in reported incidence C_k (Eq (31)), which is propagated to estimated incidence Z_k , estimated prevalence I_k , and in turn β_k (cf. §3.2).

Fig 6 suggests weak sensitivity to p_{rep} . However, noise in Z_k and I_k is amplified in β_k to the extent that Z and I are close to zero (cf. §3.2). Hence, for example, if the data-generating t_{gen} were assigned a value smaller than half its reference value of 13 days, then we would have observed more acute sensitivity to p_{rep} as a result of closer approaches to zero by Z and I (cf. §3.5.4 above).

3.5.6 S method versus SI method (Figs 5 and 6). Both the S and SI methods performed well, estimating $\beta(t)$ with median RRMSE less than 10% across most parametrizations. However, by resisting noise propagation (cf. §3.2), the SI method was significantly less sensitive to the data-generating parameters and to the addition of demographic stochasticity and observation error.

3.6 Sensitivity to mis-specification of input parameters

In §3.5, we considered the ideal situation in which the user knows the true (data-generating) values of the input parameters. Here, we examine the more realistic situation in which the

user specifies input parameters with some error. The effect of mis-specification is particularly important for parameters that are difficult to estimate accurately, such as the case reporting probability p_{rep} . The details of our analysis are outlined in §2.6.2.

We restrict our attention to application of the SI method to reported incidence data simulated with process and observation error. Differences in RRMSE between methods of data simulation and $\beta(t)$ estimation are dominated (by an order of magnitude) by the increase in RRMSE resulting from mis-specified input parameters.

Fig 7A plots the median RRMSE in estimates of $\beta(t)$ from 1000 realizations of a reported incidence time series, as a univariate function of the factor by which an input parameter—one of the initial states S_0 and I_0 , mean generation interval t_{gen} , vital rates ν_c and μ_c , and case reporting parameters p_{rep} and t_{rep} —was mis-specified. The specified value of the focal parameter was varied between $\frac{1}{4}$ and 4 times its true (data-generating) value, and the remaining parameters were specified without error.

3.6.1 Sensitivity to error in the specified initial state (S_0, I_0). Fig 7 shows that error in the specified value of S_0 is propagated non-negligibly to estimates of $\beta(t)$, while mis-specification of I_0 has practically no effect on $\beta(t)$ estimation error. Eqs (40) and (41) show that specifying incorrect values S'_0 and I'_0 for S_0 and I_0 creates errors in S_k and I_k that vanish geometrically as $k \rightarrow \infty$. However, since $t_{\text{life}} \gg t_{\text{inf}}$, the decay is significantly slower in S_k . Indeed, with reference values $\mu_c = 0.04 \text{ year}^{-1}$, $t_{\text{gen}} = \gamma^{-1} = 13 \text{ days}$, and $\Delta t = 1 \text{ week}$, we find that a factor of 10 reduction in error between times t_k and t_{k+i} requires just $i = 5$ in the infected time series, compared to $i = 3002$ in the susceptible time series (roughly 58 years with $\Delta t = 1 \text{ week}$). Hence, in practice, accurate reconstruction of $S(t)$, $I(t)$, and in turn $\beta(t)$ relies on accurate specification of S_0 , but not I_0 . We address sensitivity to mis-specification of S_0 in §3.7 below.

3.6.2 Sensitivity to error in the specified birth rate ν_c and case reporting probability p'_{rep} Mis-specifying ν_c or p_{rep} by a factor of $2^{1/10}$ (7.2%) yielded median RRMSE greater than 30%. Mis-specifying by a factor of $2^{-1/10}$ (−6.7%) led to even worse estimates of $\beta(t)$, with median

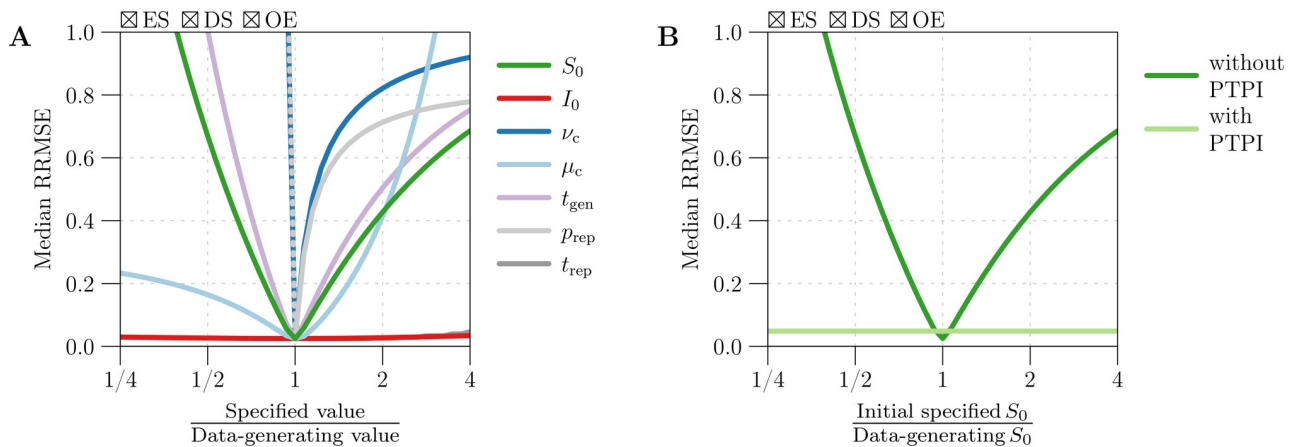


Fig 7. Sensitivity of $\beta(t)$ estimation error to the user-specified values of input parameters. [Panel A] Median RRMSE (Eq (33)) in estimates of $\beta(t)$ from simulated reported incidence time series ($\Delta t = 1 \text{ week}$, $n = 1042$), as a univariate function of the factor by which an input parameter was mis-specified. One thousand simulations were performed using fixed values (Table 1) for all data-generating parameters. The simulations accounted for environmental stochasticity [ES] ($\epsilon = 0.5$), demographic stochasticity [DS], and observation error [OE] ($p_{\text{rep}} = 0.25$, $t_{\text{rep}} = 2 \text{ weeks}$). For each simulation, corresponding mock birth and natural mortality time series were created, and $\beta(t)$ was estimated from the data using the SI method. True (data-generating) values were specified for all input parameters except the focal parameter (indicated by the legend), for which 41 values logarithmically spaced between $\frac{1}{4}$ and 4 times the true value were specified in turn. Each input parametrization yielded 1000 estimates of $\beta(t)$, whose median RRMSE was calculated (after smoothing with fixed q ; see Eq (59)) and displayed as one point in the appropriate graph. [Panel B] Result of repeating the analysis from Panel A in which S_0 was specified with varying amounts of error, but with the initially erroneous value of S_0 updated using the method of peak-to-peak iteration (PTPI; 25 iterations) prior to $\beta(t)$ estimation. The original result, obtained without PTPI, is presented for comparison.

<https://doi.org/10.1371/journal.pcbi.1008124.g007>

RRMSE exceeding 100% (not visible in Fig 7A). Eqs (42) and (47) show that specifying incorrect values v'_c and p'_{rep} for v_c and p_{rep} generates absolute errors in S_k that tend to increase over time (k) to a limit. In practice, systematic underestimation of births by the B_k time series (modeled here by $v'_c < v_c$) and overestimation of incidence by the Z_k time series ($p'_{\text{rep}} < p_{\text{rep}}$) can cause S_k to eventually take negative values. Once this happens, attempts by the S and SI methods to reconstruct $\beta(t)$ fail completely.

While this failure may seem concerning, it should be viewed as a tool for diagnosing incorrect birth and case reporting rates: if the S or SI method yields negative S_k for any k , then one should speculate that births were underestimated or that incidence was overestimated, and retry the algorithm with a scaled up B_k time series and/or with greater p_{rep} (as Z_k is computed by scaling reported incidence by a factor of p_{rep}^{-1} ; see Eqs (25a) and (26a)). Of course, overcorrection is also undesirable (*cf.* right half of Fig 7A). In our work, we have found that a brief exploration of possible adjustments—factors by which to increase B_k and/or p_{rep} —suffices to identify ones that prevent both negative S_k and pronounced transient dynamics at the start of the susceptible time series (indicating under- or overcorrection).

3.7 Solution of the S_0 estimation problem using PTPI

In §3.6, we showed that the performance of the S and SI methods is highly sensitive to misspecification of the initial number of susceptibles S_0 . Here, we assess PTPI as a way to iteratively improve initially poor estimates of S_0 prior to reconstruction of $S(t)$ and $\beta(t)$.

Fig 8 demonstrates PTPI for an example in which S_0 was overestimated by a factor of 4 by a user of the SI method. PTPI yielded increasingly accurate estimates of S_0 and correspondingly more accurate reconstructions of $S(t)$ (Fig 8B) and $\beta(t)$ (Fig 8C). Fig 7B repeats our analysis from §3.6, except using PTPI (25 iterations) to update the incorrect estimate of S_0 prior to reconstructing $\beta(t)$. We see that application of PTPI in conjunction with the SI method enables accurate $\beta(t)$ reconstruction independently of errors in the initial estimate of S_0 . This result is unsurprising in light of Fig 9, which shows that PTPI converges rapidly (in fewer than 10 iterations) to an accurate estimate of S_0 independently of the initial guess. Due to process error in the underlying dynamics, the relative error in the limiting estimate of S_0 varied between the 1000 realizations of reported incidence considered (5th–95th percentile range [−11.9, 12.5]%, median 0.9%). Process error creates variance in the time between peaks in incidence (see Fig 8A), violating the periodicity assumption of PTPI (the theoretical basis of the technique; *cf.* §2.8). Nevertheless, Figs 7–9 demonstrate that PTPI can significantly improve $S(t)$ and $\beta(t)$ reconstruction from roughly periodic incidence data.

3.8 Run time

We implemented the S and SI methods and PTPI in R and ran them on a MacBook Pro with a 2.4 GHz Quad-Core Intel Core i5 chip. The S and SI methods are both extremely fast, requiring a total of 0.124 and 0.376 seconds, respectively, to generate a reconstruction of $\beta(t)$ from 1000 years of weekly reported incidence ($\Delta t = 1$ week, $n = 52142$). Application of PTPI in conjunction with either method increases the run time with each iteration, but the total run time remains inconsequential due to the rate of convergence of the iterations to a limiting estimate of S_0 . For example, when we applied PTPI to the same simulated data, the truncation step (Box 5) added 0.094 seconds to the total run time, while the iteration step (Box 5) added 1.01 seconds per iteration on average.

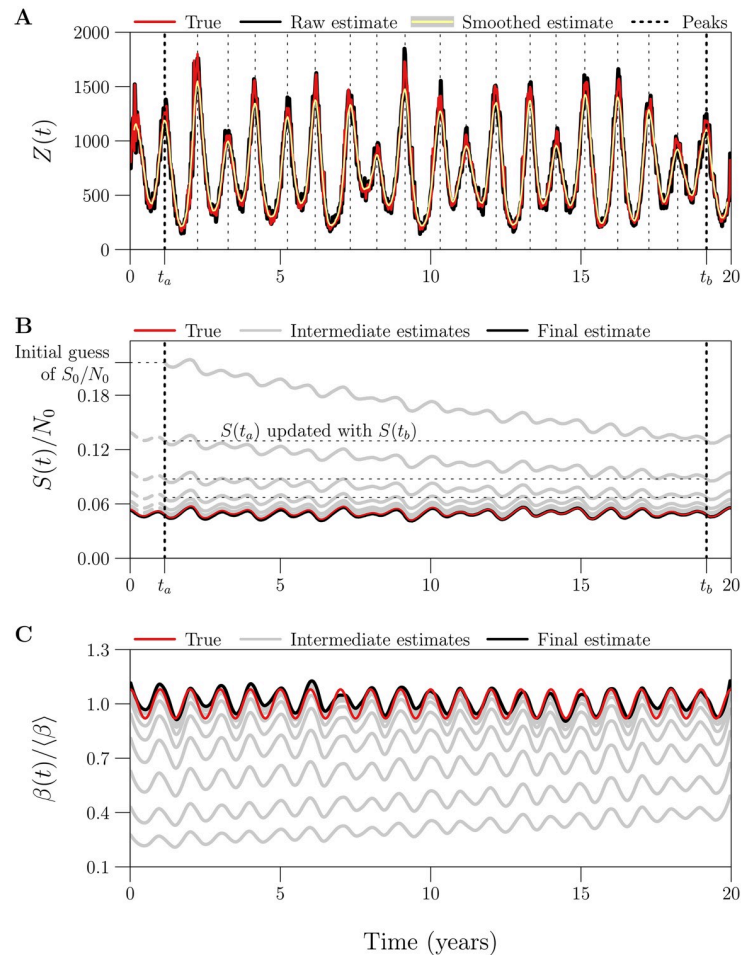


Fig 8. Example of $S(t)$ and $\beta(t)$ reconstruction with an overestimate of S_0 corrected by peak-to-peak iteration (PTPI). [Panel A] Truncation step of PTPI (Box 5). Plotted is a reconstruction of true incidence $Z(t)$ from a simulated reported incidence time series, before [Z_k , black] and after [\bar{Z}_k , yellow] smoothing with a 13-point central moving average. Vertical lines indicate peaks in \bar{Z}_k . The times of the first peak in \bar{Z}_k and the last peak occurring at the same phase of the cycle (in this case, the last peak) are denoted by t_a and t_b . [Panel B] Iteration step of PTPI (Box 6), where the initial estimates of both $S_0 = S(0)$ and $S(t_a)$ were taken to be 4 times the true (data-generating) value of S_0 . Plotted in grey are successive reconstructions of $S(t)$ between times t_a and t_b , generated by updating the estimate of $S(t_a)$ with the estimate of $S(t_b)$ obtained in the previous iteration. Dashed continuations to the left of t_a display estimation of S_0 backwards in time from estimates of $S(t_a)$. Plotted in black is the result of reconstructing $S(t)$ starting from the final estimate of S_0 , which was obtained after 25 iterations and had a relative error of roughly 1.4% (compared to 300% in the initial estimate). [Panel C] The sequence of reconstructions of $\beta(t)$ corresponding to the estimates of S_0 shown in Panel B. [Details] Twenty years of weekly reported incidence ($\Delta t = 1$ week, $n = 1042$) were simulated with environmental noise in transmission ($\epsilon = 0.5$), demographic stochasticity, and random under-reporting of cases ($p_{\text{rep}} = 0.25$), using reference values (Table 1) for the remaining parameters. $Z(t)$, $S(t)$ and $\beta(t)$ were reconstructed from reported incidence using the SI method without input error (apart from mis-specification of S_0).

<https://doi.org/10.1371/journal.pcbi.1008124.g008>

4 Discussion

We have compared three fast methods of estimating the time-varying transmission rate $\beta(t)$ from reported incidence time series, all based on discretizations of the SIR model (1). Fine and Clarkson's method [6], referred to here as the FC method, fails rapidly in practice, because it treats natural mortality in the susceptible population as negligible. Although Krylova's method [24], adapted here as the S method, corrects this limitation of the FC method and is accurate

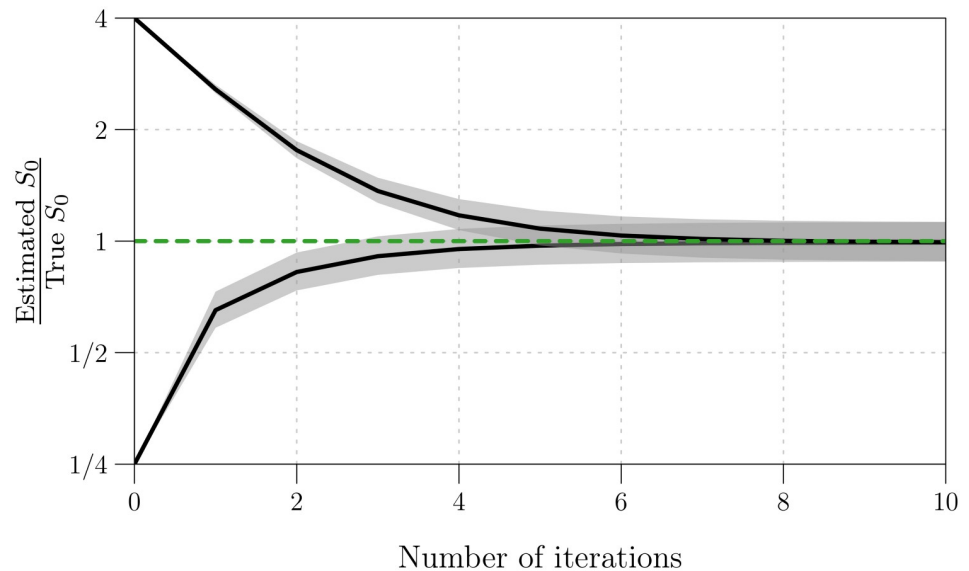


Fig 9. Convergence of estimates of S_0 obtained using peak-to-peak iteration (PTPI). S_0 was estimated by applying PTPI (25 iterations) to 1000 incidence time series (*i.e.*, 1000 realizations of a reported incidence time series, scaled by p_{rep}^{-1}). An initial guess for S_0 was taken to be $\frac{1}{4}$ or 4 times the true (data-generating) value. For each initial guess, this process generated 1000 sequences of 26 estimates of S_0 . Plotted are the median [black lines] and 5th–95th percentile range [grey bands] of the estimate of S_0 at each iteration, for the first 10 iterations. The vertical axis measures (on a logarithmic scale) the ratio of the estimated and true values of S_0 , hence convergence close to 1 [dashed green line] represents convergence of the estimates close to the true value. [Details] One thousand reported incidence time series ($\Delta t = 1$ week, $n = 1042$) were simulated with environmental noise in transmission ($\epsilon = 0.5$), demographic stochasticity, and random under-reporting of cases ($p_{\text{rep}} = 0.25$), using reference values (Table 1) for the remaining parameters, including S_0 (hence S_0 was the same in all simulations). True incidence was estimated from reported incidence via Eq (26a) (with reporting parameters p_{rep} and t_{rep} correctly specified), yielding 1000 time series of estimated incidence. Corresponding mock (constant) birth and natural mortality time series were created (with vital rates ν_c and μ_c correctly specified), and these data (estimated incidence, births, natural mortality) were passed to the PTPI algorithm, allowing for iterative re-estimation of S_0 .

<https://doi.org/10.1371/journal.pcbi.1008124.g009>

for certain simulated data, her method suffers from extreme sensitivity to process and observation error. Specifically, noise in reported incidence is spuriously propagated to its estimates of $\beta(t)$. Our algorithm for transmission rate estimation, referred to here as the SI method and based on deJonge’s method [25], is much more resilient to noise in reported incidence and therefore superior to the S method.

Like its predecessors, the SI method is sensitive to (i) certain input parameters: the initial number of susceptible individuals S_0 , the case reporting probability p_{rep} , and the mean generation interval t_{gen} ; as well as (ii) vital data: times series of births and natural mortality without substantial systematic errors.

The requirement of a good estimate of S_0 has been a major barrier to use of existing fast methods of $\beta(t)$ estimation (including those presented in [6, 24, 25]). We have proposed and demonstrated PTPI as a valid and fast technique for obtaining accurate estimates of S_0 from poor initial guesses, conditional on periodic dynamics (epidemic recurrence with a fixed period). Use of the SI method in conjunction with PTPI represents a major advance over the existing fast methods.

Estimation of the case reporting probability p_{rep} is possible using maximum likelihood approaches, including trajectory matching. However, a fast way to obtain a crude estimate of p_{rep} is to divide cumulative reported incidence over the time interval $[t_0, t_n]$, by the cumulative

incidence that is expected from the unforced SIR model (system (1) with $\beta \equiv \langle \beta \rangle$, $\nu \equiv \nu_c$, and $\mu \equiv \mu_c$) at equilibrium:

$$p_{\text{rep}} \approx \frac{\sum_{k=1}^n C_k}{\nu_c \tilde{N}_0 (1 - \frac{1}{R_0})(t_n - t_0)}. \quad (60)$$

This approximation can be made in temporal subintervals to obtain a time-varying reporting rate, which would replace the constant p_{rep} in Eq (26a). Sensitivity of the SI method to misspecification of the mean generation interval (t_{gen}) may be of greater concern, though if the distribution of the incubation period (time from infection to onset of symptoms) is narrow, then t_{gen} will be well approximated by the (observable) mean serial interval [44].

Overall, the SI method, in conjunction with PTPI, represents a highly tractable approach to reconstructing susceptibles and $\beta(t)$ from infectious disease time series that span decades or centuries. It makes fewer assumptions about the disease and population of interest than the regression-based tSIR method [7, 23] (*i.e.*, it does not require an infectious period equal to the observation interval, ignore susceptible mortality, or assume that cumulative incidence approximates cumulative births). Moreover, it is significantly less complex and much less computationally demanding than simulation-based methods of inference, such as iterated filtering [8, 19, 20] and generalized profiling [21, 22].

Even when the observed infectious disease time series is short enough that simulation-based methods are tractable, the approach to transmission rate reconstruction that we promote here can be usefully employed to provide better starting conditions at negligible computational cost.

Supporting information

S1 Text. Text supplement. A .pdf document containing annotated R code, making the results reported here completely reproducible by the reader.
(PDF)

S1 File. Source files. A .zip archive containing all of the source files needed to compile S1 Text.
(ZIP)

Acknowledgments

We thank Ben Bolker, Jonathan Dushoff, and Sang Woo Park for helpful comments and discussion.

Author Contributions

Conceptualization: Mikael Jagan, Michelle S. deJonge, Olga Krylova, David J. D. Earn.

Formal analysis: Mikael Jagan, Michelle S. deJonge, David J. D. Earn.

Funding acquisition: Mikael Jagan, Olga Krylova, David J. D. Earn.

Investigation: Mikael Jagan, Michelle S. deJonge, David J. D. Earn.

Methodology: Mikael Jagan, Michelle S. deJonge, Olga Krylova, David J. D. Earn.

Project administration: Mikael Jagan, Michelle S. deJonge, David J. D. Earn.

Resources: David J. D. Earn.

Software: Mikael Jagan.

Supervision: David J. D. Earn.

Validation: Mikael Jagan.

Visualization: Mikael Jagan.

Writing – original draft: Mikael Jagan, Michelle S. deJonge.

Writing – review & editing: Mikael Jagan, David J. D. Earn.

References

1. Dietz K. The incidence of infectious diseases under the influence of seasonal fluctuations. In: *Mathematical Models in Medicine*. vol. 11 of *Lecture Notes in Biomathematics*. Springer-Verlag Berlin / Hiedelberg; 1976. p. 1–15.
2. Earn DJD, Rohani P, Bolker BM, Grenfell BT. A simple model for complex dynamical transitions in epidemics. *Science*. 2000; 287(5453):667–670. <https://doi.org/10.1126/science.287.5453.667> PMID: 10650003
3. Shaman J, Kohn M. Absolute humidity modulates influenza survival, transmission, and seasonality. *Proceedings of the National Academy of Sciences*. 2009; 106(9):3243–3248. <https://doi.org/10.1073/pnas.0806852106>
4. London W, Yorke JA. Recurrent outbreaks of measles, chickenpox and mumps. I. Seasonal variation in contact rates. *American Journal of Epidemiology*. 1973; 98(6):453–468. <https://doi.org/10.1093/oxfordjournals.aje.a121575> PMID: 4767622
5. Hethcote HW. The mathematics of infectious diseases. *SIAM Review*. 2000; 42(4):599–653. <https://doi.org/10.1137/S0036144500371907>
6. Fine PEM, Clarkson JA. Measles in England and Wales—I: an analysis of factors underlying seasonal patterns. *International Journal of Epidemiology*. 1982; 11(1):5–14. <https://doi.org/10.1093/ije/11.1.5> PMID: 7085179
7. Finkenstädt B, Grenfell B. Time series modelling of childhood diseases: a dynamical systems approach. *Journal of the Royal Statistical Society C (Applied Statistics)*. 2000; 49(2):187–205. <https://doi.org/10.1111/1467-9876.00187>
8. He D, Ionides EL, King AA. Plug-and-play inference for disease dynamics: measles in large and small populations as a case study. *Journal of the Royal Society Interface*. 2010; 7:271–283. <https://doi.org/10.1098/rsif.2009.0151>
9. Hempel K, Earn DJD. A century of transitions in New York City's measles dynamics. *Journal of the Royal Society Interface*. 2015; 12(106):20150024. <https://doi.org/10.1098/rsif.2015.0024>
10. Pollicott M, Wang H, Weiss H. Extracting the time-dependent transmission rate from infection data via solution of an inverse ODE problem. *Journal of Biological Dynamics*. 2012; 6(2):509–523. <https://doi.org/10.1080/17513758.2011.645510> PMID: 22873603
11. Lange A. Reconstruction of disease transmission rates: applications to measles, dengue, and influenza. *Journal of Theoretical Biology*. 2016; 400:138–153. <https://doi.org/10.1016/j.jtbi.2016.04.017> PMID: 27105674
12. Wallinga J, Teunis P. Different epidemic curves for severe acute respiratory syndrome reveal similar impacts of control measures. *American Journal of Epidemiology*. 2004; 160:509–516. <https://doi.org/10.1093/aje/kwh255> PMID: 15353409
13. Smirnova A, deCamp L, Chowell G. Forecasting epidemics through nonparametric estimation of time-dependent transmission rates using the SEIR model. *Bulletin of Mathematical Biology*. 2019; 81:4343–4365. <https://doi.org/10.1007/s11538-017-0284-3> PMID: 28466232
14. Tien JH, Poinar HN, Fisman DN, Earn DJD. Herald waves of cholera in nineteenth century London. *Journal of the Royal Society Interface*. 2011; 8(58):756–760. <https://doi.org/10.1098/rsif.2010.0494>
15. Krylova O, Earn DJD. Patterns of smallpox mortality in London, England, over three centuries. *PLoS Biology*. 2020 <https://doi.org/10.1371/journal.pbio.3000506>
16. Anderson RM, May RM. *Infectious Diseases of Humans: Dynamics and Control*. Oxford, UK: Oxford University Press; 1991.

17. Morton A, Finkenstädt B. Discrete time modelling of disease incidence time series by using Markov chain Monte Carlo methods. *Journal of the Royal Statistical Society C (Applied Statistics)*. 2005; 54(3):575–594. <https://doi.org/10.1111/j.1467-9876.2005.05366.x>
18. Cauchemez S, Ferguson NM. Likelihood-based estimation of continuous-time epidemic models from time series data: application to measles transmission in London. *Journal of the Royal Society Interface*. 2008; 5(25):885–897. <https://doi.org/10.1098/rsif.2007.1292>
19. Ionides EL, Breto C, King AA. Inference for nonlinear dynamical systems. *Proceedings of the National Academy of Sciences*. 2006; 103(49):18438–18443. <https://doi.org/10.1073/pnas.0603181103>
20. King AA, Nguyen D, Ionides EL. Statistical inference for partially observed Markov processes via the R package pomp. *Journal of Statistical Software*. 2009; 69(12):1–43.
21. Ramsay JO, Hooker G, Campbell D, Cao J. Parameter estimation for differential equations: a generalized smoothing approach. *Journal of the Royal Statistical Society B (Statistical Methodology)*. 2007; 69(5):741–796. <https://doi.org/10.1111/j.1467-9868.2007.00610.x>
22. Hooker G, Ellner SP, De Vargas Roditi L, Earn DJD. Parameterizing state-space models for infectious disease dynamics by generalized profiling: measles in Ontario. *Journal of the Royal Society Interface*. 2011; 8(60):961–974. <https://doi.org/10.1098/rsif.2010.0412>
23. Becker A, T GB. tsiR: An R package for time series susceptible-infected-recovered models of epidemics. *PLoS ONE*. 2017; 12(9):0185528. <https://doi.org/10.1371/journal.pone.0185528>
24. Krylova O. Predicting epidemiological transitions in infectious disease dynamics. Smallpox in historic London (1664–1930). Hamilton, Ontario, Canada: McMaster University; 2011. Available from: <https://macsphere.mcmaster.ca/handle/11375/11231>.
25. deJonge MS. Fast estimation of time-varying transmission rates. Hamilton, Ontario, Canada: McMaster University; 2014. Available from: <https://macsphere.mcmaster.ca/handle/11375/14230>.
26. Wallinga J, Lipsitch M. How generation intervals shape the relationship between growth rates and reproductive numbers. *Proceedings of the Royal Society B (Biological Sciences)*. 2007; 274:599–604. <https://doi.org/10.1098/rspb.2006.3754>
27. Champredon D, Dushoff J. Intrinsic and realized generation intervals in infectious-disease transmission. *Proceedings of the Royal Society B (Biological Sciences)*. 2015; 282(1821):20152026. <https://doi.org/10.1098/rspb.2015.2026>
28. Krylova O, Earn DJD. Effects of the infectious period distribution on predicted transitions in childhood disease dynamics. *Journal of the Royal Society Interface*. 2013; 10:20130098. <https://doi.org/10.1098/rsif.2013.0098>
29. Brauer F, Castillo-Chavez C. *Mathematical models in population biology and epidemiology*. New York, NY: Springer; 2012.
30. Lloyd AL. Destabilization of epidemic models with the inclusion of realistic distributions of infectious periods. *Proceedings of the Royal Society B (Biological Sciences)*. 2001; 268(1470):985–993. <https://doi.org/10.1098/rspb.2001.1599>
31. Lloyd AL. Realistic distributions of infectious periods in epidemic models: changing patterns of persistence and dynamics. *Theoretical Population Biology*. 2001; 60(1):59–71. <https://doi.org/10.1006/tpbi.2001.1525> PMID: 11589638
32. Ma J, Ma Z. Epidemic threshold conditions for seasonally forced SEIR models. *Mathematical Biosciences and Engineering*. 2006; 3(1):161–172. <https://doi.org/10.3934/mbe.2006.3.161> PMID: 20361816
33. Little RJA, Rubin DB. *Statistical Analysis with Missing Data*. Hoboken, NJ: John Wiley & Sons; 2019.
34. Goldstein E, Dushoff J, Ma J, Plotkin JB, Earn DJD, Lipsitch M. Reconstructing influenza incidence by deconvolution of daily mortality time series. *Proceedings of the National Academy of Sciences*. 2009; 106:21825–21829. <https://doi.org/10.1073/pnas.0902958106>
35. He D, Earn DJD. The cohort effect in childhood disease dynamics. *Journal of the Royal Society Interface*. 2016; 13:20160156. <https://doi.org/10.1098/rsif.2016.0156>
36. Cleveland WS, Grosse E, Shyu WM. Local regression models. In: Chambers JM, Hastie TJ, editors. *Statistical models in S*. London, UK: Chapman & Hall; 1991. p. 309–376.
37. Loader C. *Local Regression and Likelihood*. New York, NY: Springer-Verlag New York; 1999.
38. Hart JD. Automated kernel smoothing of dependent data by using time series cross-validation. *Journal of the Royal Statistical Society B (Statistical Methodology)*. 1994; 56(3):529–542.
39. Gillespie DT. Stochastic simulation of chemical kinetics. *Annual Review of Physical Chemistry*. 2007; 58:35–55. <https://doi.org/10.1146/annurev.physchem.58.032806.104637> PMID: 17037977
40. Johnson P. adaptivetau: Tau-leaping stochastic simulation; 2016. Available from: <https://CRAN.R-project.org/package=adaptivetau>.
41. Elaydi S. *An Introduction to Difference Equations*. New York, NY: Springer; 2005.

42. Bauch CT, Earn DJD. Transients and attractors in epidemics. *Proceedings of the Royal Society of London B*. 2003; 270(1524):1573–1578. <https://doi.org/10.1098/rspb.2003.2410>
43. Earn DJD. Mathematical epidemiology of infectious diseases. In: Lewis MA, Chaplain MAJ, Keener JP, Maini PK, editors. *Mathematical biology*. vol. 14 of IAS Park City Mathematics Series. American Mathematical Society; 2009. p. 151–186.
44. Fine PEM. The interval between successive cases of an infectious disease. *American Journal of Epidemiology*. 2003; 158(11):1039–1047. <https://doi.org/10.1093/aje/kwg251> PMID: 14630599

Supporting Information

Fast estimation of time-varying
infectious disease transmission rates

PLOS Computational Biology

Mikael Jagan, Michelle S. deJonge, Olga Krylova, David J. D. Earn

September 23, 2020

Contents

S0 Preliminaries	1
S1 Example of $\beta(t)$ estimation using the FC, S, and SI methods	2
S1.1 Creating a list of parameter values	2
S1.2 Simulating time series data	4
S1.3 Estimating the time-varying transmission rate	5
S1.4 Measuring estimation error	9
S2 Effect of process and observation error	10
S3 Averaging the raw estimate of $\beta(t)$	13
S4 Smoothing the raw estimate of $\beta(t)$	16
S5 Sensitivity to data-generating parameters	22
S5.1 Sensitivity to \mathcal{R}_0 and α	23
S5.2 Sensitivity to S_0 , I_0 , ν_c , μ_c , t_{gen} , and p_{rep}	27
S5.3 A note on smoothing	30
S5.3.1 C_k and β_k for $t_{\text{gen}} = (2^{-1.5}, 1, 2^{1.5}) \cdot 13$ days	30
S5.3.2 $\beta_{\text{loess}}(t; q^*)$ and $\beta_{\text{loess}}(t; q_{\text{opt}})$ for $t_{\text{gen}} = (2^{-1.5}, 1, 2^{1.5}) \cdot 13$ days	32
S5.3.3 Discussion	35
S6 Sensitivity to error in input parameters	36
S6.1 A note on smoothing	39
S7 Estimating S_0 via PTPI: Example	39
S7.1 Truncation step	40
S7.2 Iteration step	43
S8 Estimating S_0 via PTPI: Convergence	47
S9 Appendix: Choice of discretization in the SI method	50
S9.1 Nine discretization schemes	50
S9.2 Comparison of RRMSE, bias, and variance	51
S9.2.1 RRMSE	51
S9.2.2 Bias and variance	55

S0 Preliminaries

This supplement to the manuscript is compiled from the source file `S1_Text.Rnw` using R version 4.0.2 (2020-06-22) [1] and these R package versions:

```
##      knitr      tikzDevice      colorRamps RColorBrewer      scales
##      1.29      0.12.3.1      2.3      1.1-2      1.1.1
##      deSolve      adaptivetau
##      1.28      2.2-3
```

Our primary aim here is to make our results entirely reproducible by the reader. Our secondary aim is to make our methods available to potential users. To this end, we introduce our R package **fastbeta**, which implements

- the FC, S, and SI methods for estimating time-varying transmission rates $\beta(t)$ from time series data; and
- peak-to-peak iteration (PTPI) for estimating the initial number of susceptible individuals S_0 from time series data.

All methods are based on the SIR model with time-varying rates of birth, death, and transmission:

$$\frac{dS}{dt} = \nu(t)\widehat{N}_0 - \beta(t)SI - \mu(t)S, \quad (1a)$$

$$\frac{dI}{dt} = \beta(t)SI - \gamma I - \mu(t)I, \quad (1b)$$

$$\frac{dR}{dt} = \gamma I - \mu(t)R, \quad (1c)$$

where $\gamma = 1/t_{\text{gen}}$.

The most recent version of **fastbeta** is located in our [GitHub repository](#) and can be installed using `install_github()` from the **remotes** package.

```
if (!require(remotes)) install.packages("remotes")
remotes::install_github("davidearn/fastbeta")
```

However, readers attempting to compile this document from source must install **fastbeta** from the `plos` branch of the repository, which houses the version used at the time of this writing.

```
if (!require(remotes)) install.packages("remotes")
remotes::install_github("davidearn/fastbeta", ref = "plos")
```

19 For complete compilation instructions, refer to `README.md`.

20 Here is a list of functions implemented in the `plos` version of `fastbeta`:

```
library(fastbeta)
ls("package:fastbeta")

## [1] "compute_rrmse"      "estimate_beta_FC" "estimate_beta_S"
## [4] "estimate_beta_SI"  "get_peak_times"   "make_data"
## [7] "make_par_list"     "ptpi"              "test_s2dgbeta"
## [10] "test_s2dgpars"     "test_s2inpars"
```

21 We will introduce these on the fly. More complete documentation can be accessed by
22 running `?fastbeta`.

23 In the sections to follow, we annotate the R code needed to reproduce results reported
24 in the manuscript. Plotting commands have been suppressed, but are preserved in
25 `S1_Text.Rnw`. Since our work involves millions of simulations, we have retained certain
26 output in the directory `RData/` to significantly reduce compilation time.

27 **S1 Example of $\beta(t)$ estimation using the FC, S, and SI** 28 **methods**

29 Fig 1 in the manuscript compares the output of the FC, S, and SI methods for a simulated
30 time series of reported incidence. To reproduce Fig 1, we simulate time series data using
31 system (1) with constant vital rates ν_c and μ_c and a seasonally forced transmission rate
32 that includes environmental noise:

$$\beta_\phi(t) = \langle \beta \rangle \left[1 + \alpha \cos \left(\frac{2\pi t}{1 \text{ year}} + \phi(t; \epsilon) \right) \right]. \quad (2)$$

33 Doing so, we obtain observations of reported incidence at equally spaced time points

$$t_k = t_0 + k\Delta t, \quad k = 0, \dots, n. \quad (3)$$

34 We then apply each algorithm (FC, S, SI) to reconstruct the seasonally forced transmission
35 rate from the data.

36 As this simulate-estimate routine is our main investigative approach going forward, we
37 describe each step in detail here (and reproduce Fig 1 in the process), but we do not repeat
38 these details in later sections.

39 **S1.1 Creating a list of parameter values**

40 Simulating a reported incidence time series from system (1) requires a list of values for all
41 data-generating parameters. Our function `make_par_list()` simplifies the task of

42 creating such a list. It does this by “filling in the blanks” when we want \mathcal{R}_0 , $\langle\beta\rangle$, N_0 , S_0 , or
 43 I_0 to depend in a complicated way on other parameters’ values.

44 Below, we call `make_par_list()`, defining all arguments explicitly. Except for
 45 `dt_weeks`, which is the observation interval Δt in weeks, the values of time and rate
 46 parameters must be supplied in units Δt and per unit Δt . In this call to
 47 `make_par_list()`, we indicate $\Delta t = 1$ week, $t_0 = 2000$ years, $t_{\text{gen}} = 13$ days, and
 48 $\nu_c = \mu_c = 0.04 \text{ year}^{-1}$.

```
## List of parameter values
par_list <- make_par_list(
  dt_weeks = 1, # observation interval
  t0 = 2000 * (365 / 7) * 1, # time of first observation
  prep = 1, # case reporting probability
  trep = 0, # case reporting delay
  hatN0 = 1e06, # population size at 0 years
  N0 = NA, # population size at `t0`
  S0 = NA, # number susceptibles at `t0`
  I0 = NA, # number infecteds at `t0`
  nu = 0.04 * (7 / 365) * 1, # birth rate (relative to `hatN0`)
  mu = 0.04 * (7 / 365) * 1, # natural mortality rate (per capita)
  tgen = 13 * (1 / 7) / 1, # mean generation interval
  Rnaught = 20, # basic reproduction number
  beta_mean = NA, # mean of seasonal forcing
  alpha = 0.08, # amplitude of seasonal forcing
  epsilon = 0 # s.d. of environmental noise
)
unlist(par_list) # printed as a named vector

## dt_weeks t0 prep trep hatN0
## 1.000000e+00 1.042857e+05 1.000000e+00 0.000000e+00 1.000000e+06
## N0 S0 I0 nu mu
## 1.000000e+06 5.405182e+04 1.318586e+03 7.671233e-04 7.671233e-04
## tgen Rnaught beta_mean alpha epsilon
## 1.857143e+00 2.000000e+01 1.078457e-05 8.000000e-02 0.000000e+00
```

49 `make_par_list()` requires that exactly one of \mathcal{R}_0 and $\langle\beta\rangle$ (arguments `Rnaught` and
 50 `beta_mean`) is defined in the function call. It sets the undefined parameter internally by
 51 enforcing the identity

$$\mathcal{R}_0 = \frac{\nu_c \hat{N}_0}{\mu_c} \cdot \frac{\langle\beta\rangle}{\gamma + \mu_c}. \quad (4)$$

52 Above, we “omitted” `beta_mean` from the function call (by supplying a value `NA`) and
 53 obtained the desired value in the output.

54 Values for N_0 , S_0 , and I_0 (arguments `N0`, `S0`, and `I0`) were also set internally. This
 55 was done via numerical integration of system (1) with constant vital rates ν_c and μ_c and a
 56 seasonally forced transmission rate that *excludes* environmental noise:

$$\beta(t) = \langle \beta \rangle \left[1 + \alpha \cos \left(\frac{2\pi t}{1 \text{ year}} \right) \right]. \quad (5)$$

57 After integrating between times $t = 0$ years and $t = t_0$ (in this case 2000 years)
 58 `make_par_list()` chooses for N_0 , S_0 and I_0 the values of $N^* = N(t_0)$, $S^* = S(t_0)$, and
 59 $I^* = I(t_0)$. This ensures that the initial state of any simulation using `par_list` is a point
 60 very near the attractor of the system being simulated.

61 In the above call to `make_par_list()`, we indicated the default values of all
 62 arguments. In future calls to this function, we will not specify arguments explicitly except
 63 for clarity or to request a value different from the default.

64 S1.2 Simulating time series data

65 To reproduce the simulation considered in Fig 1, we pass `par_list` to our function
 66 `make_data()`, which returns the simulated time series data in a data frame.

```
## Data frame containing time series data
df <- make_data(
  par_list      = par_list,      # parametrization
  n             = 20 * 365 / 7, # time series length: ~20 years
  with_dem_stoch = FALSE        # no demographic stochasticity
)
head(df)

##           t  t_years      beta  beta_phi  N      S      I
## 1 104285.7 2000.000 1.164734e-05 1.164734e-05 1e+06 54052.00 1319.000
## 2 104286.7 2000.019 1.164108e-05 1.164108e-05 1e+06 53910.11 1442.447
## 3 104287.7 2000.038 1.162241e-05 1.162241e-05 1e+06 53692.54 1573.095
## 4 104288.7 2000.058 1.159158e-05 1.159158e-05 1e+06 53398.91 1708.214
## 5 104289.7 2000.077 1.154904e-05 1.154904e-05 1e+06 53031.36 1844.220
## 6 104290.7 2000.096 1.149543e-05 1.149543e-05 1e+06 52594.95 1976.772
##           R      Q      Z      C
## 1 944629.0  0.0000      NA      NA
## 2 944647.4  867.5997  867.5997  868
## 3 944734.4 1811.0116  943.4119  943
## 4 944892.9 2830.6905 1019.6789 1020
## 5 945124.4 3924.5379 1093.8474 1094
## 6 945428.3 5087.5473 1163.0094 1163
```

67 The output contains the following information:

<code>t</code>	$\frac{t_k}{\Delta t}$	Time in units of the observation interval Δt . Equal to $\frac{t_0}{\Delta t} + (0, 1, \dots, n)$.
<code>t_years</code>	t_k	Time in years. Equal to $t_0 + (0, 1, \dots, n)\Delta t$.
<code>beta</code>	$\beta(t_k)\Delta t$	Seasonally forced transmission rate without environmental noise (Eq (5)), expressed per unit Δt per susceptible per infected.
<code>beta_phi</code>	$\beta_\phi(t_k)\Delta t$	Seasonally forced transmission rate with environmental noise (Eq (2)), expressed per unit Δt per susceptible per infected.
<code>N</code>	$N(t_k)$	Population size.
<code>S</code>	$S(t_k)$	Number of susceptible individuals.
<code>I</code>	$I(t_k)$	Number of infected individuals.
<code>R</code>	$R(t_k)$	Number of removed individuals.
<code>Q</code>	$Q(t_k)$	Cumulative incidence.
<code>Z</code>	$Z(t_k)$	Incidence.
<code>C</code>	$C(t_k)$	Reported incidence.

68 In this example, there is no environmental noise, simply because `par_list` specified
 69 `epsilon = 0`. Hence `beta` and `beta_phi` are identical in the returned data frame.

70 S1.3 Estimating the time-varying transmission rate

71 We apply the FC, S, and SI methods to estimate incidence Z , susceptibles S , infecteds I ,
 72 and the seasonally forced transmission rate β from reported incidence and vital data. We
 73 have implemented these methods in our functions `estimate_beta_FC()`,
 74 `estimate_beta_S()`, and `estimate_beta_SI()`. We will refer to these collectively as
 75 `estimate_beta()`, but note that there is no function by that name.

76 The first argument of `estimate_beta()` expects a data frame `df` with columns `t`,
 77 `C`, `B`, and (for the S and SI methods) `mu`. These specify equally spaced observation times
 78 t_k (Eq (3)) in units of the observation interval Δt (*i.e.*, $t_k/\Delta t$) and, at those times,
 79 reported incidence C_k , observed births B_k , and the observed *per capita* natural mortality
 80 rate μ_k expressed per unit Δt .

81 The second argument expects a list `par_list` with elements `prep`, `trep`, `tgen`,
 82 `S0`, and (for the SI method) `I0`. These specify values for input parameters p_{rep} , t_{rep} , t_{gen} ,
 83 S_0 , and I_0 .

84 Here, we supply the data frame `df` obtained earlier using `make_data()`. Note that
 85 this data frame does *not* have columns `B` and `mu`. When these columns are missing in the
 86 function call, `estimate_beta()` creates mock (constant) time series as follows: (i) it looks
 87 in `par_list` for additional elements `hatN0`, `nu`, and `mu`, specifying a population size \hat{N}_0
 88 and constant vital rates ν'_c and μ'_c , then (ii) it sets $B_k = \nu'_c \hat{N}_0 \Delta t$ and $\mu_k = \mu'_c$ for all k .
 89 In practice, the argument `par_list` contains the user's potentially incorrect estimates
 90 of the input parameters, such as the initial number of susceptibles individuals S_0 . For this
 91 example, there is no input error: we assign each input parameter its true (data-generating)
 92 value. That is, the `par_list` that we pass to `estimate_beta()` is precisely the
 93 `par_list` that we passed to `make_data()` earlier.

```
## List of functions
estimate_beta <- list(
  FC = estimate_beta_FC,
  S = estimate_beta_S,
  SI = estimate_beta_SI
)

## List of returned data frames
df_est <- lapply(estimate_beta, function(f) f(df, par_list))
lapply(df_est, head, n = 10)

## $FC
##           t      C      Z Z_agg      B      B_agg      S      I      beta
## 1 104285.7   NA   NA   NA 767.1233      NA 54051.82   NA      NA
## 2 104286.7  868  868   NA 767.1233      NA      NA   NA      NA
## 3 104287.7  943  943 1811 767.1233 1534.247 53775.06 1811 1.085364e-05
## 4 104288.7 1020 1020   NA 767.1233      NA      NA   NA      NA
## 5 104289.7 1094 1094 2114 767.1233 1534.247 53195.31 2114 1.061314e-05
## 6 104290.7 1163 1163   NA 767.1233      NA      NA   NA      NA
## 7 104291.7 1224 1224 2387 767.1233 1534.247 52342.56 2387 1.034483e-05
## 8 104292.7 1274 1274   NA 767.1233      NA      NA   NA      NA
## 9 104293.7 1311 1311 2585 767.1233 1534.247 51291.80 2585 1.006868e-05
## 10 104294.7 1332 1332   NA 767.1233      NA      NA   NA      NA
##
## $S
##           t      C      Z      B      mu      S      I
## 1 104285.7   NA   NA 767.1233 0.0007671233 54051.82      NA
## 2 104286.7  868  868 767.1233 0.0007671233 53909.48      NA
## 3 104287.7  943  943 767.1233 0.0007671233 53692.25 1609.707
## 4 104288.7 1020 1020 767.1233 0.0007671233 53398.18 1748.794
```

```

## 5  104289.7  1094  1094  767.1233  0.0007671233  53030.34  1891.591
## 6  104290.7  1163  1163  767.1233  0.0007671233  52593.78  2028.824
## 7  104291.7  1224  1224  767.1233  0.0007671233  52096.56  2156.784
## 8  104292.7  1274  1274  767.1233  0.0007671233  51549.72  2269.909
## 9  104293.7  1311  1311  767.1233  0.0007671233  50966.30  2362.634
## 10 104294.7  1332  1332  767.1233  0.0007671233  50362.32  2431.251
##
##          beta
## 1          NA
## 2          NA
## 3  1.180163e-05
## 4  1.171527e-05
## 5  1.159386e-05
## 6  1.147104e-05
## 7  1.133845e-05
## 8  1.120387e-05
## 9  1.106177e-05
## 10 1.092750e-05
##
## $SI
##          t      C      Z      B      mu      S      I
## 1  104285.7    NA    NA  767.1233  0.0007671233  54051.82  1318.586
## 2  104286.7   868   868  767.1233  0.0007671233  53909.53  1442.230
## 3  104287.7   943   943  767.1233  0.0007671233  53692.38  1572.434
## 4  104288.7  1020  1020  767.1233  0.0007671233  53398.43  1707.986
## 5  104289.7  1094  1094  767.1233  0.0007671233  53030.73  1844.252
## 6  104290.7  1163  1163  767.1233  0.0007671233  52594.34  1976.990
## 7  104291.7  1224  1224  767.1233  0.0007671233  52097.31  2101.398
## 8  104292.7  1274  1274  767.1233  0.0007671233  51550.68  2212.350
## 9  104293.7  1311  1311  767.1233  0.0007671233  50967.48  2305.321
## 10 104294.7  1332  1332  767.1233  0.0007671233  50363.73  2375.346
##
##          beta
## 1          NA
## 2  1.164631e-05
## 3  1.162533e-05
## 4  1.158944e-05
## 5  1.153862e-05
## 6  1.147834e-05
## 7  1.140877e-05
## 8  1.133293e-05
## 9  1.124715e-05
## 10 1.115929e-05

```


94 The output contains the following information:

t	$\frac{t_k}{\Delta t}$	Time in units of the observation interval Δt . Equal to $\frac{t_0}{\Delta t} + (0, 1, \dots, n)$. Identical to input <code>df\$t</code> .
C	C_k	Reported incidence. Identical to input <code>df\$C</code> , except that missing values and zeros (treated like missing values) have been imputed by linear interpolation.
B	B_k	Observed births. Identical to input <code>df\$B</code> if supplied. Otherwise, every element is <code>with(par_list, hatN0 * nu * 1)</code> .
mu	$\mu_k \Delta t$	Observed <i>per capita</i> natural mortality rate, expressed per unit Δt . Identical to input <code>df\$mu</code> if supplied. Otherwise, every element is <code>with(par_list, mu)</code> .
Z	Z_k	Estimate of incidence $Z(t_k)$.
S	S_k	Estimate of susceptibles $S(t_k)$.
I	I_k	Estimate of infecteds $I(t_k)$.
beta	$\beta_k \Delta t$	Raw estimate of the time-varying transmission rate $\beta(t_k)$ expressed per unit Δt per susceptible per infected.

95 Note that the FC method's output has missing values in alternating rows. This is not a
 96 mistake: the FC method aggregates incidence and births over the mean generation interval
 97 (roughly 2 weeks in this example), instead of the observation interval (1 week). As a result,
 98 estimation of $S(t_k)$ and $\beta(t_k)$ is only possible at every other observation time. Aggregation
 99 is not a requirement of the S and SI methods.

100 Be warned that `estimate_beta()` returns *raw* estimates of $\beta(t)$. Smoothing the β_k
 101 time series by fitting a loess curve $\beta_{\text{loess}}(t; q)$ is recommended in the event that it displays
 102 unwanted noise. Determining what degree of smoothing is optimal (*i.e.*, choosing a good
 103 value for the loess smoothing parameter q) is non-trivial, and therefore not undertaken by
 104 `estimate_beta()`. We discuss this issue in more detail in §S4.

105 Plotting the S_k and β_k time series returned by `estimate_beta()`, we reproduce Fig 1.
 106 Note that we are simply plotting (with a scaling) `df_estFCS`, `df_estSS`, and
 107 `df_estSIS`, and separately `df_estFCbeta`, `df_estSbeta`, and `df_estSIbeta`.

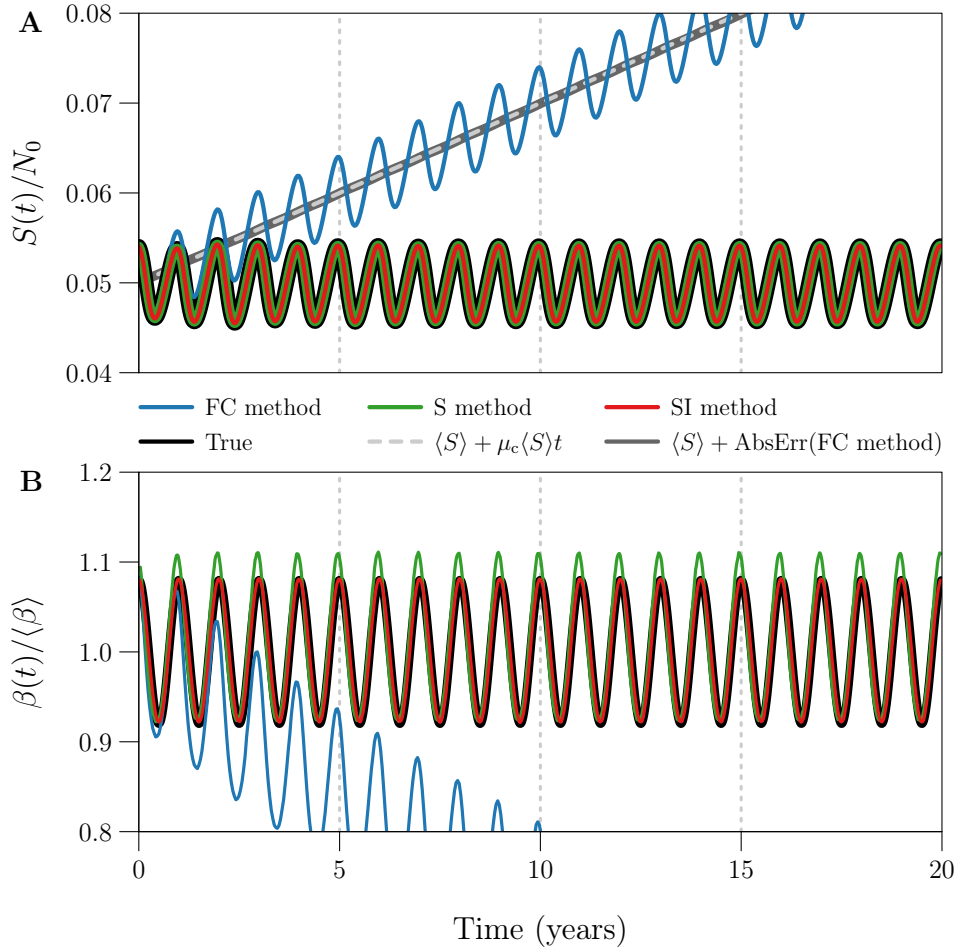


Fig 1. Example of $S(t)$ and $\beta(t)$ estimation using the FC, S, and SI methods.

108 S1.4 Measuring estimation error

109 In the manuscript, we report the relative root mean square error (RRMSE) in each β_k time
 110 series. We compute RRMSE using `compute_rrmse()`, which takes as arguments the two
 111 vectors we wish to compare, with the estimate passed second.

```
sapply(df_est, function(x) compute_rrmse(df$beta, x$beta))
```

```
##          FC          S          SI  

## 0.335487234 0.024010753 0.002139994
```

112 S2 Effect of process and observation error

113 Fig 1 in the manuscript shows the output of the S and SI methods for idealized reported
114 incidence data. Those data were simulated deterministically, *i.e.*,

- 115 ■ without environmental stochasticity [ES] (`par_list` with `epsilon = 0` passed to
116 `make_data()`),
- 117 ■ without demographic stochasticity [DS] (`with_dem_stoch = FALSE` passed to
118 `make_data()`), and
- 119 ■ without observation error [OE] (`par_list` with `prep = 1` passed to
120 `make_data()`).

121 In Fig 2, we consider the effect of adding ES, DS, and OE in turn to the original
122 deterministic simulation, on the β_k time series generated by the S and SI methods. We
123 produce these four simulations as follows:

```
## List of lists of parameter values
par_list <- list(
  xxxxxx = make_par_list(epsilon = 0, prep = 1),      # deterministic
  esxxxx = make_par_list(epsilon = 0.5, prep = 1),  # ES
  esdsxx = make_par_list(epsilon = 0.5, prep = 1),  # ES+DE
  esdsoe = make_par_list(epsilon = 0.5, prep = 0.25) # ES+DE+OE
)

## List of data frames containing time series data
df <- mapply(make_data,
  par_list = par_list,
  n = 3 * 365 / 7,
  with_dem_stoch = c(FALSE, FALSE, TRUE, TRUE),
  seed = 1305,
  SIMPLIFY = FALSE
)
names(df)

## [1] "xxxxxx" "esxxxx" "esdsxx" "esdsoe"

names(df$esdsoe)

## [1] "t"          "t_years"    "beta"       "beta_phi"  "N"         "S"
## [7] "I"          "R"          "Q"          "Z"         "C"
```

124 Here, `par_list` is a *list of lists*, containing the parameter values desired for each
 125 simulation, and `df` is a list of data frames, containing the corresponding simulated data.
 126 The next code chunk applies the S and SI methods, without input error, to each
 127 simulated reported incidence time series.

```
## List of lists of data frames containing estimation output
df_est <- list(
  ## List of data frames returned by S method
  S = mapply(estimate_beta_S,
    df = df,
    par_list = par_list,
    SIMPLIFY = FALSE
  ),
  ## List of data frames returned by SI method
  SI = mapply(estimate_beta_SI,
    df = df,
    par_list = par_list,
    SIMPLIFY = FALSE
  )
)
names(df_est)

## [1] "S" "SI"

names(df_est$SI)

## [1] "xxxxxx" "esxxxx" "esdsxx" "esdsoe"

names(df_est$SI$esdsoe)

## [1] "t" "C" "Z" "B" "mu" "S" "I" "beta"
```

128 Hence each element of `df_est` contains the output of one of the S and SI methods for all 4
 129 reported incidence time series. Plotting the resulting 8 Z_k , I_k , and β_k time series (estimates
 130 of incidence, prevalence, and the seasonally forced transmission rate) yields Fig 2.

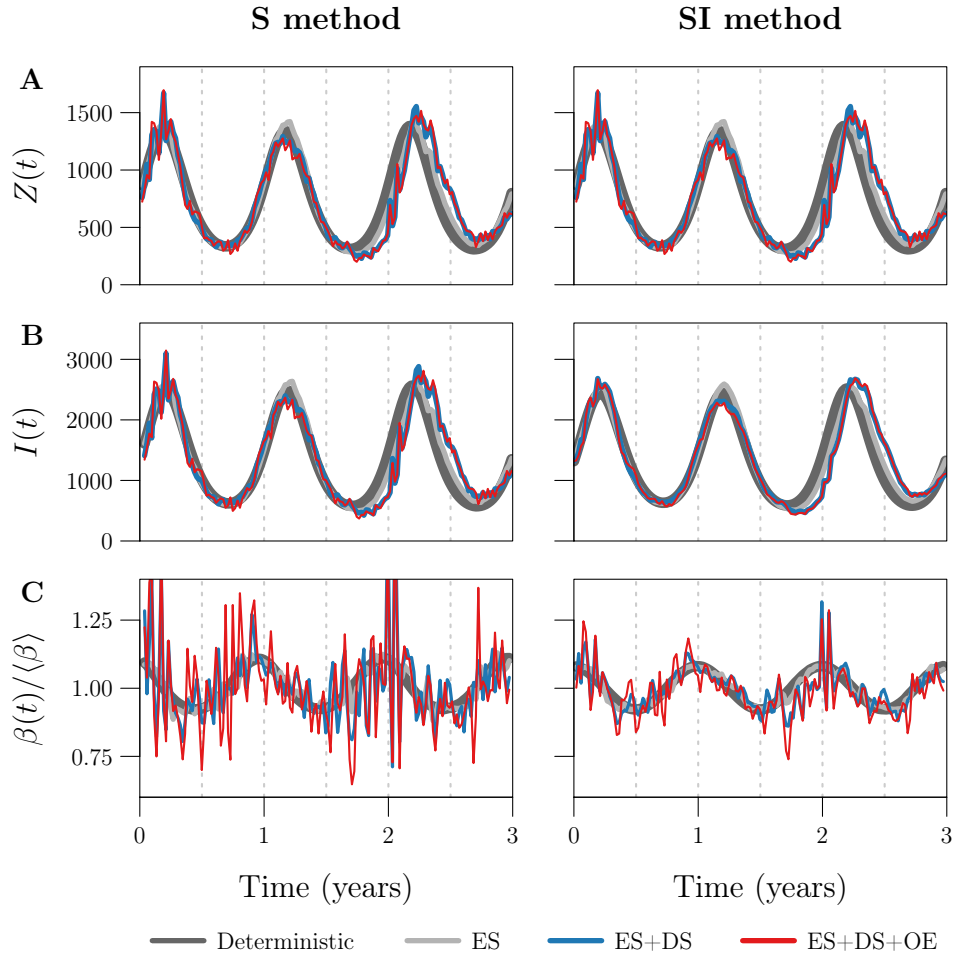


Fig 2. Effects of process and observation error on the S and SI methods.

131 We obtain the RRMSE in each β_k time series with the following line of code.

```
lapply(df_est, function(x) {
  mapply(function(y, z) compute_rrmse(y$beta, z$beta), y = df, z = x)
})

## $S
##      xxxxxx      esxxxx      esdsxx      esdsoe
## 0.02393485 0.03352897 0.12261568 0.15458400
##
## $SI
##      xxxxxx      esxxxx      esdsxx      esdsoe
## 0.002145247 0.015053954 0.053576843 0.070091436
```

132 S3 Averaging the raw estimate of $\beta(t)$

133 Fig 3 in the manuscript considers the seasonally forced $\beta(t)$ (Eq (5)) and three estimates,
134 each spanning 1000 years. It overlays the 1000 1-year cycles embedded in each estimate
135 and plots their 1-year average. To reproduce Fig 3, we simulate 1000 years of weekly
136 reported incidence, including in the simulation environmental noise in transmission
137 ($\epsilon = 0.5$), demographic stochasticity, and random under-reporting of cases ($p_{\text{rep}} = 0.25$).

```
## List of parameter values
par_list <- make_par_list(epsilon = 0.5, prep = 0.25)

## Data frame containing time series data
df <- make_data(
  par_list      = par_list,
  n             = 1000 * 365 / 7 + 1,
  with_dem_stoch = TRUE,
  seed         = 1217
)
```

138 We estimate the seasonally forced $\beta(t)$ using the S and SI methods, without input error.

```
## List of functions
estimate_beta <- list(
  S = estimate_beta_S,
  SI = estimate_beta_SI
)

## List of returned data frames. Column `beta` in `df_est[[i]]`
## stores the raw estimate generated by `estimate_beta[[i]]`.
df_est <- lapply(estimate_beta, function(f) f(df, par_list))
```

139 The raw time series estimates β_k contain spurious noise due to process and observation
140 error. Hence, for comparison, we fit a loess curve $\beta_{\text{loess}}(t; q)$ to the time series returned by
141 the SI method, where q is the loess smoothing parameter indicating (roughly) the number
142 of nearest neighbours weighted in local regression. It turns out that $q = 53$ is a good choice
143 for this parameter in this example (see §S4). To do the fitting, we call `loess()` with
144 argument `span` indicating q as a proportion of time series length. Additional arguments
145 are fully explained in the documentation, accessible by running `?loess` and
146 `?loess.control`.

```

## Object of class `loess` defining the fitted loess curve
SI_loess <- stats::loess(
  formula   = beta ~ t,
  data      = df_est$SI,
  span      = 53 / nrow(df_est$SI),
  degree    = 2,
  na.action = "na.exclude",
  control   = loess.control(surface = "direct")
)

```

147 We will calculate the average 1-year cycle in the linear interpolant $\beta_{\text{int}}(t)$ of β_k (S and
 148 SI methods), and in the loess curve $\beta_{\text{loess}}(t; q)$ fit to the same time series (SI method only).

```

## List of interpolants. `fits[[i]]` is the interpolant
## of column `beta` in `df_est[[i]]`.
fits <- lapply(df_est, function(x) {
  approxfun(x$t, x$beta, method = "linear", rule = 1)
})

## Appending the `loess` object from earlier
fits$SI_loess <- SI_loess

```

149 Before proceeding, we should verify that the β_k time series contain 1000 1-year cycles.

```

## First and last time points
t0 <- df_est$SI$t[1]
tn <- df_est$SI$t[nrow(df_est$SI)]

## 1-year period in units of the observation interval
period <- with(par_list, (365 / 7) / dt_weeks)

## Number of cycles
m <- floor((tn - t0) / period)
m

## [1] 1000

```

150 We must also specify the true 1-year cycle that each average 1-year cycle should estimate.
 151 We specify the true cycle with a reference time indicating the initial phase. For simplicity,
 152 we consider the cycle between times `t0` and `t0 + period` to be the true cycle. Phases of
 153 this cycle are specified by times `s` between 0 and `period`. To estimate the value of the
 154 true cycle at phase `s`, we evaluate each fit in `fits` (2 linear interpolants and 1 loess

155 curve) at times `t0 + s + (0:(m-1))* period` and average the resulting `m` values.
156 `get_phase_average()` computes this estimate for any `s`, for a given fit `f`.

```
get_phase_average <- function(s, f) {  
  times <- t0 + (s %% period) + (0:(m-1)) * period  
  x <- if (inherits(f, "loess")) predict(f, times) else f(times)  
  mean(x, na.rm = TRUE)  
}
```

157 Note that, whereas linear interpolants are just functions that we can evaluate at desired
158 times, loess objects must be passed to `predict()` to obtain fitted values. Note also that
159 the modulo operation `s %% period` makes `get_phase_average()` a periodic function of
160 `s`.

161 We construct the average 1-year cycle in each fit in `fits` by applying
162 `get_phase_average()` on a desired grid of `s` values.

```
s_grid <- seq(0, period, length.out = 150)  
average_one_year <- data.frame(  
  s_grid,  
  lapply(fits, function(f) sapply(s_grid, get_phase_average, f = f))  
)  
head(average_one_year)
```

##	s_grid	S	SI	SI_loess
## 1	0.0000000	1.193014e-05	1.153366e-05	1.148309e-05
## 2	0.3499521	1.194339e-05	1.154372e-05	1.148619e-05
## 3	0.6999041	1.193943e-05	1.155337e-05	1.148787e-05
## 4	1.0498562	1.191978e-05	1.155581e-05	1.148843e-05
## 5	1.3998082	1.190497e-05	1.155318e-05	1.148760e-05
## 6	1.7497603	1.189256e-05	1.154800e-05	1.148552e-05

163 We reproduce Fig 3 by plotting, for each 1000-year estimate of $\beta(t)$, the 1000 embedded
164 1-year cycles and their 1-year average, all on the same 1-year axis.

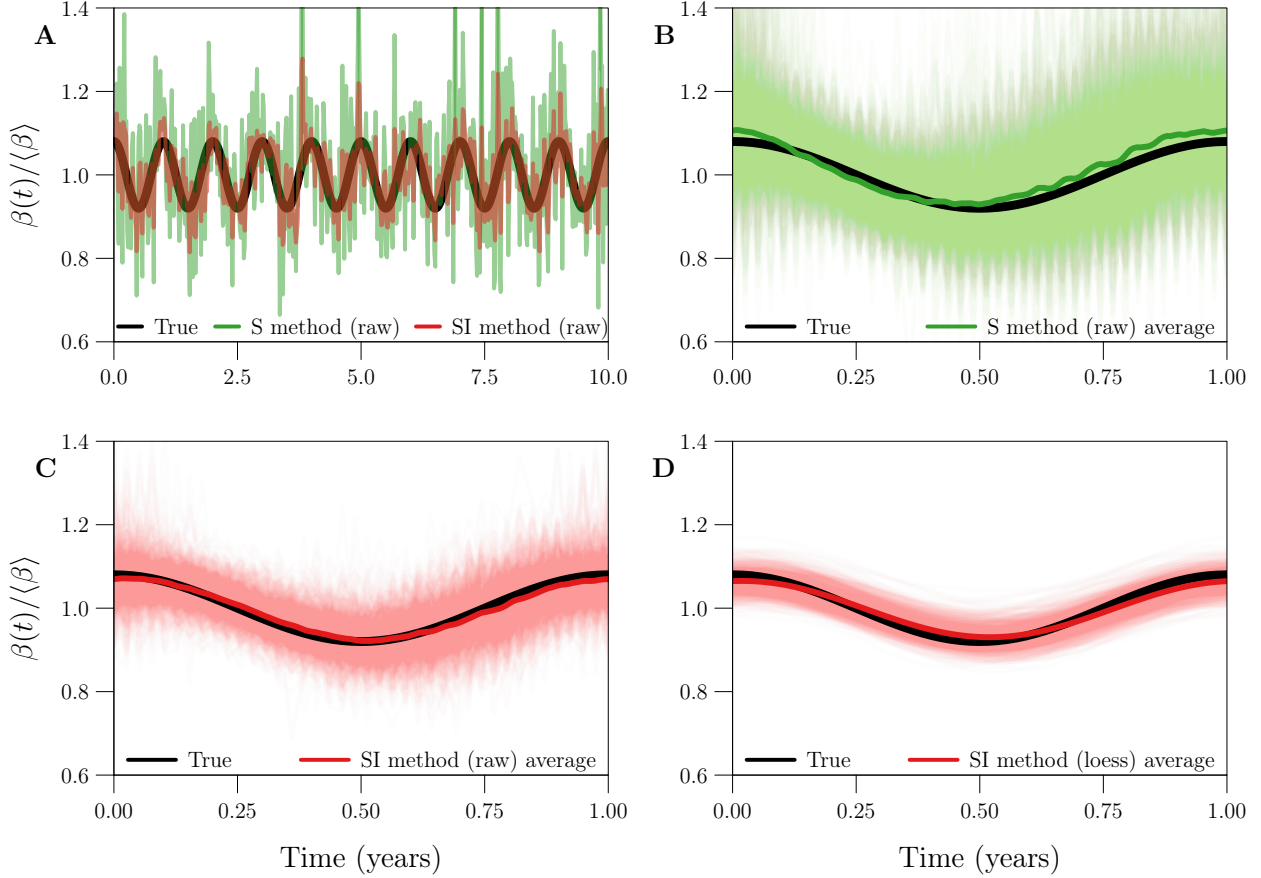


Fig 3. Bias and variance in 1-year cycles embedded in three estimates of a seasonally forced $\beta(t)$, in the absence of input error.

S4 Smoothing the raw estimate of $\beta(t)$

Figs 2C, 3B, and 3C demonstrate that, in the absence of input error, much of the error in raw estimates of $\beta(t)$ is attributable to noise in the time series. The S and SI methods produce the correct temporal pattern, but it is distorted by noise. Comparison of Figs 3C and 3D shows that fitting a smooth loess curve $\beta_{\text{loess}}(t; q)$ to the raw time series estimate β_k can lead to substantial improvement in both accuracy and interpretability.

In practice, we would like to choose the value q_{opt} of the loess smoothing parameter q that minimizes the error in $\beta_{\text{loess}}(t; q)$ relative to $\beta(t)$. However, we cannot calculate (and therefore cannot minimize) the error in $\beta_{\text{loess}}(t; q)$ when $\beta(t)$ is not known. In this situation, we can still estimate q_{opt} using statistical methods (most notably time series cross-validation [2]) or by direct inspection of $\beta_{\text{loess}}(t; q)$ for each value of q on a grid.

In our simulated data setting, we do know $\beta(t)$ and can therefore determine q_{opt} exactly. In this setting, it is instructive to quantify the reduction in error that is achieved

178 when the optimal loess estimate $\beta_{\text{loess}}(t; q_{\text{opt}})$ is chosen over the raw time series estimate β_k .
 179 Fig 4 in the manuscript addresses this issue.

180 To reproduce Fig 4, we consider 41 values of the case reporting probability p_{rep} and fix
 181 all other data-generating parameters. (Smaller values of p_{rep} generate noisier reported
 182 incidence time series, resulting in noisier β_k .) Using each value of p_{rep} , we perform 100
 183 simulations of reported incidence.

```
prep <- 10^seq(-2, 0, length.out = 41)
par_list <- make_par_list(epsilon = 0.5)
nsim <- 100
q <- 10:110
```

184 For each of these 41×100 simulations, we carry out the following steps. We estimate the
 185 seasonally forced $\beta(t)$ (Eq (5)) from the simulated reported incidence time series, without
 186 input error. (The underlying $\beta(t)$ was the same across all simulations.) For each q between
 187 10 and 110, we fit a loess curve $\beta_{\text{loess}}(t; q)$ to the raw time series estimate β_k . Finally, we
 188 record

$$\begin{aligned} \text{RRMSE}_{\text{raw}} &= \text{RRMSE in } \{(t_k, \beta_k)\}_{k=0}^n, \\ \text{RRMSE}_{\text{loess, min}} &= \min_{q \in \{10, \dots, 110\}} [\text{RRMSE in } \{(t_k, \beta_{\text{loess}}(t_k; q))\}_{k=0}^n], \\ q_{\text{opt}} &= \arg \min_{q \in \{10, \dots, 110\}} [\text{RRMSE in } \{(t_k, \beta_{\text{loess}}(t_k; q))\}_{k=0}^n]. \end{aligned}$$

189 Hence, for each value of p_{rep} , we obtain 100 values for each of $\text{RRMSE}_{\text{raw}}$, $\text{RRMSE}_{\text{loess, min}}$,
 190 and q_{opt} . We can preallocate space for this output.

```
out <- array(NA,
  dim      = c(length(prepare), nsim, 3, 2),
  dimnames = list(NULL, NULL,
    c("rrmse_raw", "rrmse_loess_min", "qopt"),
    c("S", "SI")
  )
)
```

191 The fourth dimension of the output array enables our comparison of the distributions of
 192 $\text{RRMSE}_{\text{raw}}$, $\text{RRMSE}_{\text{loess, min}}$, and q_{opt} for different methods of $\beta(t)$ estimation—in this case,
 193 the S and SI methods. Our expectation based on Figs 2C, 3B, and 3C is that the S method
 194 requires more smoothing.

195 The next code chunk does all of the hard work. Simulations are saved in the directory
 196 `RData/loess/`. Main results are saved in the file `RData/loess.RData`.

```

for (i in seq_along(prepare)) {

  ## Update `par_list` with current value of `prepare`
  par_list$prepare <- prepare[i]

  ## Create a directory for this loop's `.RData`
  dirname <- paste0(
    "RData/loess/",
    ## log10 current value of `prepare`
    "prepare_log10v-", sprintf("%+05.0f", log(prepare[i], 10) * 1000), "/"
  )
  if (!dir.exists(dirname)) {
    dir.create(dirname, recursive = TRUE)
  }

  for (j in seq_len(nsim)) {

    message(
      "`prepare` value ", i, " of ", length(prepare), ", ",
      "sim ", j, " of ", nsim
    )

    ## File name for simulation
    filename <- paste0(dirname, "sim", sprintf("%04.0f", j), ".RData")

    ## Simulate reported incidence data, if you haven't already
    if (file.exists(filename)) {
      load(filename)
    } else {
      df <- make_data(
        par_list      = par_list,
        n             = 20 * 365 / 7,
        with_dem_stoch = TRUE,
        seed          = j
      )
      save(df, file = filename)
    }

    ## Estimate the seasonally forced transmission rate from
    ## reported incidence
    estimate_beta <- list(

```

```

    S = estimate_beta_S,
    SI = estimate_beta_SI
  )
df_est <- lapply(estimate_beta, function(f) f(df, par_list))

## Compute the error in each raw estimate
out[i, j, "rrmse_raw", ] <- sapply(df_est, function(x) {
  compute_rrmse(df$beta, x$beta)
})

## Preallocate memory for the error in each loess estimate
## (one for each value of `q`, for each raw estimate)
rrmse_after_loess <- array(NA,
  dim      = c(length(q), 2),
  dimnames = list(NULL, c("S", "SI")))
)

## Standardize missing values in the raw estimates. `loess()`
## handles `NA` but complains about `NaN` and `Inf`.
df_est <- lapply(df_est, function(x) {
  x$beta[!is.finite(x$beta)] <- NA
  x
})

for (k in seq_along(q)) {

  ## Fit a smooth loess curve to each raw estimate
  loess_fit <- lapply(df_est, function(x) {
    stats::loess(
      formula = beta ~ t,
      data    = x,
      span    = q[k] / nrow(x),
      degree  = 2,
      na.action = "na.exclude",
      control = loess.control(
        surface = "direct",
        statistics = "none"
      )
    )
  })
}

```

```

    ## Compute the error in each loess estimate
    rrmse_after_loess[k, ] <- sapply(loess_fit, function(x) {
      compute_rrmse(df$beta, predict(x))
    })

  }

  ## Find the minimum error over all loess estimates.
  ## Also retrieve the value of `q` that minimized error.
  out[i, j, "rrmse_loess_min", ] <- apply(rrmse_after_loess, 2, min)
  out[i, j, "qopt", ] <- apply(rrmse_after_loess, 2, function(x) {
    q[which.min(x)]
  })

}

}

attr(out, "arg_list") <- list(
  prep      = prep,
  par_list  = par_list,
  q         = q
)
save(out, file = "RData/loess.RData")

```

197 For each value of p_{rep} , we desire the median and 5th and 95th percentiles of $\text{RRMSE}_{\text{raw}}$,
 198 $\text{RRMSE}_{\text{loess,min}}$, and q_{opt} .

```
pct <- apply(out, c(1, 3, 4), quantile, probs = c(0.05, 0.5, 0.95))
```

199 Plotting these as functions of p_{rep} , we reproduce Fig 3.

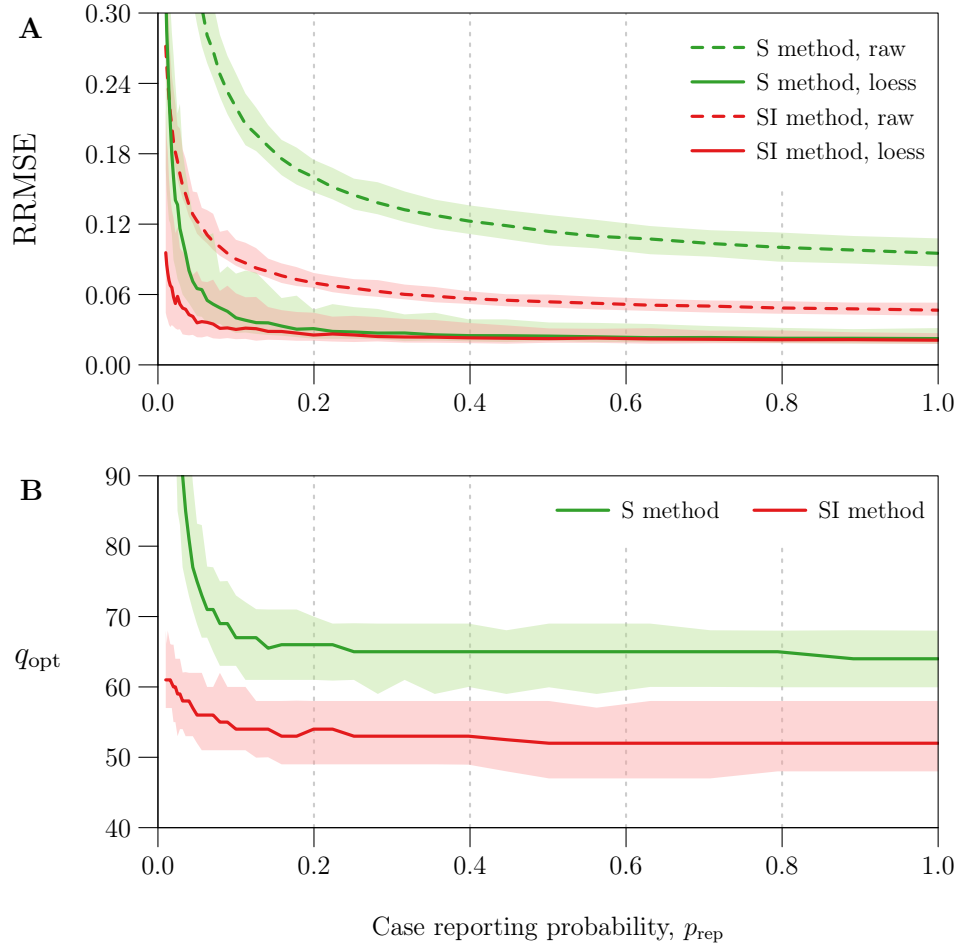


Fig 4. Reduction in $\beta(t)$ estimation error with optimal loess smoothing.

200 In the manuscript, we report the minimum percentage reduction in RRMSE across all
 201 simulations. Borrowing our earlier notation, this is the minimum value of

$$100 \times \left(1 - \frac{\text{RRMSE}_{\text{loess,min}}}{\text{RRMSE}_{\text{raw}}} \right). \quad (6)$$

```

apply(out, 4, function(x) {
  min(100 * (1 - x[, , "rrmse_loess_min"] / x[, , "rrmse_raw"]), na.rm = TRUE)
})

##          S          SI
## 46.38507 17.47202

```

202 We also report the median value of q_{opt} across all simulations for which $p_{\text{rep}} \geq 0.1$.

```

qstar <- apply(out[prep >= 0.1, , "qopt", ], 3, quantile,
  probs = 0.5,
  names = FALSE
)
qstar

## S SI
## 65 53

```

203 In our remaining analysis, we set $q = q^*$ when smoothing any β_k time series, taking

$$q^* = \begin{cases} 65 & \text{with the S method,} \\ 53 & \text{with the SI method.} \end{cases} \quad (7)$$

204 For a given time series, this setting may not be optimal ($q^* \neq q_{\text{opt}}$), but can be justified, as
 205 we explain in the sections to follow.

206 S5 Sensitivity to data-generating parameters

207 Error in estimates of the seasonally forced $\beta(t)$ (Eq (5)) from simulated reported incidence
 208 data is a function of data-generating parameters, given by

$$\boldsymbol{\theta} = (\langle\beta\rangle, \alpha, \epsilon, \widehat{N}_0, S_0, I_0, \nu_c, \mu_c, t_{\text{gen}}, p_{\text{rep}}, t_{\text{rep}}, t_0, \Delta t, n). \quad (8)$$

209 In order to measure the sensitivity of $\beta(t)$ estimation error to $\boldsymbol{\theta}$, we must define grids of
 210 parameter values. For this task, it is helpful to associate with each parameter a reference
 211 value:

$$\begin{array}{c|c} \langle\beta\rangle & \beta^* \\ \alpha & 0.08 \\ \epsilon & 0.5 \end{array} \quad
\begin{array}{c|c} \widehat{N}_0 & 10^6 \\ S_0 & S^* \\ I_0 & I^* \end{array} \quad
\begin{array}{c|c} \nu_c & 0.04 \text{ year}^{-1} \\ \mu_c & 0.04 \text{ year}^{-1} \\ t_{\text{gen}} & 13 \text{ days} \end{array} \quad
\begin{array}{c|c} t_0 & 2000 \text{ years} \\ \Delta t & 1 \text{ week} \\ n & 1042 \\ p_{\text{rep}} & p_{\text{rep}}^* \\ t_{\text{rep}} & t_{\text{rep}}^* \end{array} \quad (9)$$

212 Here, S^* and I^* are the values of S and I at a point very near the attractor of system
 213 (1) with constant vital rates ν_c and μ_c and a seasonally forced transmission rate (Eq (5)).
 214 It follows that S^* and I^* vary with parameters of the system (specifically, $\langle\beta\rangle$, α , ν_c , μ_c ,
 215 and t_{gen}). See §S1.1 for details on how S^* and I^* are obtained using `make_par_list()`
 216 given values for other parameters.

217 β^* is the value of $\langle\beta\rangle$ that satisfies Eq (4) with $\mathcal{R}_0 = 20$, $\widehat{N}_0 = 10^6$,
 218 $\nu_c = \mu_c = 0.04 \text{ year}^{-1}$, and $t_{\text{gen}} = \gamma^{-1} = 13 \text{ days}$:

$$\begin{aligned} \beta^* &= 20 \cdot \frac{0.04 \text{ year}^{-1}}{10^6 \cdot 0.04 \text{ year}^{-1}} \cdot \left(\frac{1}{13} \text{ day}^{-1} + 0.04 \text{ year}^{-1} \right) \\ &\approx 5.6234 \times 10^{-4} \text{ year}^{-1}. \end{aligned} \quad (10)$$

219 Finally,

$$p_{\text{rep}}^* = \begin{cases} 1 & \text{for analysis without OE} \\ 0.25 & \text{for analysis with OE} \end{cases} \quad t_{\text{rep}}^* = \begin{cases} 0 \text{ weeks} & \text{for analysis without OE} \\ 2 \text{ weeks} & \text{for analysis with OE} \end{cases} \quad (11)$$

220 where an “analysis with OE” is one in which we desire simulations of reported incidence
221 with observation error.

222 S5.1 Sensitivity to \mathcal{R}_0 and α

223 Fig 5 in the manuscript describes how $\beta(t)$ estimation error depends on features of $\beta(t)$
224 itself. For the seasonally forced $\beta(t)$ (Eq (5)), these features are the mean $\langle\beta\rangle$ and
225 amplitude α . Fig 5 casts error as a function of \mathcal{R}_0 and α , rather than $\langle\beta\rangle$ and α , but this
226 formulation is equivalent, because \mathcal{R}_0 is proportional to $\langle\beta\rangle$ (Eq (4)). It is also more
227 interpretable: unlike $\langle\beta\rangle$, \mathcal{R}_0 has a natural epidemiological meaning and is dimensionless
228 (its numerical value does not depend on the chosen units of time).

229 To reproduce Fig 5, we set all data-generating parameters other than $\langle\beta\rangle$ and α equal
230 to their reference value in (9). We consider the grid of (\mathcal{R}_0, α) pairs with levels
231 $\mathcal{R}_0 = 2, 3, \dots, 32$ and $\alpha = 0, 0.01, \dots, 0.2$ —defining $\langle\beta\rangle$ for each \mathcal{R}_0 using Eq (4)—and
232 simulate 1000 reported incidence time series using each of these 31×21 parametrizations.

```
Rnought <- seq(2, 32, by = 1)
alpha <- seq(0, 0.2, by = 0.01)
nsim <- 1000
```

233 We estimate $\beta(t)$ from each simulated reported incidence time series, without input error,
234 fit a loess curve $\beta_{\text{loess}}(t; q)$ to the raw estimate β_k , and record the RRMSE in $\beta_{\text{loess}}(t_k; q)$.
235 For comparison, this is done using both the S and SI methods. We fix $q = q^*$ (Eq (7))
236 independently of the β_k time series being smoothed. (See §S5.3 for discussion of the
237 consequences of using fixed q in this analysis.)

238 This algorithm is implemented in our function `test_s2dgbeta()` (“sensitivity to
239 data-generating $\beta(t)$ ”), which takes as arguments

- 240 ■ `par_list_ref`, a list containing the reference values of all data-generating
241 parameters;
- 242 ■ `Rnought` and `alpha`, numeric vectors specifying the desired grid of (\mathcal{R}_0, α) pairs;
- 243 ■ `with_dem_stoch`, a logical scalar indicating whether simulations should account for
244 demographic stochasticity;
- 245 ■ `nsim`, the number of simulations to perform using each (\mathcal{R}_0, α) pair;

246 ■ `loess_par`, a numeric vector of length 2 specifying the value of the loess smoothing
247 parameter q used when fitting loess curves to raw transmission rate estimates β_k .
248 `loess_par[1]` is used with the S method. `loess_par[2]` is used with the SI
249 method.

250 `s2dgbeta()` returns a 4-dimensional array, whose `[i, j, k, m]` th entry is the RRMSE
251 in an estimate of $\beta(t)$ (S method if `m = 1`, SI method if `m = 2`) from simulation k of
252 `nsim` using the (i, j) th (\mathcal{R}_0, α) grid point.

253 First, we consider simulations with environmental stochasticity ($\epsilon = 0.5$), without
254 demographic stochasticity, and without observation error ($p_{\text{rep}} = 1, t_{\text{rep}} = 0$).

```
rrmse_esxxxx <- test_s2dgbeta(  
  par_list_ref = make_par_list(epsilon = 0.5, prep = 1, trep = 0),  
  Rnaught      = Rnaught,  
  alpha        = alpha,  
  with_dem_stoch = FALSE,  
  nsim         = nsim,  
  loess_par    = qstar  
)  
save(rrmse_esxxxx, file = "RData/s2dgbeta_esxxxx.RData")
```

255 Second, we consider simulations with environmental stochasticity ($\epsilon = 0.5$), with
256 demographic stochasticity, and without observation error ($p_{\text{rep}} = 1, t_{\text{rep}} = 0$).

```
rrmse_esdsxx <- test_s2dgbeta(  
  par_list_ref = make_par_list(epsilon = 0.5, prep = 1, trep = 0),  
  Rnaught      = Rnaught,  
  alpha        = alpha,  
  with_dem_stoch = TRUE,  
  nsim         = nsim,  
  loess_par    = qstar  
)  
save(rrmse_esdsxx, file = "RData/s2dgbeta_esdsxx.RData")
```

257 Third, we consider simulations with environmental stochasticity ($\epsilon = 0.5$), with
258 demographic stochasticity, and with observation error ($p_{\text{rep}} = 0.25, t_{\text{rep}} = 2$ weeks).

```
rrmse_esdsoe <- test_s2dgbeta(  
  par_list_ref = make_par_list(epsilon = 0.5, prep = 0.25, trep = 2),  
  Rnaught      = Rnaught,  
  alpha        = alpha,  
  with_dem_stoch = TRUE,
```

```

    nsim          = nsim,
    loess_par     = qstar
  )
save(rrmse_esdsoe, file = "RData/s2dgbeta_esdsoe.RData")

```

259 We apply `get_rrmse_50pct()` to the output of `test_s2dgbeta()` in order to
 260 compute the median RRMSE in each set of `nsim` estimates of $\beta(t)$.

```

get_rrmse_50pct <- function(rrmse, method) {
  apply(rrmse[, , , method], c(1, 2), quantile, probs = 0.5)
}

```

261 `get_rrmse_50pct()` takes as arguments `rrmse` (any of the three arrays defined earlier)
 262 and `method` (`"S"` or `"SI"`). It returns an array whose `[i, j]`th entry is the median
 263 RRMSE for the (i, j) th (\mathcal{R}_0, α) grid point.

264 Fig 5 displays heatmaps of median RRMSE obtained from the output of
 265 `get_rrmse_50pct()`. There is one heatmap for each choice of the arguments `rrmse` and
 266 `method` (3×2 heatmaps in total). Navy fill indicates median RRMSE less than the
 267 minimum shown on the colour scale.

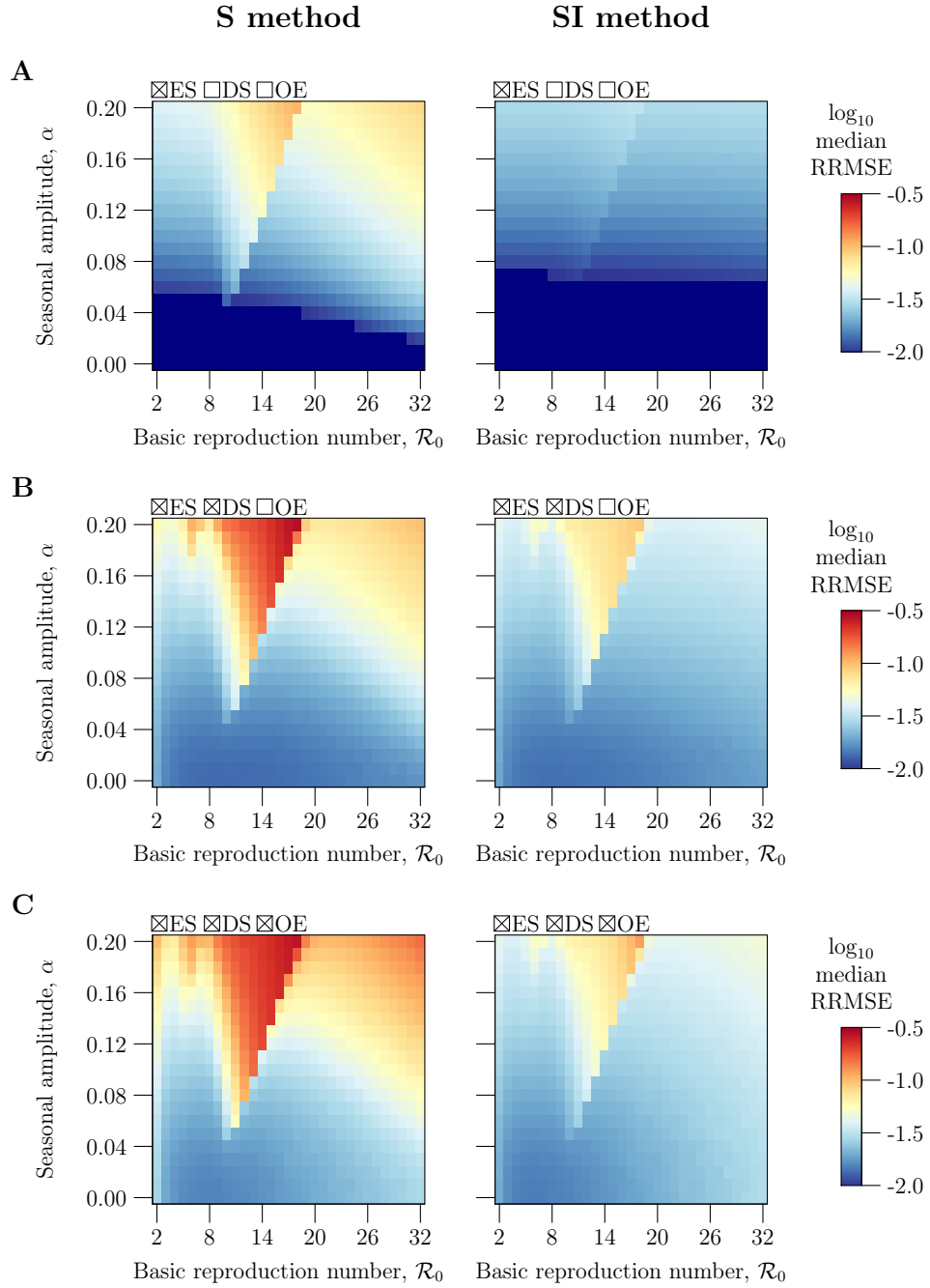


Fig 5. Sensitivity of $\beta(t)$ estimation error to the mean $\langle\beta\rangle$ and amplitude α of seasonal forcing. The $\langle\beta\rangle$ axis has been scaled to measure the basic reproduction number \mathcal{R}_0 (Eq (4)).

268 S5.2 Sensitivity to S_0 , I_0 , ν_c , μ_c , t_{gen} , and p_{rep}

269 Fig 6 describes how $\beta(t)$ estimation error varies as a function of data-generating
270 parameters other than $\langle\beta\rangle$ and α : the initial states S_0 and I_0 , vital rates ν_c and μ_c , mean
271 generation interval t_{gen} , and case reporting probability p_{rep} .

272 To reproduce Fig 6, we explore lines in the data-generating parameter space by
273 assigning all parameters their reference value in (9), except a focal parameter (one of S_0 ,
274 I_0 , ν_c , μ_c , t_{gen} , and p_{rep}), which we assign each of 41 values logarithmically spaced between
275 $\frac{1}{4}$ and 4 times its reference value. Using each of these 5×41 or 6×41 parametrizations (we
276 fix $p_{\text{rep}} = 1$ when we desire simulations without observation error), we simulate 1000
277 reported incidence time series.

```
scale_factors <- 2^seq(-2, 2, length.out = 41)
nsim <- 1000
```

278 We estimate $\beta(t)$ from each simulated reported incidence time series, without input error,
279 fit a loess curve $\beta_{\text{loess}}(t; q)$ to the raw estimate β_k , and record the RRMSE in $\beta_{\text{loess}}(t_k; q)$.
280 For comparison, this is done using both the S and SI methods. We fix $q = q^*$ (Eq (7))
281 independently of the β_k time series being smoothed. (See §S5.3 for discussion of the
282 consequences of using fixed q in this analysis.)

283 This algorithm is implemented in our function `test_s2dgpars()`. (“sensitivity to
284 data-generating parameters”). Its arguments are identical to those of `test_s2dgpars()`,
285 except, instead of `Rnaught` and `alpha`, `test_s2dgpars()` has arguments

- 286 ■ `pars_to_vary`, a character vector listing the data-generating parameters to be
287 treated as a focal parameter;
- 288 ■ `scale_factors`, a numeric vector listing the factors by which the reference value of
289 each focal parameter is scaled to obtain the grid of values considered for that
290 parameter.

291 `test_s2dgpars()` returns a 4-dimensional array, whose `[i, j, k, m]` th entry is the
292 RRMSE in an estimate of $\beta(t)$ (S method if `m = 1`, SI method if `m = 2`) from simulation
293 `k` of `nsim` in which `pars_to_vary[j]` is assigned its reference value times
294 `scale_factors[i]`.

295 First, we consider simulations with environmental stochasticity ($\epsilon = 0.5$), without
296 demographic stochasticity, and without observation error ($p_{\text{rep}} = 1$, $t_{\text{rep}} = 0$ weeks).

```
rrmse_esxxxx <- test_s2dgpars(
  pars_to_vary = c("S0", "I0", "nu", "mu", "tgen"),
  par_list_ref = make_par_list(epsilon = 0.5, prep = 1, trep = 0),
  scale_factors = scale_factors,
```

```

with_dem_stoch = FALSE,
nsim           = nsim,
loess_par      = qstar
)
save(rrmse_esxxxx, file = "RData/s2dgpars_esxxxx.RData")

```

297 Second, we consider simulations with environmental stochasticity ($\epsilon = 0.5$), with
298 demographic stochasticity, and without observation error ($p_{\text{rep}} = 1$, $t_{\text{rep}} = 0$ weeks).

```

rrmse_esdsxx <- test_s2dgpars(
  pars_to_vary   = c("S0", "I0", "nu", "mu", "tgen"),
  par_list_ref   = make_par_list(epsilon = 0.5, prep = 1, trep = 0),
  scale_factors  = scale_factors,
  with_dem_stoch = TRUE,
  nsim           = nsim,
  loess_par      = qstar
)
save(rrmse_esdsxx, file = "RData/s2dgpars_esdsxx.RData")

```

299 Third, we consider simulations with environmental stochasticity ($\epsilon = 0.5$), with
300 demographic stochasticity, and with observation error ($p_{\text{rep}} = 0.25$, $t_{\text{rep}} = 2$ weeks).

```

rrmse_esdsoe <- test_s2dgpars(
  pars_to_vary   = c("S0", "I0", "nu", "mu", "tgen", "prep"),
  par_list_ref   = make_par_list(prepare = 0.25, trep = 2),
  scale_factors  = scale_factors,
  with_dem_stoch = TRUE,
  nsim           = nsim,
  loess_par      = qstar
)
save(rrmse_esdsoe, file = "RData/s2dgpars_esdsoe.RData")

```

301 In this third analysis, when S_0 , I_0 , ν_c , μ_c , or t_{gen} is varied, p_{rep} is fixed and assigned its
302 reference value, 0.25. When p_{rep} itself is varied, we consider for p_{rep} each value in the vector
303 `scale_factors * 0.25`.

304 As with `test_s2dgbeta()`, we apply `get_rrmse_50pct()` to the output of
305 `test_s2dgpars()` in order to compute the median RRMSE in each set of `nsim` estimates
306 of $\beta(t)$.

307 Fig 6 displays the output of `get_rrmse_50pct()`, plotting median RRMSE as a
308 function of each data-generating parameter. To be precise, the horizontal axis measures the
309 ratio of the data-generating and reference values of the focal parameter, which ranges from

310 $\frac{1}{4}$ to 4 regardless of the focal parameter. This allows results for different parameters to be
 311 compared in one panel.

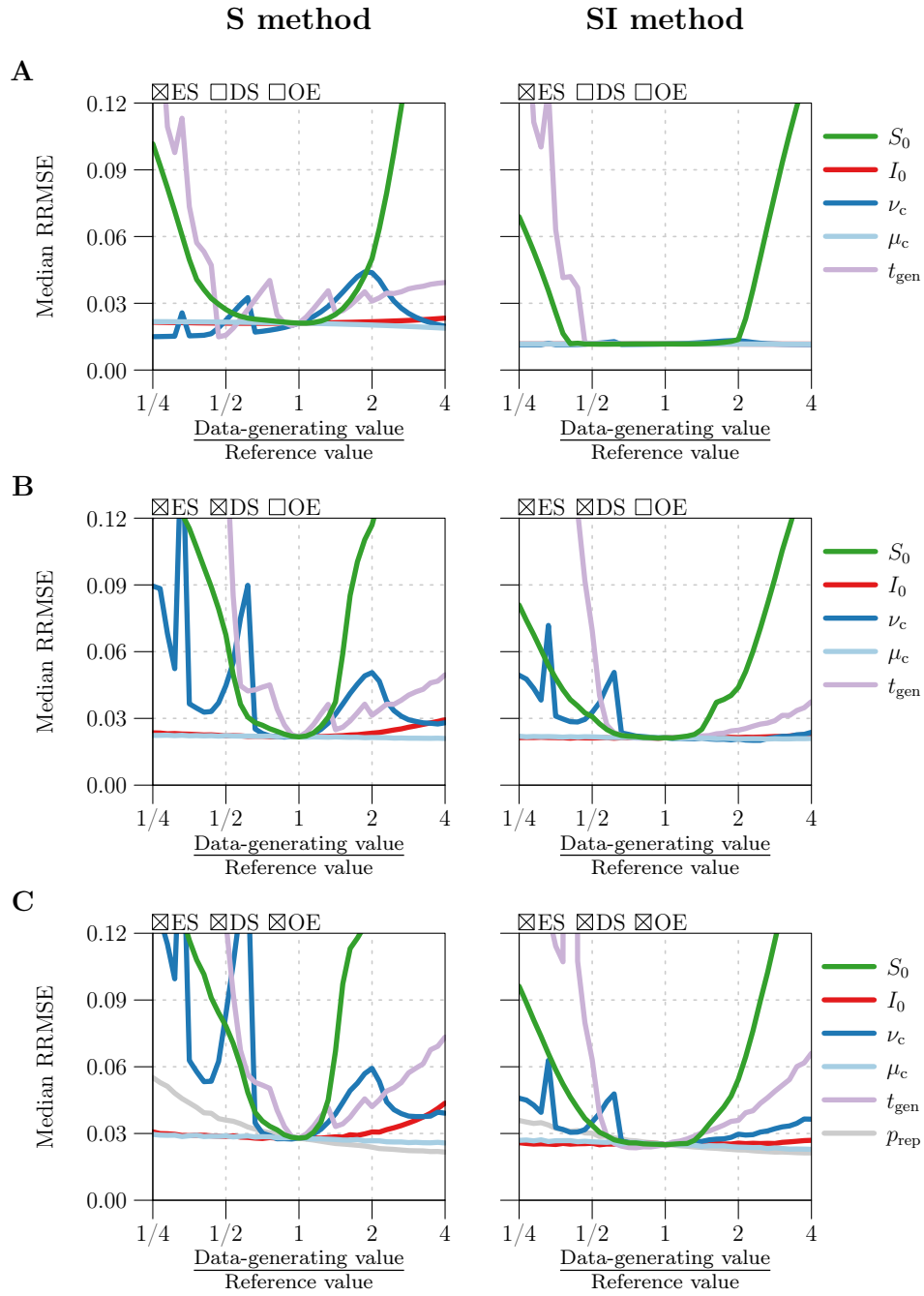


Fig 6. Sensitivity of $\beta(t)$ estimation error to data-generating parameters other than $\langle\beta\rangle$ and α .

312 S5.3 A note on smoothing

313 To generate Figs 5 and 6, we fixed $q = q^*$ (Eq (7)) when fitting loess curves $\beta_{\text{loess}}(t; q)$ to
314 raw transmission rate estimates β_k . For a given β_k time series, this setting may not have
315 been optimal ($q^* \neq q_{\text{opt}}$), meaning that the RRMSE calculated for $\beta_{\text{loess}}(t_k; q)$ was greater
316 with $q = q^*$ than it would have been had we found q_{opt} and used $q = q_{\text{opt}}$.

317 This is potentially problematic, because sensitivity to data-generating parameters is
318 mediated by propagation of noise from the simulated reported incidence data to β_k . We
319 may have observed less sensitivity to a parameter (for example, t_{gen} in Fig 6) had we
320 smoothed more when there was extreme noise in β_k (*i.e.*, had we set $q = q_{\text{opt}}$ when
321 $q_{\text{opt}} > q^*$). We did not do this, because finding q_{opt} for each of the 5×10^6 time series
322 considered by Figs 5 and 6 would have increased the total computation time by a factor of
323 100. Hence Figs 5 and 6 may overestimate the sensitivity of $\beta(t)$ estimation error to
324 data-generating parameters.

325 Nevertheless, we expect the quantitative effect of choosing q^* over q_{opt} to be relatively
326 small. Consider the graph corresponding to t_{gen} in the right panel of Fig 6C, which displays
327 median RRMSE close to (0.12, 0.03, 0.045) when t_{gen} is $(2^{-1.5}, 1, 2^{1.5}) \cdot 13$ days, respectively
328 (13 days being the reference value). For these values of t_{gen} , it is instructive to compare (i)
329 simulated reported incidence time series C_k , (ii) raw transmission rate estimates β_k from
330 C_k , and (iii) the corresponding loess estimates $\beta_{\text{loess}}(t; q^*)$ and $\beta_{\text{loess}}(t; q_{\text{opt}})$.

331 S5.3.1 C_k and β_k for $t_{\text{gen}} = (2^{-1.5}, 1, 2^{1.5}) \cdot 13$ days

332 First, we simulate a reported incidence time series C_k using each of $t_{\text{gen}} = (2^{-1.5}, 1, 2^{1.5}) \cdot 13$
333 days. All three simulations account for environmental stochasticity ($\epsilon = 0.5$), demographic
334 stochasticity, and observation error ($p_{\text{rep}} = 0.25$).

```
## List of reference parameter values
par_list_ref <- make_par_list(epsilon = 0.5, prep = 0.25)

## List of lists of data-generating parameter values
par_list <- mapply(make_par_list,
  tgen      = 2^c(-1.5, 0, 1.5) * par_list_ref$tgen,
  beta_mean = par_list_ref$beta_mean,
  Rnaught  = NA,
  epsilon  = 0.5,
  prep     = 0.25,
  SIMPLIFY = FALSE
)

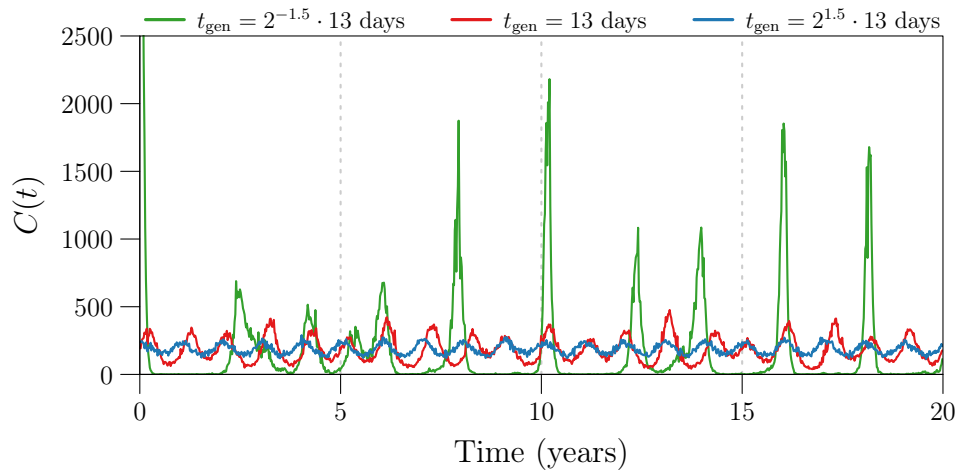
## List of data frames containing time series data
df <- mapply(make_data,
```

```

par_list = par_list,
n = 20 * 365 / 7,
with_dem_stoch = TRUE,
seed = c(1836, 6183, 3618),
SIMPLIFY = FALSE
)

```

335 Plotting each C_k time series yields the following result. Note that we are simply plotting
336 `df[[i]]$C` for $i = 1, 2, 3$.



337 We see that a period-doubling bifurcation occurs between $t_{\text{gen}} = 13$ days and
338 $t_{\text{gen}} = 2^{-1.5} \cdot 13$ days, with C_k attaining a much smaller minimum in the time series with a
339 2-year cycle (generated by $t_{\text{gen}} = 2^{-1.5} \cdot 13$ days).

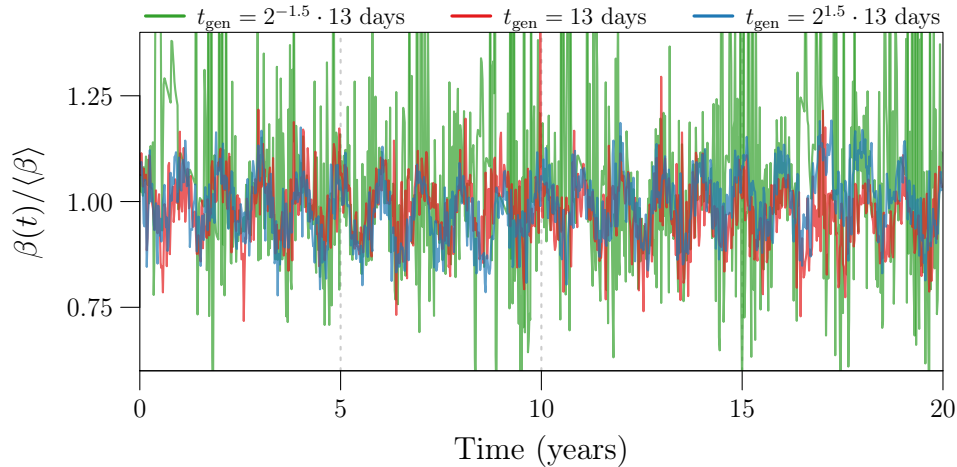
340 Due to much closer approaches to zero by incidence and prevalence with
341 $t_{\text{gen}} = 2^{-1.5} \cdot 13$ days, noise in C_k is amplified to a much greater extent in the raw
342 transmission rate estimate β_k . We show this by applying the SI method without input
343 error to estimate the underlying, seasonally forced transmission rate $\beta(t)$ (Eq (5))—which
344 was the same across simulations—from each C_k time series.

```

## List of data frames containing estimation output
df_est <- mapply(estimate_beta_SI,
  df = df,
  par_list = par_list,
  SIMPLIFY = FALSE
)

```

345 Plotting β_k shows that, indeed, propagation of noise from C_k to β_k is much more severe
346 when $t_{\text{gen}} = 2^{-1.5} \cdot 13$ days. Note that we are simply plotting `df_est[[i]]$beta`, scaled
347 by `with(par_list, 1/beta_mean)`, for $i = 1, 2, 3$.



348 We calculate the RRMSE in each of these estimates as follows.

```

rrmse_raw <- mapply(
  function(x, y) compute_rrmse(x$beta, y$beta),
  x = df,
  y = df_est
)
rrmse_raw

## [1] 0.26917391 0.06715921 0.05893578

```

349 S5.3.2 $\beta_{\text{loess}}(t; q^*)$ and $\beta_{\text{loess}}(t; q_{\text{opt}})$ for $t_{\text{gen}} = (2^{-1.5}, 1, 2^{1.5}) \cdot 13$ days

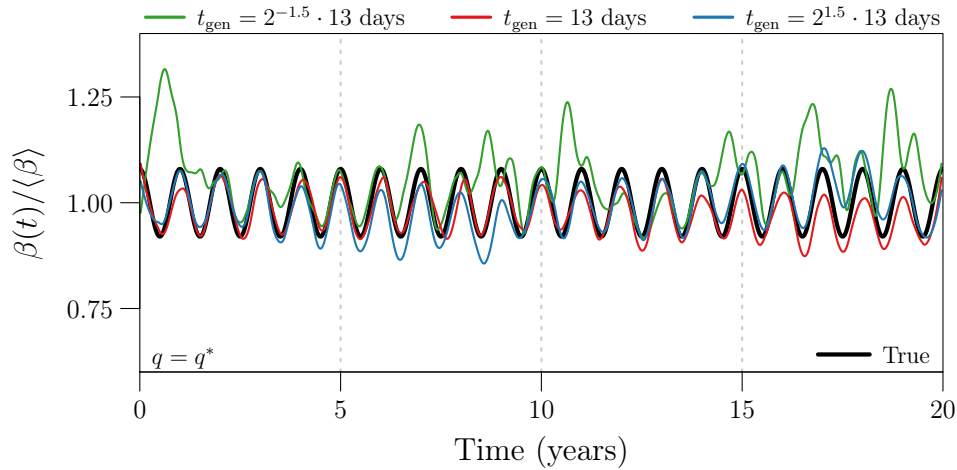
350 All three of these estimates of $\beta(t)$ are greatly improved with loess smoothing. First, we
 351 consider smoothing all three β_k time series with $q = q^*$.

```

## List of `loess` objects encoding the fitted loess curves
loess_fit <- lapply(df_est,
  function(x) {
    loess(
      formula = beta ~ t,
      data = x,
      span = qstar["SI"] / nrow(x),
      degree = 2,
      na.action = "na.exclude",
      control = loess.control(surface = "direct")
    )
  }
)

```

352 Plotting these loess estimates $\beta_{\text{loess}}(t; q^*)$ yields the following result. Note that we are
 353 plotting (with a scaling) `predict(loess_fit[[i]])` for $i = 1, 2, 3$.



354 We calculate the RRMSE in each of these estimates as follows.

```
rmse_loess_qstar <- mapply(
  function(x, y) compute_rrmse(x$beta, predict(y)),
  x = df,
  y = loess_fit
)
rmse_loess_qstar

## [1] 0.10502016 0.03356297 0.03478337
```

355 Next, we consider smoothing each β_k time series with $q = q_{\text{opt}}$. Of course, we must first
 356 find q_{opt} .

```
q <- 10:150

## Array of values of RRMSE. Entry `[i, j]` contains the RRMSE
## in the loess estimate obtained from `df_est[[j]]$beta` using
## `q[i]` for the loess smoothing parameter.
rmse_loess <- mapply(
  function(x, y) {
    sapply(q, function(z) {
      loess_fit <- loess(
        formula = beta ~ t,
        data = y,
        span = z / nrow(y),
        degree = 2,

```

```

    na.action = "na.exclude",
    control   = loess.control(
      surface   = "direct",
      statistics = "none"
    )
  )
  compute_rrmse(x$beta, predict(loess_fit))
})
},
x = df, y = df_est, SIMPLIFY = TRUE
)
dim(rrmse_loess)

## [1] 141  3

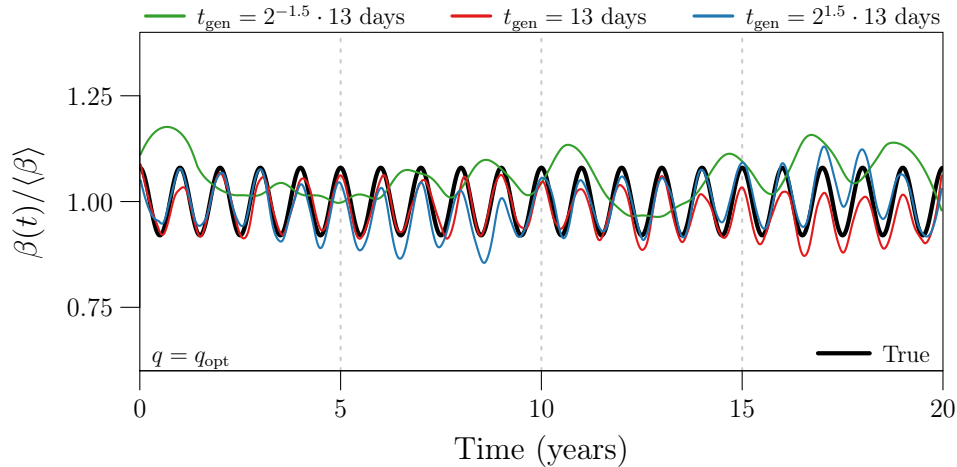
## Optimal value for loess smoothing parameter is that
## which minimizes RRMSE
qopt <- apply(rrmse_loess, 2, function(x) q[which.min(x)])
qopt

## [1] 150  50  52

## List of `loess` objects encoding the fitted loess curves
loess_fit <- mapply(
  function(x, y) {
    loess(
      formula   = beta ~ t,
      data      = x,
      span      = y / nrow(x),
      degree    = 2,
      na.action = "na.exclude",
      control   = loess.control(surface = "direct")
    )
  },
  x = df_est, y = qopt, SIMPLIFY = FALSE
)

```

357 As expected, the β_k time series corresponding to $t_{\text{gen}} = 2^{-1.5} \cdot 13$ days requires the most
358 smoothing (greatest q_{opt}). Plotting these *optimal* loess estimates $\beta_{\text{loess}}(t; q_{\text{opt}})$ yields the
359 following result. Once again, we are plotting (with a scaling) `predict(loess_fit[[i]])`
360 for $i = 1, 2, 3$.



361 The RRMSE in each of these estimates is calculated as before.

```

rrmse_loess_qopt <- mapply(
  function(x, y) compute_rrmse(x$beta, predict(y)),
  x = df,
  y = loess_fit
)
rrmse_loess_qopt

## [1] 0.09848373 0.03346263 0.03475891

```

362 S5.3.3 Discussion

363 Comparing β_k , $\beta_{\text{loess}}(t; q^*)$, and $\beta_{\text{loess}}(t; q_{\text{opt}})$ for each value of t_{gen} , we find that when noise
 364 in β_k is severe (in this example, when $t_{\text{gen}} = 2^{-1.5} \cdot 13$ days), even an optimal degree of
 365 smoothing cannot recover the true $\beta(t)$ from the noise, due to underlying bias. No amount
 366 of variance reduction can correct the error due to bias. For this reason, smoothing β_k using
 367 q^* for the loess smoothing parameter q was never much worse than smoothing using the
 368 optimal value q_{opt} , even when $q^* \ll q_{\text{opt}}$ (as was the case with $t_{\text{gen}} = 2^{-1.5} \cdot 13$ days):

```

## Summary of results
data.frame(
  rrmse_raw,
  qstar = as.numeric(qstar["SI"]),
  rrmse_loess_qstar,
  qopt,
  rrmse_loess_qopt
)

```

##	rrmse_raw	qstar	rrmse_loess_qstar	qopt	rrmse_loess_qopt
## 1	0.26917391	53	0.10502016	150	0.09848373
## 2	0.06715921	53	0.03356297	50	0.03346263
## 3	0.05893578	53	0.03478337	52	0.03475891

369 This suggests that the decision to fix $q = q^*$ when generating Figs 5 and 6 does not greatly
370 mischaracterize the effect of parameters like t_{gen} on $\beta(t)$ estimation error. Had we found
371 q_{opt} for each raw estimate β_k , we would have calculated quantitatively similar RRMSE.

372 S6 Sensitivity to error in input parameters

373 Error in estimates of the seasonally forced transmission rate (Eq (5)) from simulated
374 reported incidence data is also a function of the user-specified values of input parameters,
375 given by

$$\theta' = (S'_0, I'_0, \nu'_c, \mu'_c, t'_{\text{gen}}, p'_{\text{rep}}, t'_{\text{rep}}). \quad (12)$$

376 Input error arises when the user’s input mischaracterizes the data-generating process. In
377 our simulated data setting, this occurs when the specified value of an input parameter
378 differs from the value used to simulate data (*e.g.*, when $S'_0 \neq S_0$, and so on).

379 Fig 7A in the manuscript describes how $\beta(t)$ estimation error varies as a function of
380 input error. To reproduce Fig 7A, we simulate 1000 reported incidence time series using the
381 reference values in (9) for all data-generating parameters. From each reported incidence
382 time series, we estimate the underlying $\beta(t)$ using the S and SI methods with different
383 errors in the input. Specifically, we explore lines in the input parameter space by assigning
384 all input parameters their true (data-generating) value, except a focal parameter (one of
385 $S_0, I_0, \nu_c, \mu_c, t_{\text{gen}}, p_{\text{rep}}$, and t_{rep}), which we assign each of 41 values logarithmically spaced
386 between $\frac{1}{4}$ and 4 times its true value. Hence, in total, we consider 7×41 parametrizations
387 of the S and SI methods. We fit loess curves $\beta_{\text{loess}}(t; q)$ to each raw transmission rate
388 estimate β_k generated in this process, fixing $q = q^*$ (Eq (7)), and record the RRMSE in
389 $\beta_{\text{loess}}(t_k; q^*)$ (See §S6.1 for discussion of the consequences of using fixed q in this analysis.)

390 The above algorithm is implemented in our function `test_s2inpars()` (“sensitivity to
391 input parameters”), which takes as arguments

- 392 ■ `par_list_ref`, a list containing values for all data-generating parameters, used in
393 all simulations;
- 394 ■ `pars_to_vary`, a character vector listing the input parameters to be treated as a
395 focal parameter;
- 396 ■ `scale_factors`, a numeric vector listing the factors by which the data-generating
397 value of each focal parameter is scaled to obtain the grid of input values considered
398 for that parameter;

- 399 ■ `with_dem_stoch`, a logical scalar indicating whether simulations should account for
400 demographic stochasticity;
- 401 ■ `nsim`, the number of simulations to perform;
- 402 ■ `loess_par`, a numeric vector of length 2 specifying the value of the loess smoothing
403 parameter q used when fitting loess curves to raw transmission rate estimates β_k .
404 `loess_par[1]` is used with the S method. `loess_par[2]` is used with the SI
405 method.

406 `test_s2inpars()` returns a 4-dimensional array, whose `[i, j, k, m]` th entry is the
407 RRMSE in the estimate of $\beta(t)$ from simulation k of `nsim`, generated by assigning
408 `pars_to_vary[j]` its true (data-generating) value times `scale_factors[i]` in the input
409 to the S (`m = 1`) or SI (`m = 2`) method.

410 We reproduce Fig 7A starting with the following call to `test_s2inpars()`.

```

rrmse_esdsoe <- test_s2inpars(
  pars_to_vary   = c("S0", "I0", "nu", "mu", "tgen", "prep", "trep"),
  par_list_ref   = make_par_list(epsilon = 0.5, prep = 0.25, trep = 2),
  scale_factors  = 2^seq(-2, 2, length.out = 41),
  with_dem_stoch = TRUE,
  nsim           = 1000,
  loess_par      = qstar
)
save(rrmse_esdsoe, file = "RData/s2inpars_esdsoe.RData")

```

411 Fig 7A plots the median RRMSE obtained with each parametrization of the SI method.
412 We retrieve medians from `rrmse_esdsoe` in the next code chunk. Note that some
413 parametrizations cause the SI method to fail. For example, modest underestimation of ν_c
414 by ν'_c or of p_{rep} by p'_{rep} causes S_k —the SI method estimate of $S(t_k)$ —to become negative.
415 When this happens, `test_s2inpars()` assigns RRMSE the value `NA`. Below, we
416 calculate the median RRMSE only for those parametrizations that yield a full set of 1000
417 values of RRMSE (no `NA`s).

```

## Preallocate memory for median RRMSE:
## one value for each parametrization of the SI method
rrmse_50pct <- NA * rrmse_esdsoe[, , 1, "SI"]
dim(rrmse_50pct)

## [1] 41 7

## Define vector indexing parametrizations for which RRMSE

```

```

## was never `NA`
ind_no_na <- which(
  apply(!is.na(rrmse_esdsoe[, , , "SI"]), c(1, 2), all)
)

## Calculate median RRMSE for the indexed parametrizations
rrmse_50pct[ind_no_na] <- sapply(ind_no_na, function(i) {
  ai <- arrayInd(i, dim(rrmse_50pct))
  quantile(rrmse_esdsoe[ai[1], ai[2] , , "SI"],
    probs = 0.5,
    na.rm = TRUE
  )
})

```

418 Fig 7B repeats the analysis from Fig 7A concerning mis-specification of S_0 , except with
 419 initially erroneous estimates of S_0 corrected using peak-to-peak iteration (PTPI; see §S7
 420 below for an actual illustration of this technique) before being passed to the S and SI
 421 methods. We generate results with PTPI by repeating the last call to `test_s2inpars()`
 422 with the additional argument `ptpi_iter = 25`, indicating that PTPI should be employed
 423 and stopped after 25 iterations. Since PTPI only affects results for S_0 , we set
 424 `pars_to_vary = "S0"`.

```

rrmse_esdsoe_ptpi <- test_s2inpars(
  pars_to_vary = "S0",
  par_list_ref = make_par_list(epsilon = 0.5, prep = 0.25, trep = 2),
  scale_factors = 2^seq(-2, 2, length.out = 41),
  with_dem_stoch = TRUE,
  nsim = 1000,
  loess_par = qstar,
  ptpi_iter = 25
)
save(rrmse_esdsoe_ptpi, file = "RData/s2inpars_esdsoe_ptpi.RData")

```

425 There are no issues with RRMSE being assigned `NA` in this analysis, so calculating median
 426 RRMSE is more straightforward.

```

rrmse_ptpi_50pct <- apply(
  rrmse_esdsoe_ptpi[, "S0", , "SI"], 1, quantile,
  probs = 0.5,
  names = FALSE
)

```

427 We reproduce Fig 7 by plotting median RRMSE—saved in `rrmse_50pct` and
 428 `rrmse_ptpi_50pct`—as a function of the ratio of the specified value of the focal
 429 parameter to the true (data-generating) value.

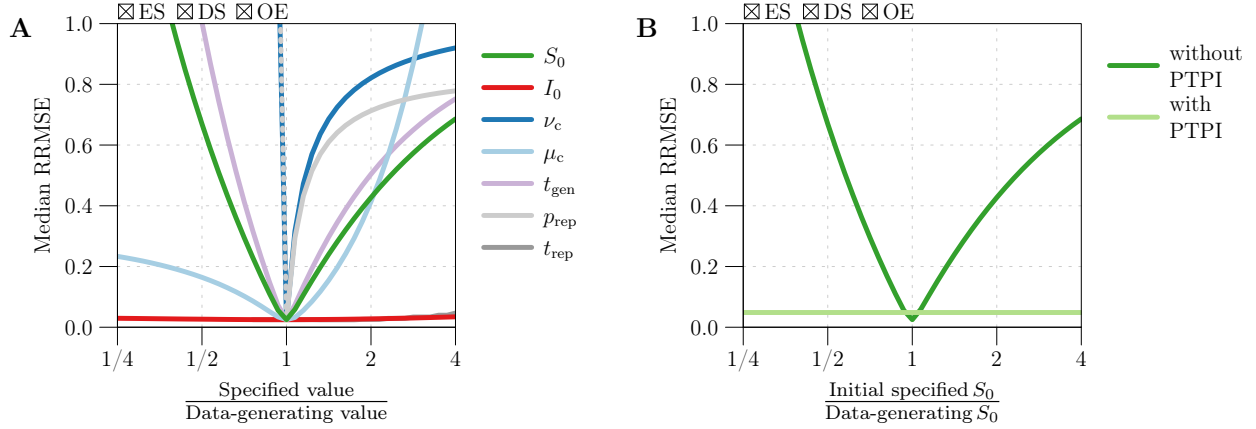


Fig 7. Sensitivity of $\beta(t)$ estimation error to the user-specified values of input parameters.

430 S6.1 A note on smoothing

431 The exact choice of the loess smoothing parameter q in this analysis is not critical, because
 432 error in the raw transmission rate estimate β_k is primarily due to bias caused by
 433 mis-specified input parameters. Moderate oversmoothing or undersmoothing of β_k has a
 434 negligible effect on RRMSE when β_k is extremely biased. (Fig 8 in the manuscript shows
 435 this clearly for the case of mis-specified S_0 .) Hence the decision to fix $q = q^*$ (Eq (7)) as
 436 done here does not have a visible quantitative effect.

437 S7 Estimating S_0 via PTPI: Example

438 Fig 8 in the manuscript illustrates the use of peak-to-peak iteration (PTPI) to estimate the
 439 initial number of susceptible individuals $S_0 = S(t_0)$ from times series Z_k , B_k , and μ_k of
 440 (estimated) incidence, births, and the *per capita* natural mortality rate. The PTPI
 441 algorithm relies on the following:

- 442 (a) Periodicity of Z_k , meaning that Z_k displays recurrent epidemics.
- 443 (b) Accuracy of Z_k , B_k , and μ_k . Systematic errors in these time series bias the
 444 reconstruction of susceptibles by PTPI, and ultimately the estimate of S_0 to which
 445 the iterations converge. This makes sense, given that susceptible dynamics are the
 446 direct result of imbalance between susceptible recruitment through birth and
 447 susceptible depletion through infection and death.

448 To reproduce Fig 8, we simulate a reported incidence time series C_k with known
 449 underlying S_0 (to be estimated).

```
## List of data-generating parameter values
par_list <- make_par_list(epsilon = 0.5, prep = 0.25)

## Data frame containing time series data
df <- make_data(
  par_list      = par_list,
  n             = 20 * 365 / 7,
  with_dem_stoch = TRUE,
  seed         = 1350
)

## True value of `S0` to be estimated
df$S[1]

## [1] 54052
```

450 We estimate true incidence Z from reported incidence C_k as in the SI method:

$$Z(t_k) \approx Z_k = \frac{1}{p_{\text{rep}}} C_{k+r}, \quad r = \frac{[t_{\text{rep}}]_{\Delta t}}{\Delta t}, \quad (13)$$

451 We do this using the true (data-generating) values of p_{rep} and t_{rep} , so that Z_k estimates Z
 452 without systematic error. (We consider this ideal case in order to demonstrate the validity
 453 of the PTPI algorithm. The sensitivity of the method to input error is not explored here
 454 explicitly, but is likely captured by the expressions for $\text{Err}(S_k, \xi \leftarrow \omega\xi)$ derived in §2.7.2 of
 455 the manuscript.)

```
## Time series of estimated incidence
Z <- estimate_beta_SI(df, par_list)$Z
```

456 We will pass this Z_k time series to the PTPI algorithm. The complete algorithm consists of
 457 a truncation step, described in Box 4 in the manuscript, followed by an iteration step,
 458 described in Box 5 in the manuscript. Below, we explain their implementation in R,
 459 generating Fig 8 in the process.

460 S7.1 Truncation step

461 The goal of the truncation step is to find the time t_a of the first peak in \bar{Z}_k and the time t_b
 462 of the last peak occurring at the same phase of the cycle. Here, \bar{Z}_k is a central moving
 463 average applied to the Z_k time series to remove unwanted noise. (Noise creates “peaks” in
 464 Z_k that we wish to ignore.)

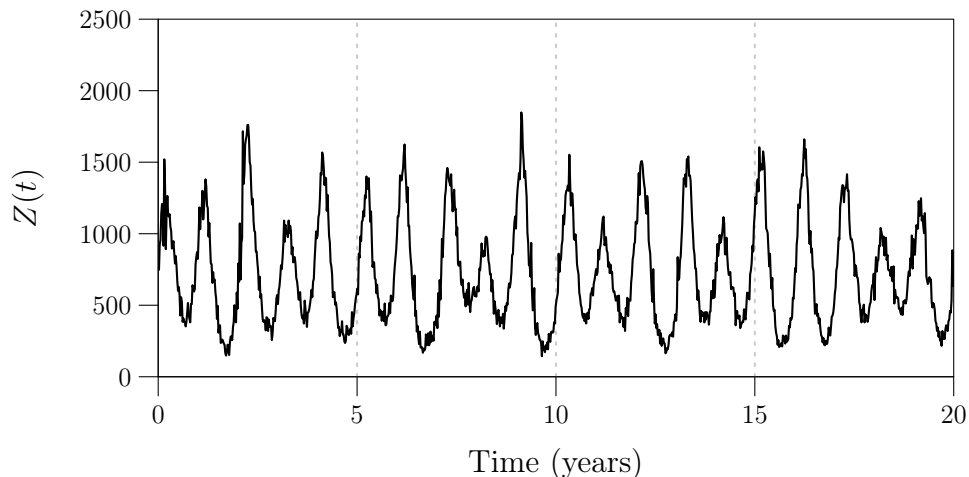
465 Our function `get_peak_times()` automates the task of (i) applying a central moving
 466 average to any equally spaced, (roughly) periodic time series, then (ii) finding peak times.
 467 It takes as arguments

- 468 ■ `x`, a numeric vector specifying an equally spaced, (roughly) periodic time series;
- 469 ■ `period`, a numeric scalar specifying the period of `x` in units of the observation
 470 interval;
- 471 ■ `bw_mavg`, an integer scalar (a bandwidth) indicating that the central moving average
 472 applied to `x` should include `2 * bw_mavg + 1` points;
- 473 ■ `bw_peakid`, an integer scalar (a bandwidth) indicating that `x_mavg[i]` should be
 474 considered a peak if and only if `x_mavg[i] > x_mavg[j]` for all `j` such that
 475 `0 < |i - j| < bw_peakid`.

476 In the last item above, `x_mavg` is a vector of length `length(x)` containing the central
 477 moving average applied to `x`. `x_mavg[i]` is equal to
 478 `mean(x[(i-bw_mavg):(i+bw_mavg)])` for all `i` from `bw_mavg+1` to `length(x)-bw_mavg`,
 479 and equal to `NA` everywhere else (*i.e.*, at the the edges).

480 `get_peak_times()` returns a list containing `x_mavg` and two index vectors `all` and
 481 `phase`. `all` indexes all peaks in `x_mavg`, while `phase` indexes only those peaks in phase
 482 with the first peak (and is therefore a subset of `all`).

483 Before we construct a call to `get_peak_times()`, we must ascertain that our time
 484 series Z_k of estimated incidence is roughly periodic and determine the period. Plotting Z_k ,
 485 it is clear that it is periodic with a 1-year cycle.



486 In general, it may be helpful to inspect the power spectrum of Z_k to determine the period,
 487 but we do not do this here.

488 We locate the peaks in \bar{Z}_k with the following call to `get_peak_times()`.

```

## List of index vectors for peaks in incidence time series
peaks <- get_peak_times(
  x      = Z,
  period = with(par_list, (365 / 7) / dt_weeks),
  bw_mavg = 6,
  bw_peakid = 8
)

## All peaks
peaks$all[1:10]

## [1] 61 118 171 218 274 322 383 429 478 539

## All peaks in phase with first
peaks$phase[1:10]

## [1] 61 118 171 218 274 322 383 429 478 539

```

489 Above, we assigned `period` the value of 1 year in units of the observation interval. We
490 chose bandwidths `bw_mavg = 6` and `bw_peakid = 8` using a simple tuning procedure.
491 First, we chose the smallest value of `bw_mavg` that eliminated noise near peaks in Z_k . This
492 was determined by visual inspection of the moving average \bar{Z}_k (`peaks$x_mavg`). Next, we
493 chose an arbitrary value of `bw_peakid` greater than 5 and less than half of `period`. This
494 ensured that the definition of a peak was meaningful (a point greater than many of its
495 nearest neighbours) and that peaks were not being compared against other peaks. The
496 exact choice of `bw_peakid` tends not to be critical provided \bar{Z}_k is smooth near the peaks.

497 Note that the two index vectors `all` and `phase` returned by `get_peak_times()` are
498 identical. In this example, all peaks in \bar{Z}_k are in phase, because the time between peaks is
499 precisely the period (1 year). This is not true in general. For example, a 2-year cycle can
500 have major and minor peaks that are out of phase. In this case, `all` would index both
501 major and minor peaks, but `phase` would index either minor peaks or major peaks (but
502 not both).

503 Plotting true incidence Z (`df$Z`), estimated incidence Z_k (`Z`), and the central moving
504 average \bar{Z}_k (`peaks$x_mavg`), as well as indicators of the times of peaks in \bar{Z}_k in phase
505 with the first peak (`peaks$phase`), we reproduce Fig 8A (see below). Fig 8A verifies that
506 all of the peaks of interest were identified by `get_peak_times()`.

507 We conclude the truncation step of the PTPI algorithm by retrieving the index of the
508 first peak in \bar{Z}_k and the index of the last peak occurring at the same phase of the cycle.

```
## Index of first peak
a <- with(peaks, phase[1])
## Index of last peak in phase with first peak
b <- with(peaks, phase[length(phase)])
```

509 The precise times t_a and t_b of these peaks are given by `df$t[c(a, b)]`.

510 S7.2 Iteration step

511 The goal of the iteration step is to use times series Z_k , B_k , and μ_k of (estimated) incidence,
 512 births, and the *per capita* natural mortality rate to iteratively update an initial estimate of
 513 $S_0 = S(t_0)$. This updating procedure depends on the result of the truncation step. The
 514 iteration step is implemented in our function `ptpi()`, which takes as arguments

- 515 ■ `df`, a data frame with columns `Z`, `B`, and `mu` specifying time series Z_k , B_k and μ_k
 516 of (estimated) incidence, births, and the *per capita* natural mortality rate;
- 517 ■ `par_list`, a list with elements `hatN0`, `nu`, and `mu`, specifying a population size
 518 \hat{N}_0 and constant vital rates ν_c and μ_c , which are used to create mock vital data in the
 519 event that `df` does not possess columns `B` or `mu` (`ptpi()` will set $B_k = \nu_c \hat{N}_0 \Delta t$
 520 and $\mu_k = \mu_c$ for all k);
- 521 ■ `a`, an integer scalar indicating the index of the first peak in `df$Z`;
- 522 ■ `b`, an integer scalar indicating the index of the last peak in `df$Z` in phase with the
 523 first peak;
- 524 ■ `initial_S0_est`, a numeric scalar indicating an initial estimate of S_0 ;
- 525 ■ `iter`, an integer scalar indicating the number of iterations to perform before
 526 stopping.

527 We carry out the iteration step with the following call to `ptpi()`. For this example,
 528 we suppose that our initial guess of S_0 is 4 times greater than its true value, and ask for
 529 our estimate to be updated 25 times. We provide the peak indices `a` and `b` obtained in
 530 the truncation step (see above). Finally, in the first argument, we specify our incidence
 531 time series and nothing else, and in the second argument, we specify the data-generating
 532 values of \hat{N}_0 , ν_c , and μ_c . This means that `ptpi()` will construct mock vital data without
 533 any systematic error and use it in conjunction with the supplied incidence time series.

```
## List containing PTPI output
ptpi_out <- ptpi(
  df = data.frame(Z),
```

```

par_list      = par_list,
a             = a,
b             = b,
initial_S0_est = df$S[1] * 4,
iter         = 25
)

```

534 `ptpi()` returns a list with elements

- 535 ■ `S_mat`, a numeric matrix with `nrow(df)` rows and `iter+1` columns, containing the
536 susceptible time series generated in each iteration;
- 537 ■ `S0`, a numeric vector of length `iter+1` listing the initial estimate of $S_0 = S(t_0)$ and
538 the estimate obtained in each iteration (equivalent to `S_mat[1,]`);
- 539 ■ `S0_final`, a numeric scalar indicating the final estimate of S_0 (equivalent to
540 `S0[length(S0)]`);
- 541 ■ `SA`, a numeric vector of length `iter+1` listing the initial estimate of $S_a = S(t_a)$
542 (equal to the initial estimate of S_0) and the estimate obtained in each iteration
543 (equivalent to `S_mat[a,]`);
- 544 ■ `SA_final`, a numeric scalar indicating the final estimate of S_a (equivalent to
545 `SA[length(SA)]`).

546 Examining `ptpi_out`, we find that the iterations converged to an accurate estimate of S_0 .

```

## Ordered estimates of `S0`
ptpi_out$S0

## [1] 216208.00 138745.04 94654.54 73216.89 62793.50 57725.45 55261.27
## [8] 54063.13 53480.58 53197.33 53059.61 52992.64 52960.09 52944.26
## [15] 52936.56 52932.82 52931.00 52930.11 52929.68 52929.47 52929.37
## [22] 52929.32 52929.30 52929.29 52929.28 52929.28

## Relative error in final estimate of S0
(ptpi_out$S0_final - df$S[1]) / df$S[1]

## [1] -0.02077116

```

547 Fig 8B (see below) displays the `iter+1` susceptible time series S_k obtained in each
548 iteration of PTPI. To reproduce Fig 8B, we plot the columns of `ptpi_out$S_mat`, scaled
549 by `with(par_list, 1/N0)`.

```
## Matrix with ordered susceptible time series as columns
ptpi_out$S_mat[1:10, 1:5]
```

```
##      [,1]      [,2]      [,3]      [,4]      [,5]
## [1,] 216208 138745.0 94654.54 73216.89 62793.50
## [2,]      NA 138657.8 94601.07 73179.87 62764.47
## [3,]      NA 138394.6 94371.71 72966.93 62559.52
## [4,]      NA 138099.7 94110.54 72722.18 62322.74
## [5,]      NA 137625.1 93669.64 72297.67 61906.22
## [6,]      NA 137078.8 93157.10 71801.53 61418.04
## [7,]      NA 136581.0 92692.94 71353.74 60978.22
## [8,]      NA 136327.4 92473.04 71150.21 60782.64
## [9,]      NA 135470.3 91649.54 70343.06 59983.44
## [10,]     NA 134793.7 91006.60 69716.46 59364.78
```

550 Note that the first column contains `NA`, but only up to index `a` (not shown), where the
551 first iteration starts.

552 Fig 8C (see below) displays the SI method estimate of the transmission rate
553 corresponding to each estimate of S_0 listed in `ptpi_out$S0`. To reproduce Fig 8C, we pass
554 each estimate of S_0 to `estimate_beta_SI()`, specifying the true (data-generating) value
555 of every other input parameter. We fit a loess curve $\beta_{\text{loess}}(t; q^*)$ to each raw transmission
556 rate estimate β_k , and record $\beta_{\text{loess}}(t_k; q^*)$ as a column in a matrix `beta_mat`. Finally we
557 plot the columns of `beta_mat`, scaled by `with(par_list, 1/beta_mean)`.

```
## Matrix with ordered transmission rate time series as columns
beta_mat <- sapply(ptpi_out$S0,
  function(x) {
    par_list_with_err <- within(par_list, S0 <- x)
    df_est <- estimate_beta_SI(df, par_list_with_err)
    loess_fit <- loess(
      formula = beta ~ t,
      data = df_est,
      span = qstar["SI"] / nrow(df_est),
      degree = 2,
      na.action = "na.exclude",
      control = loess.control(surface = "direct")
    )
    predict(loess_fit)
  }
)
beta_mat[1:10, 1:5]
```

```
##           [,1]           [,2]           [,3]           [,4]           [,5]
## [1,]           NA           NA           NA           NA           NA
## [2,] 2.978043e-06 4.632868e-06 6.774538e-06 8.736727e-06 1.016727e-05
## [3,] 2.925529e-06 4.557144e-06 6.675664e-06 8.623999e-06 1.004922e-05
## [4,] 2.875193e-06 4.484526e-06 6.580771e-06 8.515711e-06 9.935726e-06
## [5,] 2.827043e-06 4.415025e-06 6.489875e-06 8.411877e-06 9.826795e-06
## [6,] 2.781082e-06 4.348645e-06 6.402980e-06 8.312501e-06 9.722428e-06
## [7,] 2.737311e-06 4.285386e-06 6.320081e-06 8.217575e-06 9.622613e-06
## [8,] 2.695731e-06 4.225250e-06 6.241182e-06 8.127098e-06 9.527348e-06
## [9,] 2.656352e-06 4.168251e-06 6.166301e-06 8.041095e-06 9.436658e-06
## [10,] 2.619180e-06 4.114399e-06 6.095452e-06 7.959580e-06 9.350560e-06
```

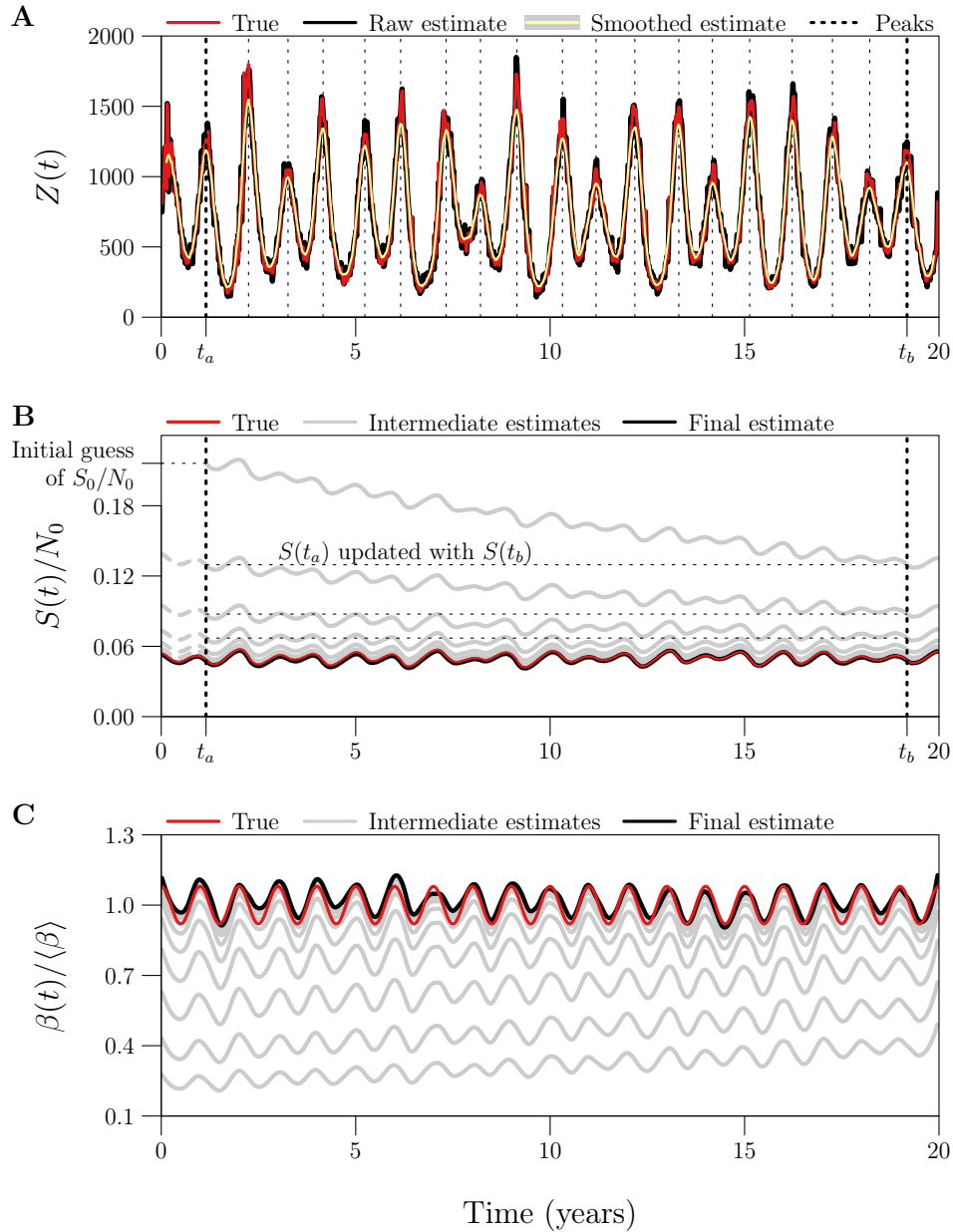


Fig 8. Example of $S(t)$ and $\beta(t)$ reconstruction with an overestimate of S_0 corrected by peak-to-peak iteration.

558 **S8 Estimating S_0 via PTPI: Convergence**

559 Fig 9 in the manuscript displays the result of applying PTPI (25 iterations) to estimate S_0
 560 from 1000 realizations of a reported incidence time series, starting from each of two initial

561 guesses: $\frac{1}{4}$ and 4 times the true value. The aim of this analysis is to assess the bias and
562 variance in the limiting estimate of S_0 .

563 To reproduce Fig 9, we record the estimate obtained at each iteration (for each initial
564 guess and simulation) in an array. The following code chunk preallocates space for this
565 output and creates a list of parameter values to be used in simulations of reported
566 incidence.

```
## Array with entry `[i, j, k]` equal to the `i`th estimate of `S0`  
## generated from the `j`th initial guess and the `k`th simulated  
## reported incidence time series  
out <- array(NA, dim = c(26, 2, 1000))  
  
## List of data-generating parameter values  
par_list <- make_par_list(epsilon = 0.5, prep = 0.25)
```

567 The next code chunk fills in the `out` array with our desired output and saves it in
568 `RData/ptpi_convergence.RData`.

```
for (k in 1:1000) {  
  ## Data frame containing time series data  
  df <- make_data(  
    par_list      = par_list,  
    n             = 20 * 365 / 7,  
    with_dem_stoch = TRUE,  
    seed = k  
  )  
  
  ## PTPI: truncation step  
  Z <- estimate_beta_SI(df, par_list)$Z  
  peaks <- get_peak_times(  
    x      = Z,  
    period = with(par_list, (365 / 7) / dt_weeks),  
    bw_mavg = 6,  
    bw_peakid = 8  
  )  
  
  ## PTPI: iteration step  
  out[, , k] <- sapply(c(0.25, 4),  
    function(x) {  
      ptpi_out <- ptpi(  
        df      = data.frame(Z),  
        par_list = par_list,  
        x       = x  
      )  
    })
```

```

    a      = with(peaks, phase[1]),
    b      = with(peaks, phase[length(phase)]),
    initial_S0_est = with(par_list, S0 * x),
    iter   = 25
  )
  ptpi_out$S0 # all 26 estimates of `S0` in a vector
}
)
}
attr(out, "par_list") <- par_list
save(out, file = "RData/ptpi_convergence.RData")

```

569 We want the median and 5th and 95th percentiles of the estimate of S_0 obtained at each
 570 iteration (for each initial guess).

```

pct <- apply(out, c(1, 2), quantile,
  probs = c(0.05, 0.5, 0.95)
)

```

571 Plotting these as a functions of iteration, we reproduce Fig 9.

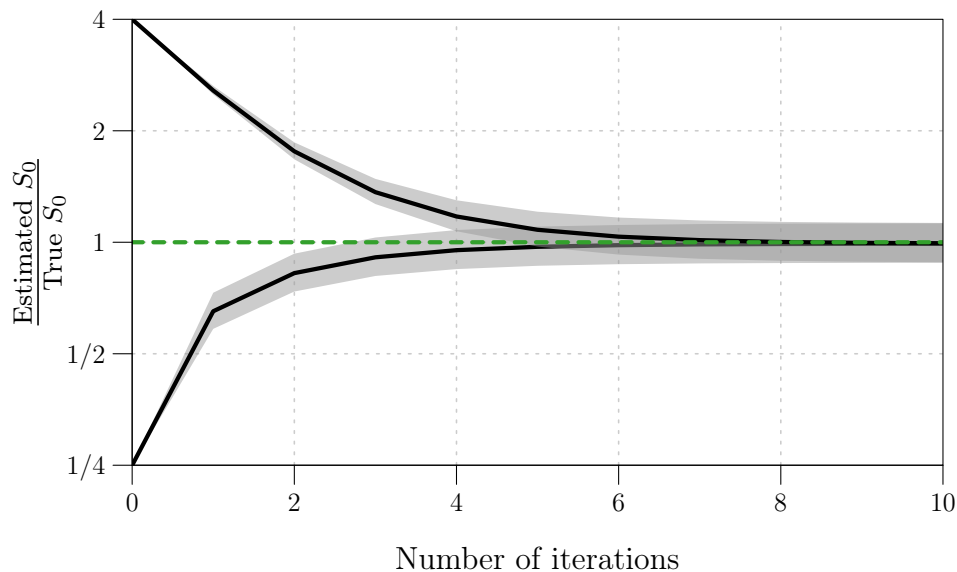


Fig 9. Convergence of estimates of S_0 obtained using peak-to-peak iteration.

572 In the manuscript, we report the median and 5th and 95th percentiles of the relative
 573 error in the estimate of S_0 obtained in the last iteration (for each initial guess). These are
 574 calculated as follows.

```

with(par_list, (pct[, 26, ] - S0) / S0)

##           [,1]           [,2]
## 5% -0.119343123 -0.119343062
## 50% -0.008528768 -0.008528708
## 95% 0.125379218 0.125379276

```

S9 Appendix: Choice of discretization in the SI method

The SI method modifies a method presented in [3] by deJonge. Here, we cast the SI method and deJonge’s method as two possible algorithms from a set of nine, differing according to (i) how

$$\frac{dS}{dt} = \nu(t)\widehat{N}_0 - \beta(t)SI - \mu(t)S, \quad (14a)$$

$$\frac{dI}{dt} = \beta(t)SI - \gamma I - \mu(t)I \quad (14b)$$

are discretized (forward Euler, backward Euler, or trapezoidal method) in order to estimate susceptibles $S(t)$ and infecteds $I(t)$, and (ii) how

$$\frac{dQ}{dt} = \beta(t)SI \quad (15)$$

is discretized (forward Euler, backward Euler, or both) in order to estimate the transmission rate $\beta(t)$. (“Both” means that the two estimates of $\beta(t)$ obtained by forward and backward Euler are averaged to generate a final estimate.) DeJonge’s method uses forward Euler throughout, whereas the SI method uses the trapezoidal method for Eqs (14) and both forward and backward Euler for Eq (15).

Here, we show that the SI method is more accurate than deJonge’s method and the seven other algorithms. We further show that the SI method and deJonge’s method are nearly unbiased (asymptotically) in the absence of input error.

S9.1 Nine discretization schemes

Our function `estimate_beta_SI()` takes a third argument `method`, which must be assigned a vector of length 2. `method[1]` has options `"forward"`, `"backward"`, and `"trapezoid"` (default), telling `estimate_beta_SI()` how to numerically integrate Eqs (14). `method[2]` has options `"forward"`, `"backward"`, and `"both"`, (default) telling `estimate_beta_SI()` how to numerically integrate Eq (15).

595 Eqs (16) below lay out the algorithm carried out by `estimate_beta_SI()`, conditional
 596 on `method[1]` and `method[2]`.

$$Z_k \leftarrow \frac{1}{p_{\text{rep}}} C_{k+r} \quad (16a)$$

$$S_k \leftarrow \begin{cases} (1 - \mu_{k-1}\Delta t)S_{k-1} + B_k - Z_k & \text{if } \text{method}[1] = \text{"forward"} \\ \frac{S_{k-1} + B_k - Z_k}{1 + \mu_k \Delta t} & \text{if } \text{method}[1] = \text{"backward"} \\ \frac{(1 - \frac{1}{2}\mu_{k-1}\Delta t)S_{k-1} + B_k - Z_k}{1 + \frac{1}{2}\mu_k \Delta t} & \text{if } \text{method}[1] = \text{"trapezoid"} \end{cases} \quad (16b)$$

$$I_k \leftarrow \begin{cases} [1 - (\gamma + \mu_{k-1})\Delta t]I_{k-1} + Z_k & \text{if } \text{method}[1] = \text{"forward"} \\ \frac{I_{k-1} + Z_k}{1 + (\gamma + \mu_k)\Delta t} & \text{if } \text{method}[1] = \text{"backward"} \\ \frac{[1 - \frac{1}{2}(\gamma + \mu_{k-1})\Delta t]I_{k-1} + Z_k}{1 + \frac{1}{2}(\gamma + \mu_k)\Delta t} & \text{if } \text{method}[1] = \text{"trapezoid"} \end{cases} \quad (16c)$$

$$\beta_k \leftarrow \begin{cases} \frac{Z_{k+1}}{S_k I_k \Delta t} & \text{if } \text{method}[2] = \text{"forward"} \\ \frac{Z_k}{S_k I_k \Delta t} & \text{if } \text{method}[2] = \text{"backward"} \\ \frac{Z_k + Z_{k+1}}{2S_k I_k \Delta t} & \text{if } \text{method}[2] = \text{"both"} \end{cases} \quad (16d)$$

597 Hence the SI method corresponds to `method = c("trapezoid", "both")`, while
 598 deJonge's method corresponds to `method = c("forward", "forward")`.

599 S9.2 Comparison of RRMSE, bias, and variance

600 We will compare the nine algorithms described in Eqs (16) using two metrics. First, we
 601 consider performance as measured by the RRMSE in the raw transmission rate estimates
 602 β_k . Second, we consider bias in the average 1-year cycle, calculated from the linear
 603 interpolant of β_k as in §S3.

604 S9.2.1 RRMSE

605 We simulate 100 reported incidence time series C_k using each of 41 values for the case
 606 reporting probability p_{rep} , logarithmically spaced between 0.01 and 1. (Smaller values of
 607 p_{rep} generate noisier C_k , leading to noisier β_k .)

```
prep <- 10^seq(-2, 0, length.out = 41)
par_list <- make_par_list(epsilon = 0.5)
nsim <- 100
```

608 We estimate the underlying, seasonally forced transmission rate $\beta(t)$ (Eq (5)) from each
 609 simulated reported incidence time series using each algorithm described in Eqs (16), and
 610 record the RRMSE in each raw estimate β_k . We can preallocate space for this output.

```

method1_names <- c("forward", "backward", "trapezoid")
method2_names <- c("forward", "backward", "both")
out <- array(NA,
  dim      = c(length(prepare), nsim, 3, 3),
  dimnames = list(NULL, NULL, method1_names, method2_names)
)

```

611 The next code chunk implements the steps in this routine, saving main results in the
612 file `RData/euler.RData`. We can reuse simulations from §S4, which were saved in the
613 directory `RData/loess/`.

```

for (i in seq_along(prepare)) {

  ## Update `par_list` with current value of `prepare`
  par_list$prepare <- prepare[i]

  ## Create a directory for this loop's `.RData`
  dirname <- paste0(
    "RData/loess/",
    ## log10 current value of `prepare`
    "prepare_log10v-", sprintf("%+05.0f", log(prepare[i], 10) * 1000), "/"
  )
  if (!dir.exists(dirname)) {
    dir.create(dirname, recursive = TRUE)
  }

  for (j in seq_len(nsim)) {

    message(
      "`prepare` value ", i, " of ", length(prepare), ", ",
      "sim ", j, " of ", nsim
    )

    ## File name for simulation
    filename <- paste0(dirname, "sim", sprintf("%04.0f", j), ".RData")

    ## Simulate reported incidence data, if you haven't already
    if (file.exists(filename)) {
      load(filename)
    } else {
      df <- make_data(
        par_list      = par_list,

```

```

    n          = 20 * 365 / 7,
    with_dem_stoch = TRUE,
    seed       = j
  )
  save(df, file = filename)
}

for (m1 in method1_names) {
  for (m2 in method2_names) {

    ## Estimate the seasonally forced transmission rate
    ## from reported incidence
    df_est <- estimate_beta_SI(df, par_list, method = c(m1, m2))

    ## Record the error
    out[i, j, m1, m2] <- compute_rrmse(df$beta, df_est$beta)

  }
}

}

}

attr(out, "arg_list") <- list(
  prep      = prep,
  par_list  = par_list
)
save(out, file = "RData/euler.RData")

```

614 We desire the median and 5th and 95th percentiles of RRMSE for each value of p_{rep} , for
 615 each of the nine algorithms used to estimate $\beta(t)$.

```
pct <- apply(out, c(1, 3, 4), quantile, probs = c(0.05, 0.5, 0.95))
```

616 Plotting these as functions of p_{rep} , and stratifying the results by `method[1]` (panel title)
 617 and `method[2]` (legend label) yields the following figure.

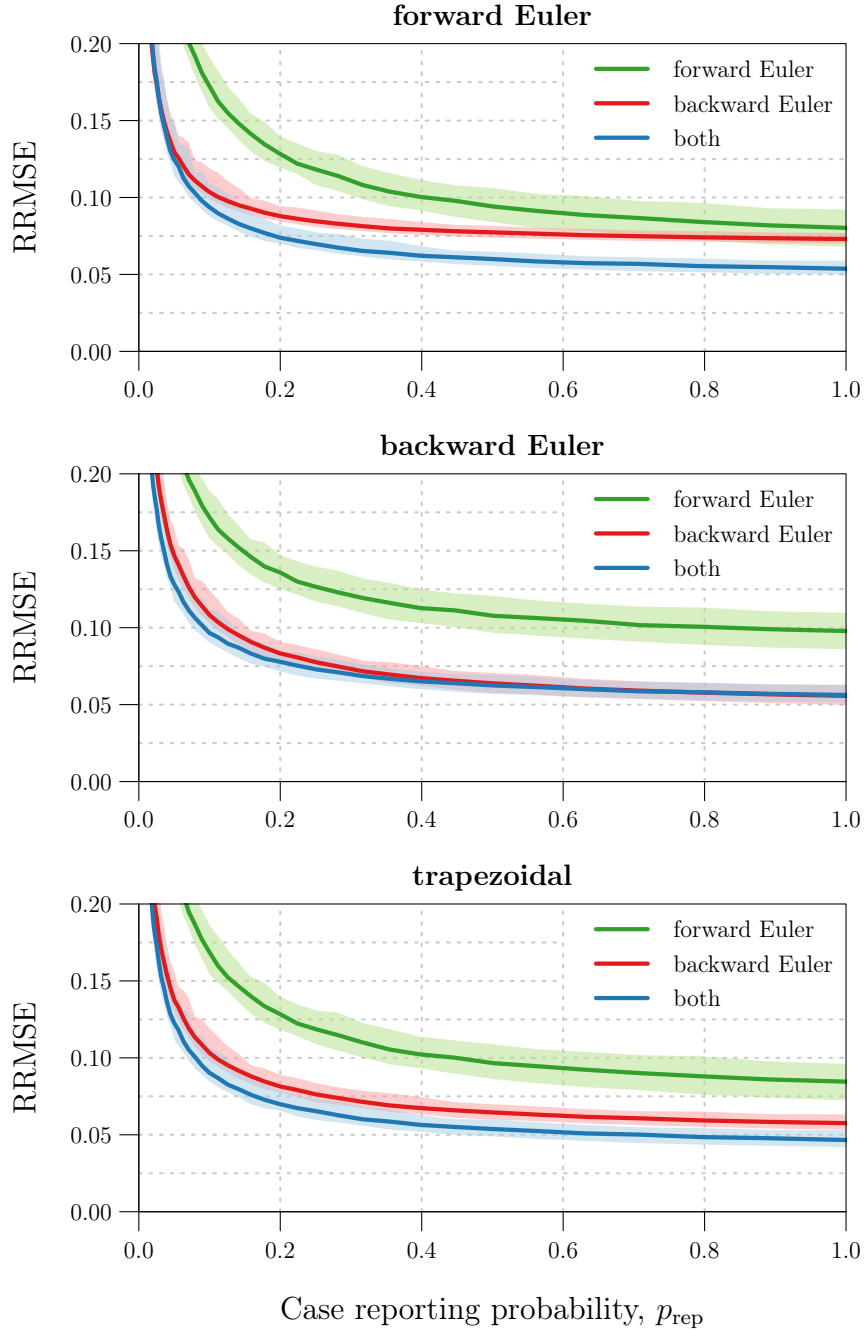


Fig 10. Performance of the nine discretization schemes, as measured by RRMSE in the raw transmission rate estimate β_k . Panel titles specify the discretization of Eqs (14). Legend labels specify the discretization of Eq (15).

618 For every choice of `method[1]` (panel title), the best choice of `method[2]` (legend
 619 label) was typically `"both"`. On the other hand, for a given choice of `method[2]`, the

620 best choice of `method[1]` (by a small margin) was typically the one that avoided
621 mismatch with `method[2]`. That is, when forward and backward Euler were used to
622 discretize Eq (15), RRMSE was typically smallest when forward and backward Euler,
623 respectively, were used to discretize Eqs (14). Similarly, when both forward and backward
624 Euler were used to discretize Eq (15), RRMSE was typically smallest when the trapezoidal
625 method was used to discretize Eqs (14). This combination, with
626 `method = c("trapezoid", "both")`, gave the best performance overall.

627 S9.2.2 Bias and variance

628 In §S3, we looked at bias and variance in the 1-year cycles embedded in raw transmission
629 rate estimates β_k spanning 1000 years. There, we compared the S and SI methods. Here,
630 we compare the nine algorithms described in Eqs (16).

631 We simulate 1000 years of weekly observations of reported incidence, including in the
632 simulation environmental noise in transmission ($\epsilon = 0.5$), demographic stochasticity, and
633 random under-reporting of cases ($p_{\text{rep}} = 0.25$).

```
par_list <- make_par_list(epsilon = 0.5, prep = 0.25)
df <- make_data(
  par_list      = par_list,
  n             = 1000 * 365 / 7 + 1,
  with_dem_stoch = TRUE,
  seed         = 1352
)
```

634 We estimate the seasonally forced $\beta(t)$ using all nine discretization schemes, without input
635 error.

```
df_est <- mapply(
  function(x) {
    mapply(
      function(y) {
        estimate_beta_SI(df, par_list, method = c(x, y))
      },
      y = method2_names, SIMPLIFY = FALSE
    )
  },
  x = method1_names, SIMPLIFY = FALSE
)
```

636 We linearly interpolate each raw time series estimate β_k .


```
fits <- lapply(df_est, function(x) {
  lapply(x, function(y) {
    approxfun(y$t, y$beta, method = "linear", rule = 1)
  })
})
```

637 As in §S3, we define the initial observation time `t0`, period `period`, and number of cycles
 638 `m`, then use `get_phase_average()` to calculate the average 1-year cycle in the linear
 639 interpolants.

```
## First and last time points, retrievable
## from any data frame in the list
t0 <- df_est[[1]][[1]]$t[1]
tn <- df_est[[1]][[1]]$t[nrow(df_est[[1]][[1]])]

## 1-year period in units of the observation interval
period <- with(par_list, (365 / 7) / dt_weeks)

## Number of cycles
m <- floor((tn - t0) / period)

get_phase_average <- function(s, f) {
  x <- f(t0 + (s %% period) + (0:(m-1)) * period)
  mean(x, na.rm = TRUE)
}

s_grid <- seq(0, period, length.out = 150)
average_one_year <- lapply(fits, function(x) {
  data.frame(
    s_grid,
    lapply(x, function(f) sapply(s_grid, get_phase_average, f = f))
  )
})
```

640 We plot the 1000 individual cycles and their average on the same 1-year axis, yielding a
 641 9-panel plot.

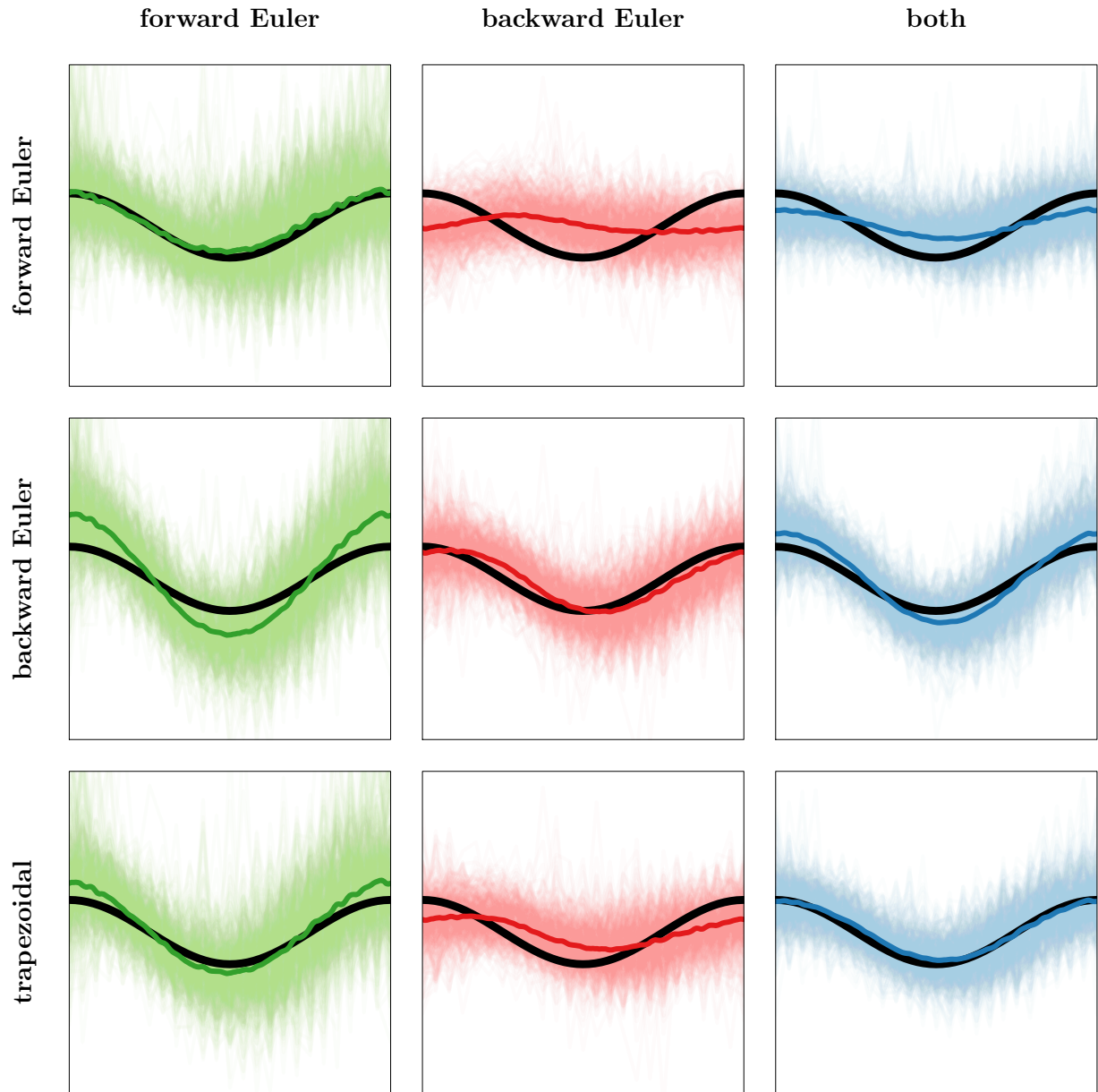


Fig 11. Bias and variance incurred by the nine discretization schemes. Row names specify the discretization of [Eqs \(14\)](#). Column names specify the discretization of [Eq \(15\)](#).

642 Following the pattern of [Fig 10](#), [Fig 11](#) shows that mismatch between `method[1]` and
 643 `method[2]` is detrimental: in the off-diagonal panels, the average 1-year cycle fails to
 644 capture the correct seasonal amplitude. In addition, use of backward Euler to discretize
 645 [Eqs \(14\)](#) appears ill-advised: in the panels from the second row, the average 1-year cycle
 646 lags the true cycle. Finally, it is apparent that the SI method (bottom right panel) and
 647 deJonge's method (top left panel) are both nearly unbiased.

648 All methods appear prone to propagating noise from reported incidence (due to process
649 and observation error) to β_k . However, the SI method and deJonge's method stand out as
650 being the least and most susceptible, respectively, to propagation of spurious noise. This
651 likely accounts for the difference in their performance shown in Fig 10.

References

1. R Core Team. R: A language and environment for statistical computing; 2020. Available from: <https://www.R-project.org>.
2. Hart JD. Automated kernel smoothing of dependent data by using time series cross-validation. *Journal of the Royal Statistical Society B (Statistical Methodology)*. 1994;56(3):529–542.
3. deJonge MS. Fast estimation of time-varying transmission rates. Hamilton, Ontario, Canada: McMaster University; 2014. Available from: <https://macsphere.mcmaster.ca/handle/11375/14230>.